Synthetic studies towards an organometallic rotaxane.

A thesis submitted to the

UNIVERSITY OF CAPE TOWN

in fulfilment of the requirements for the degree of

MASTER OF SCIENCE

by

Jacques Maré

BSc (Hons)

Department of Chemistry

University of CapeTown

Rondebosch

7700

Republic of South Africa

April 1996

Acknowledgements

I would like to express my gratitude to the following people and institutions.

Professor R. Hunter for his advice, encouragement and intellectual guidance during this work.

Professor Moss for his supervision and encouragement throughout the duration of this project.

Members of the organometallic research team as well as members of the organic and steroidal research groups epecially Professor J. R. Bull for their advice.

My friend and colleague, Rainer Clauss.

Dr K. Dimitriova and Mr N. Hendricks for running the numerous NMR spectra.

Mr P. Benincasa for the microanalyses and mass spectrometry as well as

Dr K. Boshoff for mass spectrometry.

The Foundation for Research Development and the University of Cape Town for financial assitance.

My family, especially my mother and brother for their continued support.

Abstract

The synthesis of interlocking molecules such as rotaxanes and catenanes is a branch of supramolecular chemistry of particular current interest. The aim of this work was to assess the viability of the synthesis of an organometallic rotaxane in which the transition metal is covalently bonded to a carbon atom of an alkyl group.

We have synthesised novel organometallic π-electron donor alkyl and polyether compounds such as the alkyl thread π-donor compound, $CpFe(CO)_2(CH_2)_3OC_6H_4O(CH_2)_3Fe(CO)_2Cp$, and the polyether π-donor compound, $CpFe(CO)_2(CH_2)_3O(CH_2CH_2O)_2C_6H_4(OCH_2CH_2)_2O(CH_2)_3Fe(CO)_2Cp$.

The stability of these compounds has been further enhanced through derivatization by reaction with PPh_3 yielding chiral iron-acyl species.

The formation of a rotaxane using the host cyclophane, cyclobis(paraquat-p-phenylene), formed by a template effect, has been investigated using our chiral organometallic polyether.

Abbreviations

Compd.	compound
Cp	$(\eta^5\text{-}C_5H_5)$
DMF	dimethylformamide
DMSO-d_6	deuterated dimethylsulfoxide.
THF	tetrahydrofuran
"Bluebox"	cyclobis(paraquat-p-phenylene).

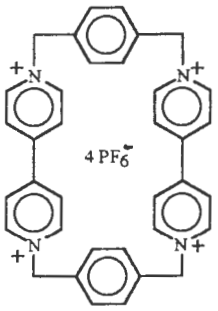

"Horseshoe"

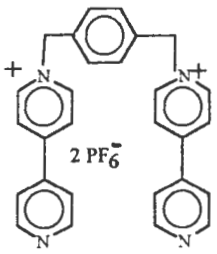

FAB - MS	Fast atom bombardment mass spectrometry.
NMR	nuclear magnetic resonance
M^+	molecular ion
m/e	mass to charge ratio
m.p.	melting point

nm	nanometer
TMS	tetramethylsilane
tr	triplet
q	quintet
s	singlet
d	doublet
br s	broad singlet
X	halogen
Δ	heat
$t_{1/2}$	half life

Table of Contents.

Chapter 1

Introduction.

1.1. Preparation of Rotaxanes By Statistical Methods

The early preparation of rotaxanes was accomplished by statistical methods, in which no specific molecular features were used in the construction of the thread or macrocycle to encourage association of the two components to form a rotaxane thus giving this method of rotaxane synthesis the advantage of extreme simplicity.
Harrison[1] prepared a mixture of rotaxanes using a thermal threading procedure. A mixture of alkane macrocycles containing all homologues from C_{14} to C_{42} was heated at 120°C in the presence of 1,10-bis(triphenylmethoxy)decane. This yielded the rotaxane formed by the threading of 1,10-bis(triphenylmethoxy)decane through the C_{29} alkane macrocycle, identified using thin layer chromatography and separated by column chromatography.

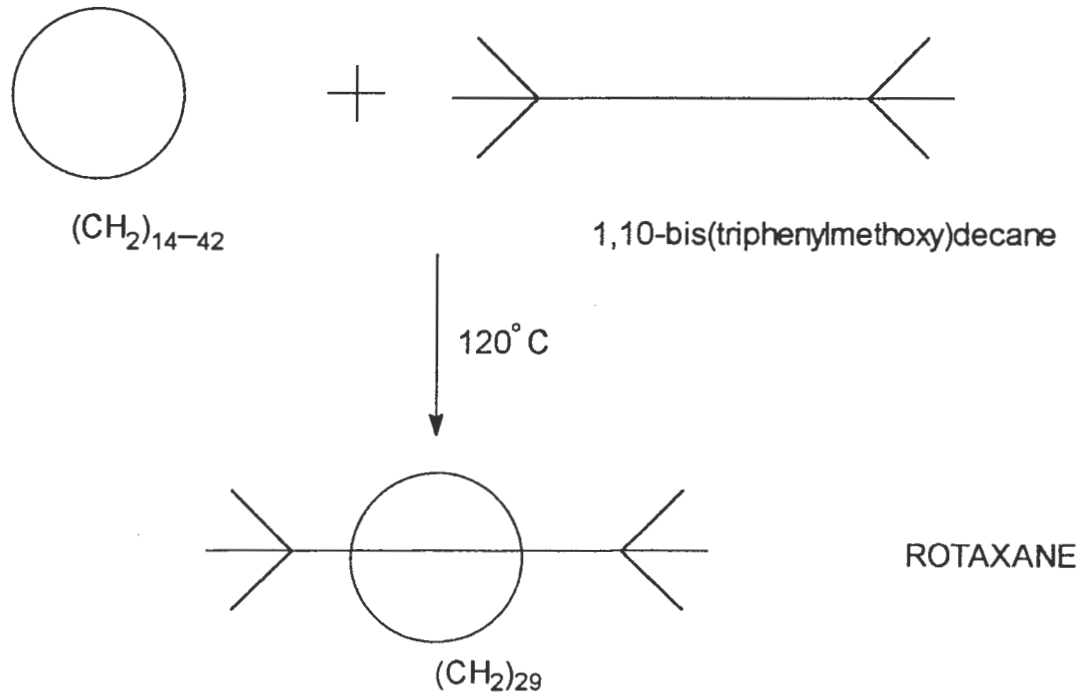

Figure 1.1. Synthesis of a rotaxane by a statistical method.

Heating of this rotaxane at 120°C caused the extrusion of the C_{29} alkane macrocycle with a $t_{1/2}$ of 19 minutes. Harrison[1] explains that C_{28} and smaller macrocycles are too small to permit threading of the bulky blocking groups while C_{30} and larger macrocycles form unstable transient rotaxanes which separate into their components at room temperature. Harrison[1] demonstrated this by repeating the experiment in the presence of a catalytic ammount of trichloroacetic acid which reversibly cleaved a triphenylmethyl blocking group allowing threading of the unblocked chain which resulted in the isolation of a mixture of rotaxanes containing macrocycles from C_{25} to C_{29}. Harrison[1] notes that no traces of rotaxanes formed with C_{30} and higher macrocycles were found.

Harrison[2] similarly synthesised a mixture of rotaxanes by a statistical method.
A mixture of macrocycles containing all homologues from C_{14} to C_{42} was heated with 1,13-di(tris-4-t-butylphenylmethoxy)tridecane in the presence of napthalene-β-sulphonic acid which reversibly cleaved the triaryl ether blocking groups of the thread. After equilibrium was attained, the reaction was quenched by the addition of base and the threaded products were separated by chromatography. The threaded products were then treated with acid which cleaved the ether blocking groups of the thread and this released the macrocycles. Gas chromatography of the released macrocycles allowed the determination of the yield of rotaxanes for each ring size. The yields were found to vary from 0.0013% for C_{24} to 1.6% for C_{33}.
Thus Harrison[1,2] has demonstrated that rotaxanes can be synthesised by statistical methods and further that the most important factors to consider when using these methods are the size of the macrocycle versus the size of the blocking groups and the reaction conditions (i.e. thermal threading versus acid catalysed threading.)
The drawback to this method is that the yields are extremely low.

1.2. Template Synthesis using metal cations.

This method of template synthesis[3] makes use of tetrahedral copper(I) to direct the assembly of chelating components. Two of the strategies used are shown in figure 1.2.1. below and are labelled as strategy A and B. Both strategies result in the synthesis of a catenane V with the intermediate labelled IV from strategy B being a rotaxane.

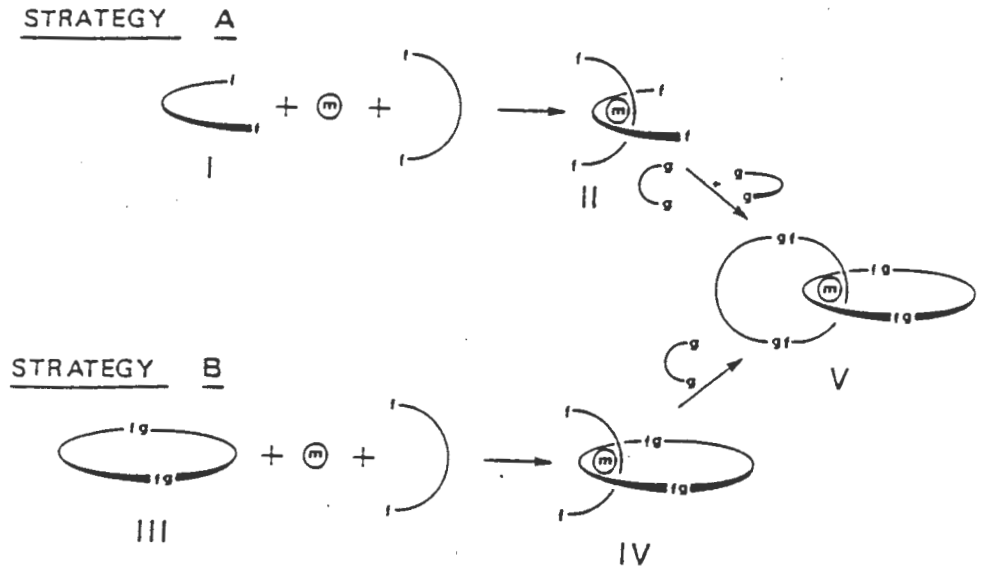

Figure 1.2.1. Strategies A and B.

Initially[4] 1,10-phenanthroline is converted to 2,9-dianisyl-1,10-phenanthroline by addition of lithioanisole, followed by deprotection with pyridinium hydrochloride to yield 2,9-di-(4-hydroxyphenyl)-1,10-phenanthroline, **31**.

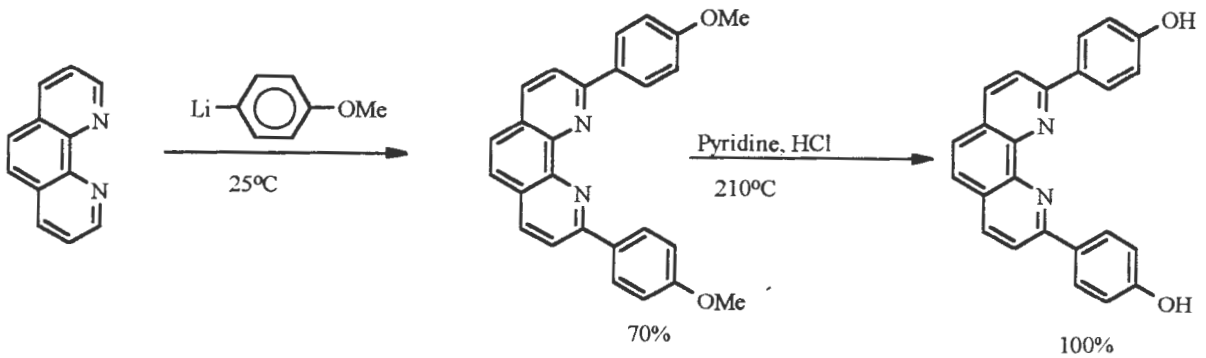

31

Figure 1.2.2 Synthesis of 2,9-(4-hydroxyphenyl)-1,10-phenanthroline, **31**.

Various precursors have been synthesised from 2,9-diphenol-1.10-phenanthroline and have been used in the synthesis of a 3-catenane[5], a fullerene stoppered rotaxane, as well as 2-catenanes and polyrotaxanes.

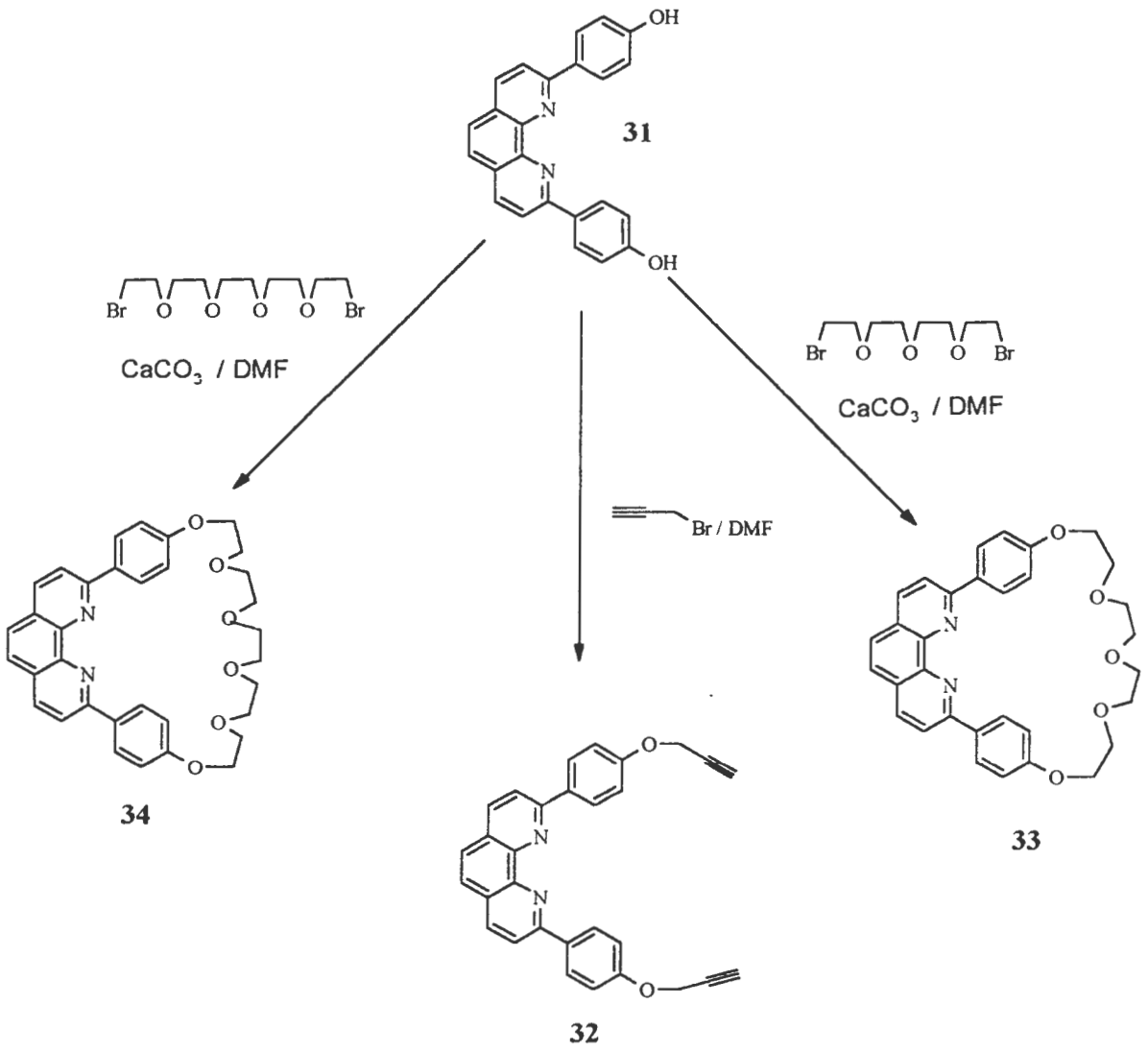

Figure 1.2.3. Preparation of ligands using the precursor, **31.**

This method of template synthesis has recently been used by Sauvage[6] in the synthesis of a fullerene stoppered rotaxane. The macrocyclic ligand, **33**, used in this synthesis, was prepared using 1,12-dibromo-3,6,9,-trioxododecane as shown in figure 1.2.3. above. The open chain diyne, **32**, was prepared in 80% yield from 2,9-diphenol-1.10-phenanthroline, **31** and 3-bromopropyne in DMF in the presence of a large excess of Cs_2CO_3.

The oxidative coupling reaction was carried out between the termini of the alkynes of **32** and an alkynyl fullerene stopper using the Hay catalyst [CuCl-TMEDA-O_2] in dichloromethane and yielded the fullerene stoppered rotaxane in 15% yield when 5 equivalents of the fullerene derivative were reacted with one equivalent of the open chain diyne, **32**. (TMEDA = N,N,N',N',-tetramethylethylenediamine.)

Sauvage[6] notes that the dimeric fullerene derivative was isolated in 20% yield, presumably relative to the amount of fullerene starting material. The synthesis of this rotaxane is shown below, with reaction conditions, i, being CuCl-TMEDA-O_2, CH_2Cl_2, room temperature.

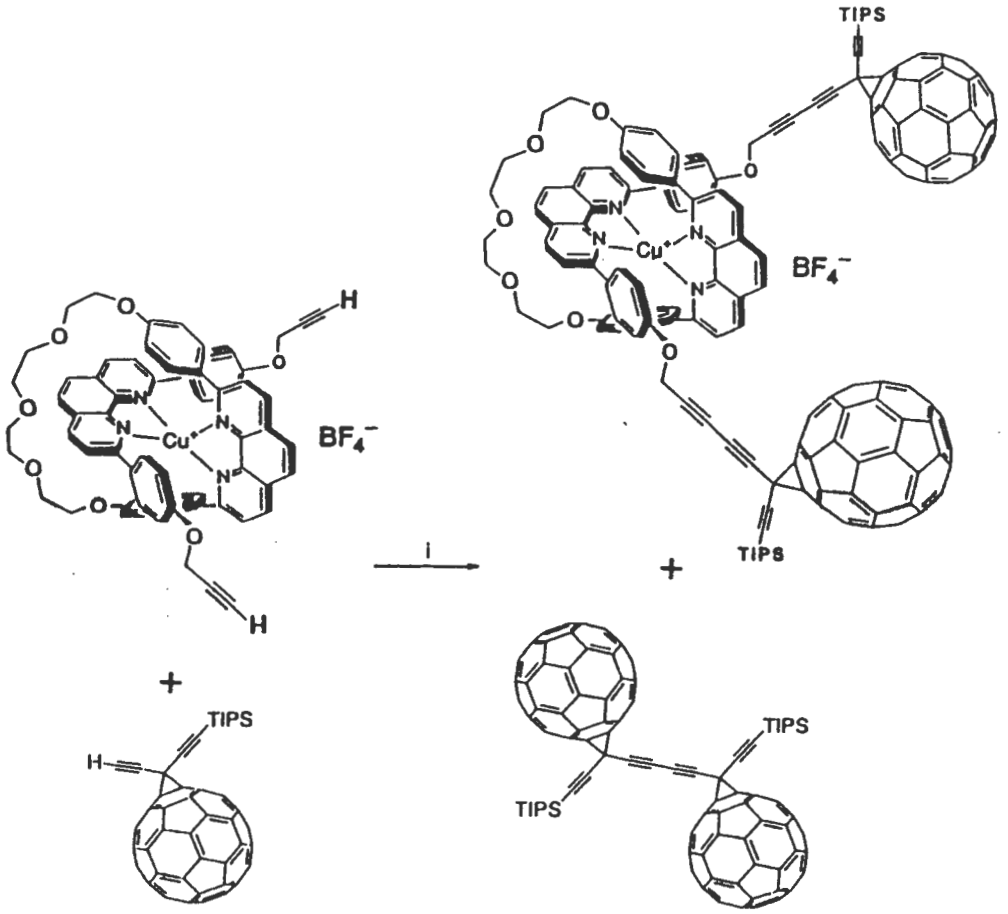

Figure 1.2.4. Synthesis of a fullerene stoppered rotaxane.

The Cu(I) ion is usually removed from the templated synthesis using an excess of KCN. However, in this instance demetallation with KCN yielded a mixture of compounds and the desired non-coordinated fullerene rotaxane could not be isolated in a pure form but could be detected by FAB-MS. Further developments in the templated synthesis of rotaxanes[7,8] using multi-chelate threads resulted in the synthesis of polyrotaxanes with particularly interesting and complex topology.

The synthetic routes are shown in figure 1.2.5 below. Route **a** was used to synthesise the fullerene stoppered rotaxane as explained above; routes **b** and **c** have been used to create both rigid-multimetallic rotaxane type complexes[8] as well as highly flexible multimetallic rotaxane type complexes[7].

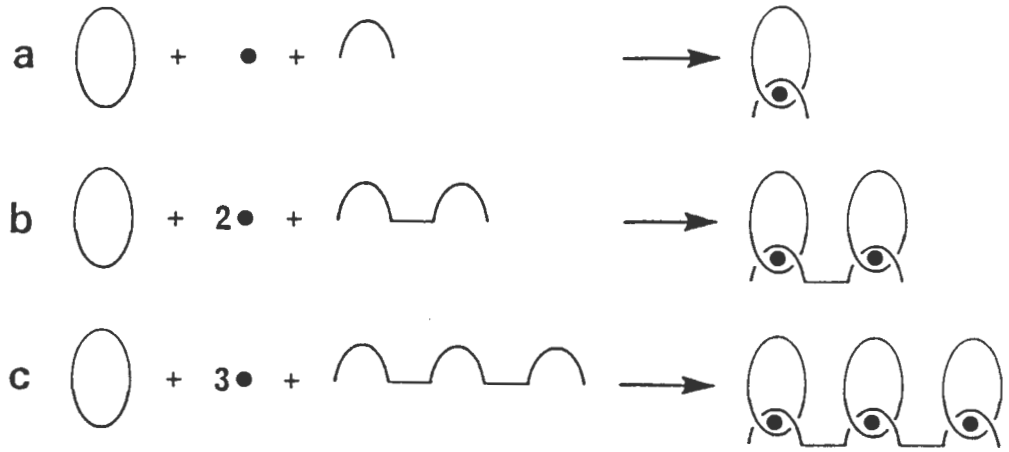

Figure 1.2.5. Strategies used for the templated synthesis of multimetallic rotaxanes. Lehn and co-workers[8] have used strategies **b** and **c** to synthesize rigid multimetallic rotaxane type complexes in high yield as shown in figure 1.2.6 below.

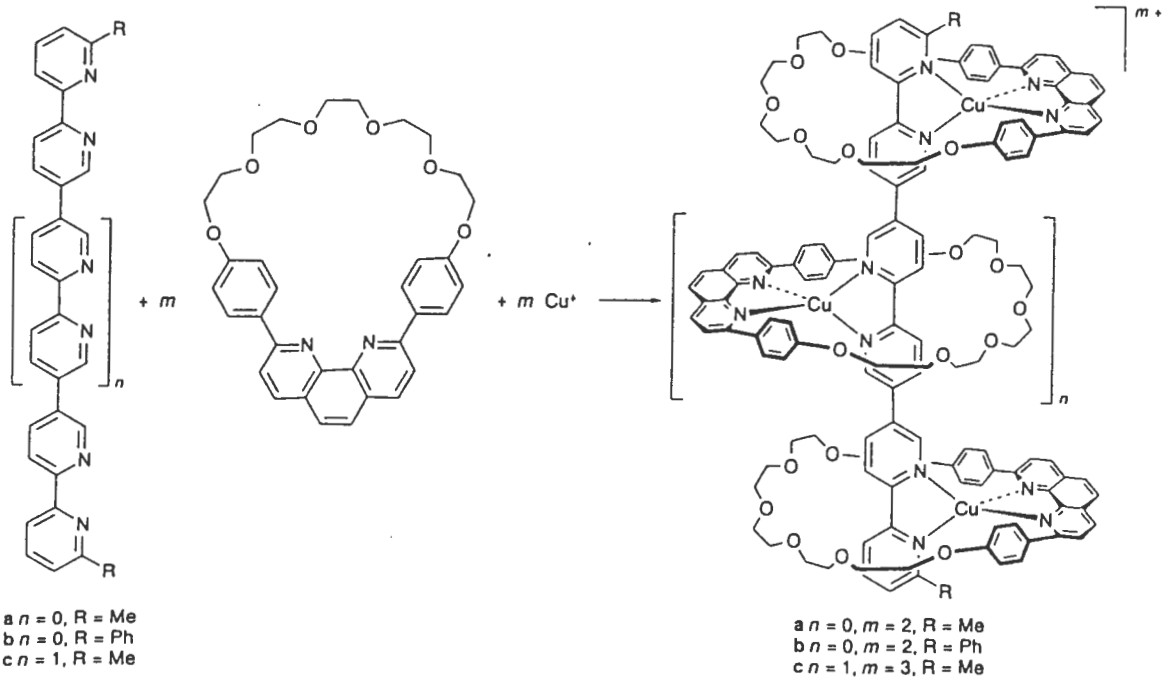

Figure 1.2.6. Self-assembly of rigid multimetallic rotaxane type complexes.

The construction of these systems uses linear ligands built on 2,2' bypyridine subunits and the macrocyclic ligand, **34**, the synthesis of which was previously described[6].

Chambron and co-workers[7] prepared both flexible and rigid multimetallic rotaxane type complexes using multi-dentate phenanthroline based threads shown in figure 1.2.7. below.

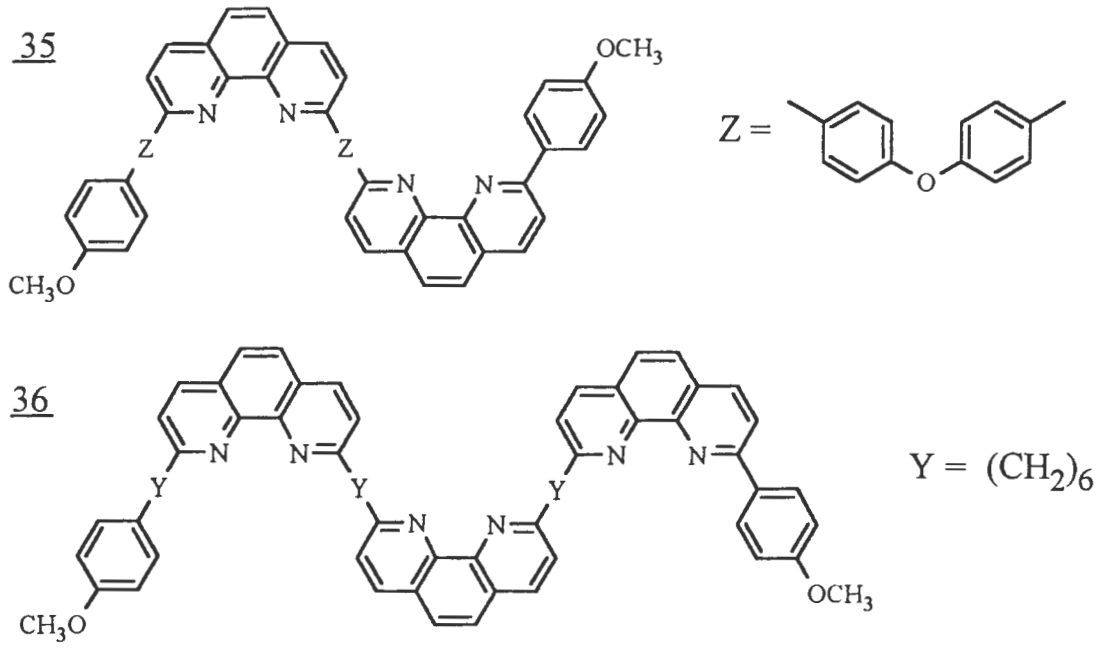

Figure 1.2.7. Rigid, **35**, and flexible, **36**, multimetallic, multidentate threads.

Combination of the rigid bidentate thread, **35**, with two equivalents of monodentate macrocyclic ligand, **34**, yielded the 3-rotaxane [**35**, $(\mathbf{34})_2,\mathbf{Cu}_2]^{2+}$ as shown in figure 1.2.8 below.

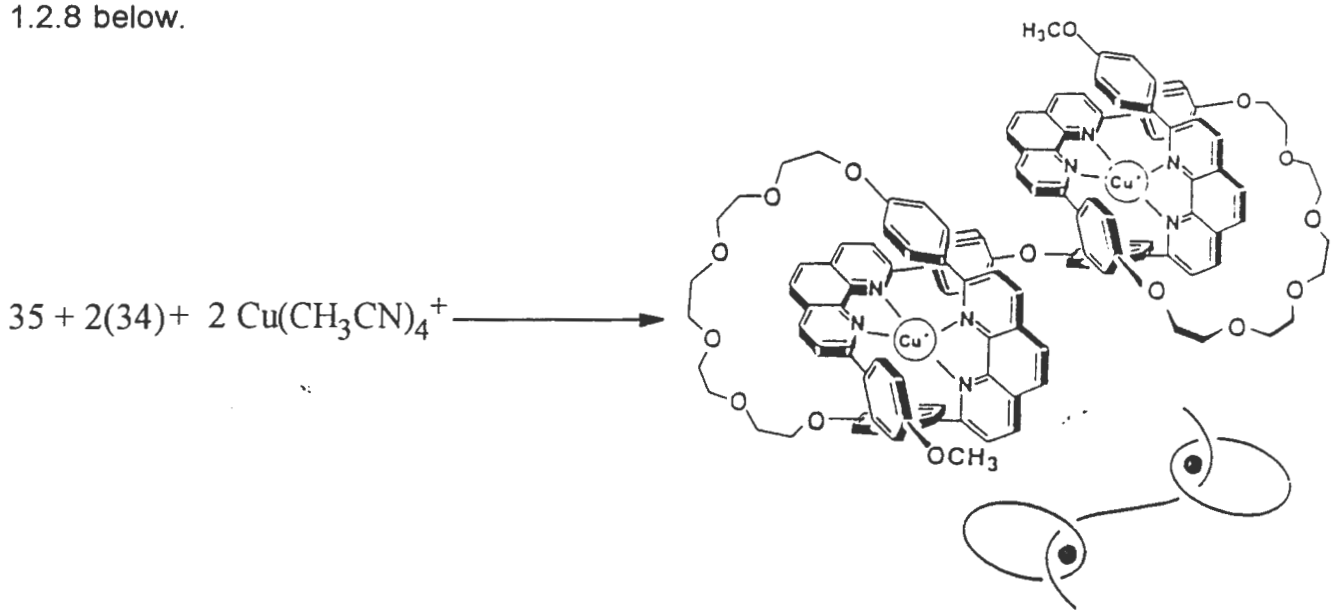

Figure 1.2.8.Synthesis of 3-rotaxane [**35**, $(\mathbf{34})_2$, $\mathbf{Cu}_2]^{2+}$.

Similarly, combination of the flexible tridentate thread, **36**, with one equivalent of monodentate macrocyclic ligand, **34**, yielded the 2-rotaxane [**36**, **(34)**, $\mathbf{Cu_2}]^{2+}$.
The molecular topology of this rotaxane is particularly unique and interesting as the thread curls back and coordinates on itself to give an intramolecular chelate effect as shown in figure 1.2.9 below. The structure of this compound was proved using electrospray mass spectrometry[7].

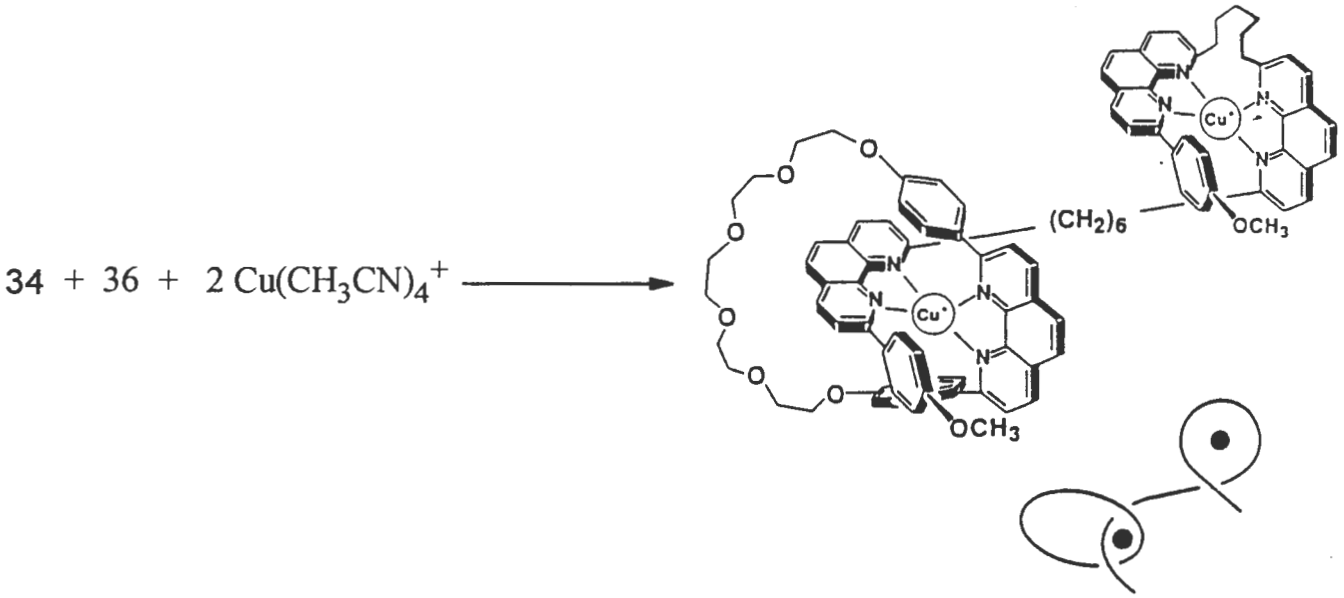

Figure 1.2.9. Synthesis of 2-rotaxane [**36**, **(34)**, $\mathbf{Cu_2}]^{2+}$

1.3. Self assembly using π-donors and π-acceptors.

The potential use of π-donors and π-acceptors[9], for self assembly, first became apparent with the observation that the charged complex, $[Pt(bipy)(NH_3)_2][PF_6]_2$ forms a 1:1 crystalline adduct with dibenzo-30-crown-10 (DB30-C-10).

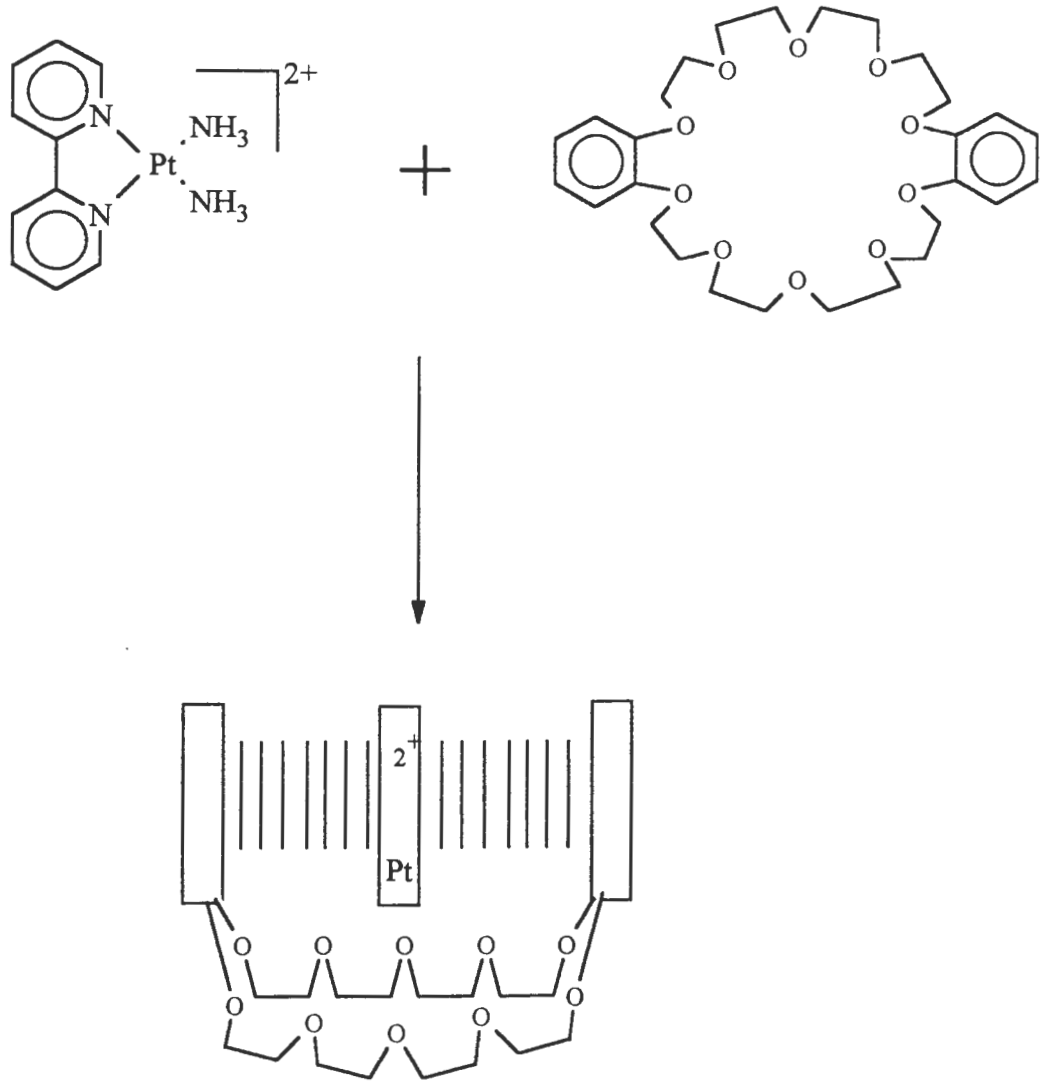

Figure 1.3.1 The horseshoe like structure of the $[Pt(bipy)(NH_3)_2]^{2+}$ DB30C10 adduct.

The crystal structure revealed that the crown, normally a rather large, extended molecule, wraps around the platinum bipyridyl complex in a horseshoe-like fashion. This is due to weak covalent non-bonding interactions in the adduct, including [N-H·····O] hydrogen bonding and π-π stacking interactions between the electron deficient bipyridyl ligand and the electron rich dibenzo-30-crown-10 macrocycle.

The next step towards the synthesis of rotaxanes using π-π stacking interactions was the synthesis of cyclobis(paraquat-p-phenylene) tetracation[10, 17] and the elucidation of the crystal structure of this cyclophane. Stoddart and co-workers[10] described the structure of the cyclobis(paraquat-p-phenylene) tetracation as a rigid centrosymetric rectangular box-like conformation with the two paraquat units forming the longer side while the two para-xylylene residues form the shorter sides. The tetracationic cyclophane adopted a bowed geometry, with the macrocyclic strain relieved throughout the cyclophane by out-of-plane bending of all six aryl rings. The overall dimensions of the cyclophane are 10.3 Å between the two para-xylylene sides and 6.8 Å between the two dipyridyl sides. The crystal structure and space-filling diagram are shown in Figure 1.3.2 below.

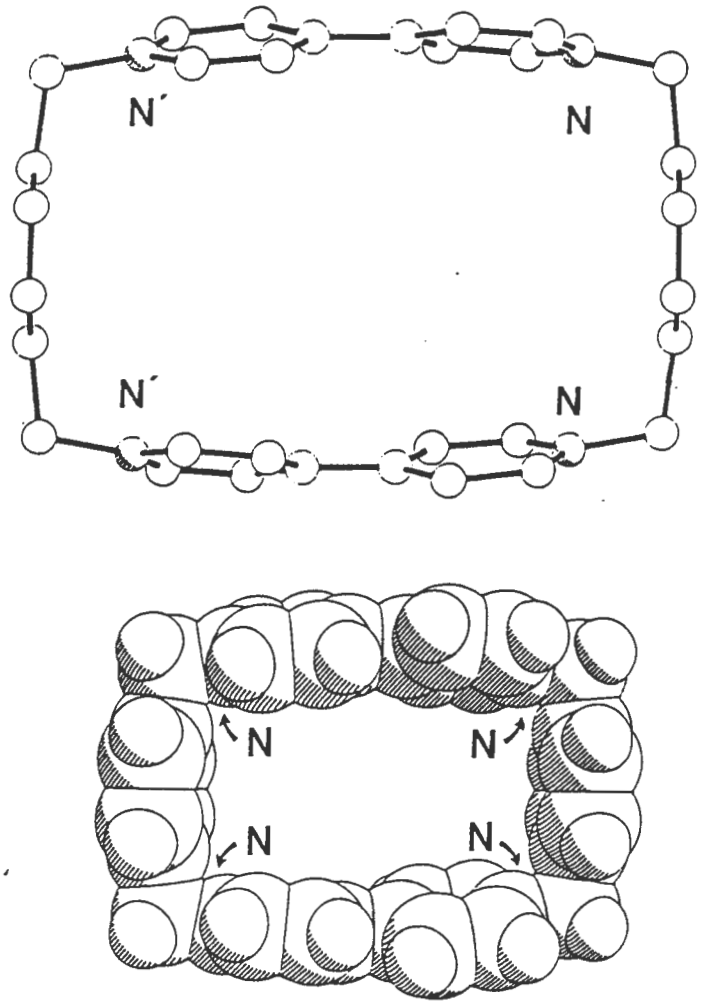

Figure 1.3.2. Crystal structure and space-filling diagram of the cyclophane cyclobis(paraquat-p-phenylene) tetracation.

The next advance was the observation[11] that the π-electron rich ether, 1,4-dimethoxybenzene could be inserted through the centre of the centrosymetric cyclophane, cyclobis(paraquat-p-phenylene) tetracation, with the methoxy substituents above and below the rim of the tetracation as shown in Figure 1.3.3 below. The authors[11] noted that the only significant change in the conformation of the cyclophane, in this inclusion compound, as compared to the conformation of the host on its own, was the reduction of the twist angle between the two bipridinium rings from 19° to 4° in the case of the inclusion compound. The authors, therefore, concluded that the cyclophane has the ability to flex to accomodate the π-electron rich substrate.

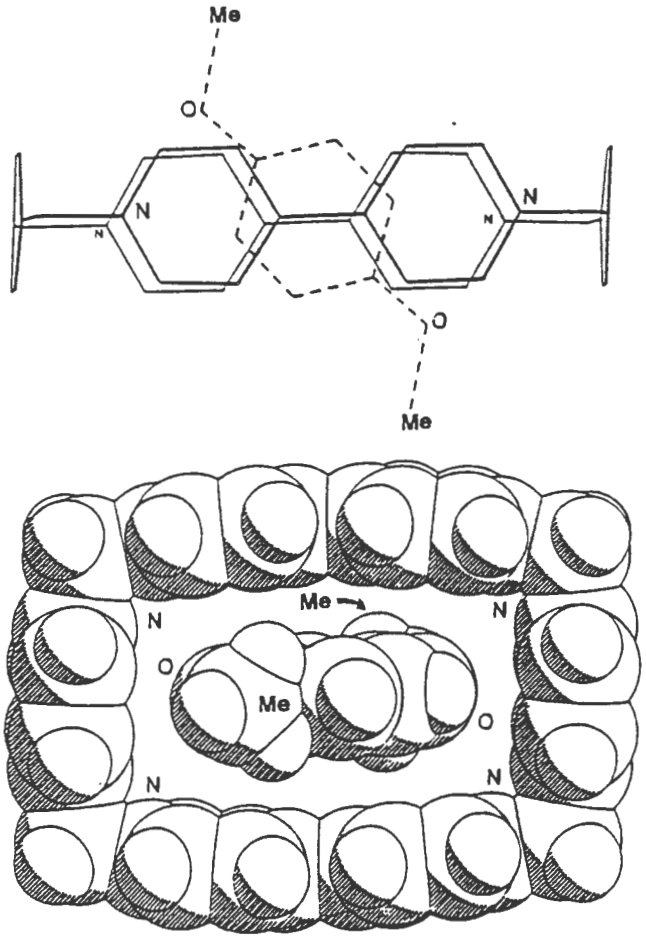

Figure 1.3.3. Skeletal arrangement of the inclusion compound formed between cyclobis(paraquat-p-phenylene)tetracationand1,4-dimethoxybenzene.

Subsequently, the observation[12] that 1,5-dimethoxynaphthalene inserts through the centre of the rigid cavity of this tetracationic cyclophane, provided further evidence for the potential versatility of cyclobis(paraquat-p-phenylene)tetracation as a host cyclophane for a rotaxane. The growing confidence of Stoddart and co-workers in this host was reflected in the title of the article[12] "Towards a Molecular Abacus."

The insertion of 1,5-dimethoxynaphthalene through the centre of the cyclophane was claimed by Stoddart and coworkers[12] for both the solid phase, (on the basis of a crystal structure) and for the solution phase, on the basis of ^{1}H NMR spectroscopy in CD_3CN solution. The tetracationic cyclophane adopted a bowed geometry as shown in Figure 1.3.4 below, with the macrocyclic strain relieved by out of plane bending of all six aryl rings. Interplanar spacing of 3.41 Å between the π-electron rich 1,5-dimethoxynaphthalene and π-electron deficient cyclobis(paraquat-p-phenylene) tetracation, were identified as giving rise to charge transfer interactions associated with donor-acceptor π-stacking. In addition, edge-to-face interactions of H_4 and H_8 of 1,5-dimethoxynaphthalene directed towards the para-phenylenedimethyl residues of cyclobis(paraquat-p-phenylene)tetracation give additional stabilization to this inclusion complex.

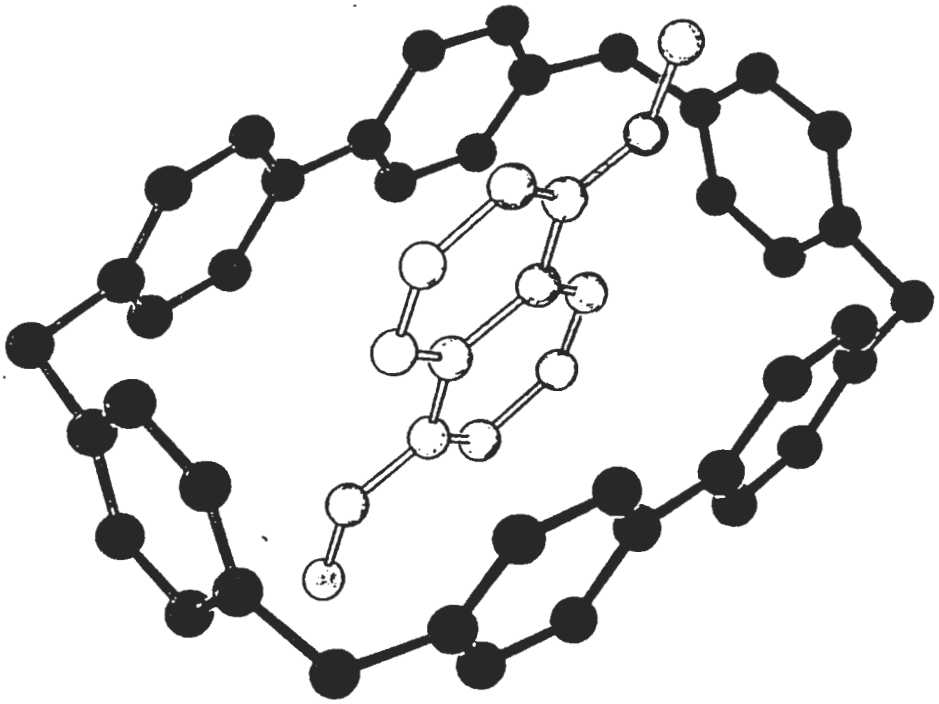

Figure 1.3.4. Complex formed between the (darkly shaded) cyclophane, cyclobis(paraquat-p-phenylene)tetracation and 1,5-dimethoxynaphthalene (lightly shaded).

Subsequently, rotaxanes[13-15] were developed using polyoxymethylene threads (typically having 8 or more oxygen atoms) to link π-electron rich hydroquinol donors thus creating two or more π-electron rich donor sites or "stations" in the thread.

X-ray structural analysis[13] of rotaxanes **25•21*** and **25•22** showed that in both instances the thread was inserted through the centre of the tetracationic cyclophane, **25**, such that the middle hydroquinone ring was encircled by the cyclophane and the polyether chains curled back around the cyclophane to allow the aromatic π-donors on the ends of the thread to stack against the outward face of the bipyridinium π-acceptor units of **25**.

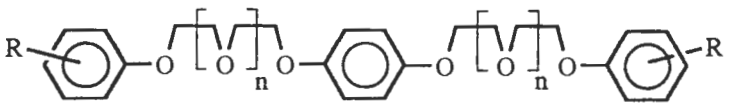

21 n = 3, R = 4-$PhCH_2O$ **22** n = 2, R = 3,5-$(MeO)_2$

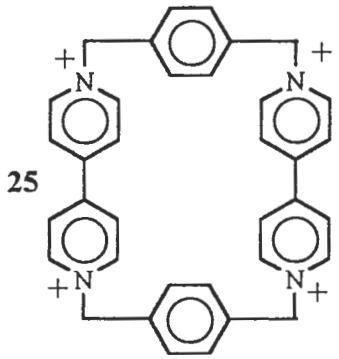

25

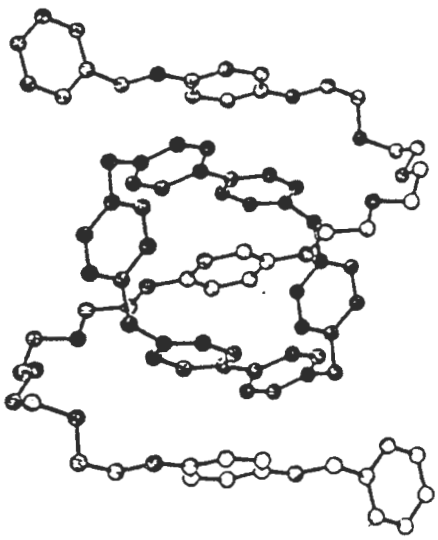

25•21

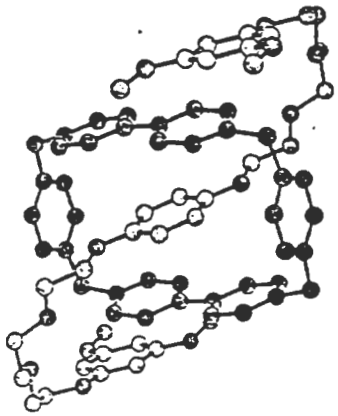

25•22

Figure 1.3.5. The threads, **21** and **22,** the cyclophane, **25** and crystal structures of the rotaxanes **25•21** and **25•22**.

(* **25•21** Denotes a novel rotaxane prepared using cyclophane, **25**, and thread, **21**.)

The synthesis of both of these rotaxanes was accomplished by a *threading procedure*, meaning that the tetracationic cyclophane, **25**, was synthesised prior to the synthesis of the rotaxane and the rotaxanes were prepared by combining **25** (as the PF_6 salt) with the thread (either **21** or **22**.) in acetonitrile solution.

For both rotaxanes **25•21** and **25•22** the encircled hydroquinone π-donor was separated from the bypyridinium π-acceptor units of **25** by ca. 3.5 Å. The authors[13] noted that for the two rotaxanes **25•21** and **25•22** there existed a common conformation of the first 10 atoms emanating from the included hydroquinone ring. The inner surface of the polyether loops, that passed over the junction of the bi pyridinium units and para-phenylene units, were arranged such that the oxygen atoms were in close proximity to the positively charged nitrogen atoms, thereby satisfying the electrostatic requirements of the tetracatonic cyclophane and adding to the associative interactions which bound the polyether threads and the tetracationic cyclophanes and gave these rotaxanes. This particular associative interaction the authors[14] classified as pole-dipole attractions.

An alternative procedure, known as a *clipping procedure*[14] was used to synthesize the rotaxane **25•23** in 32% yield and is shown in the Figure 1.3.6 below.

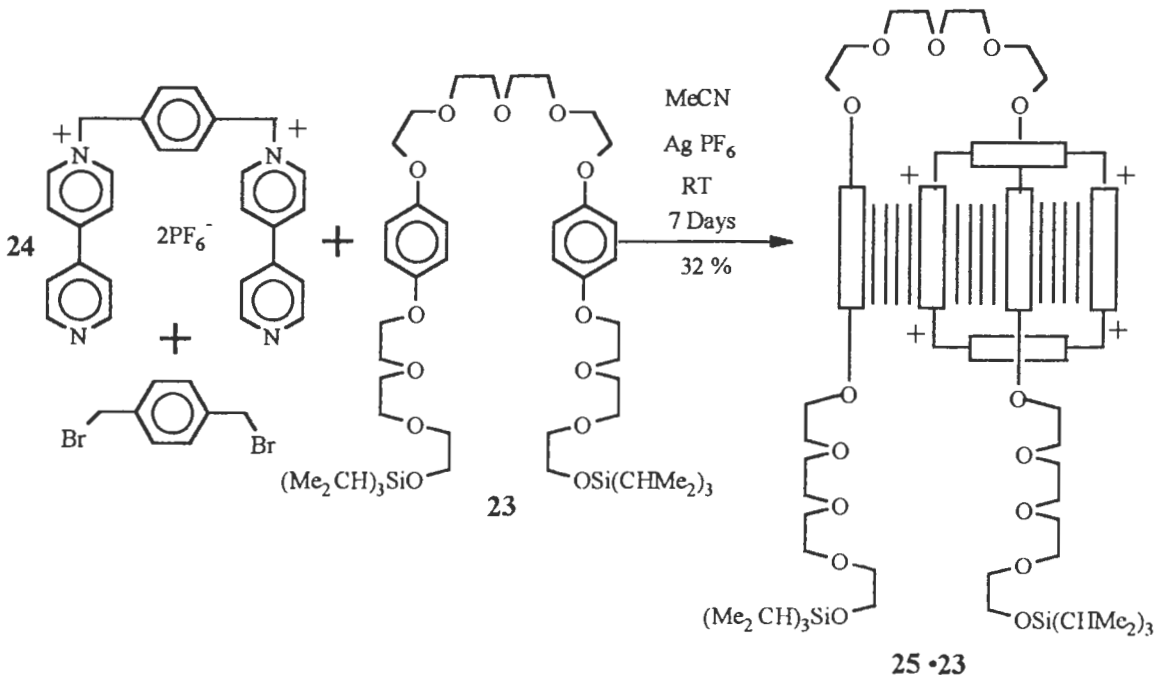

Figure 1.3.6. Reaction scheme for the *clipping procedure* used to synthesise the rotaxane **25•23**.

This *clipping procedure* is described as an example of a template synthesis since non-covalent bonding is responsible for the association of the components **24**, **23** and bis(bromomethyl)benzene to form the rotaxane, **25·23**. With reference to the synthesis of a 2-rotaxane[18], a mechanism has been proposed for the *clipping procedure*[9, 16, 18] and is presented below, for the case of the synthesis of the rotaxane **25·23**.

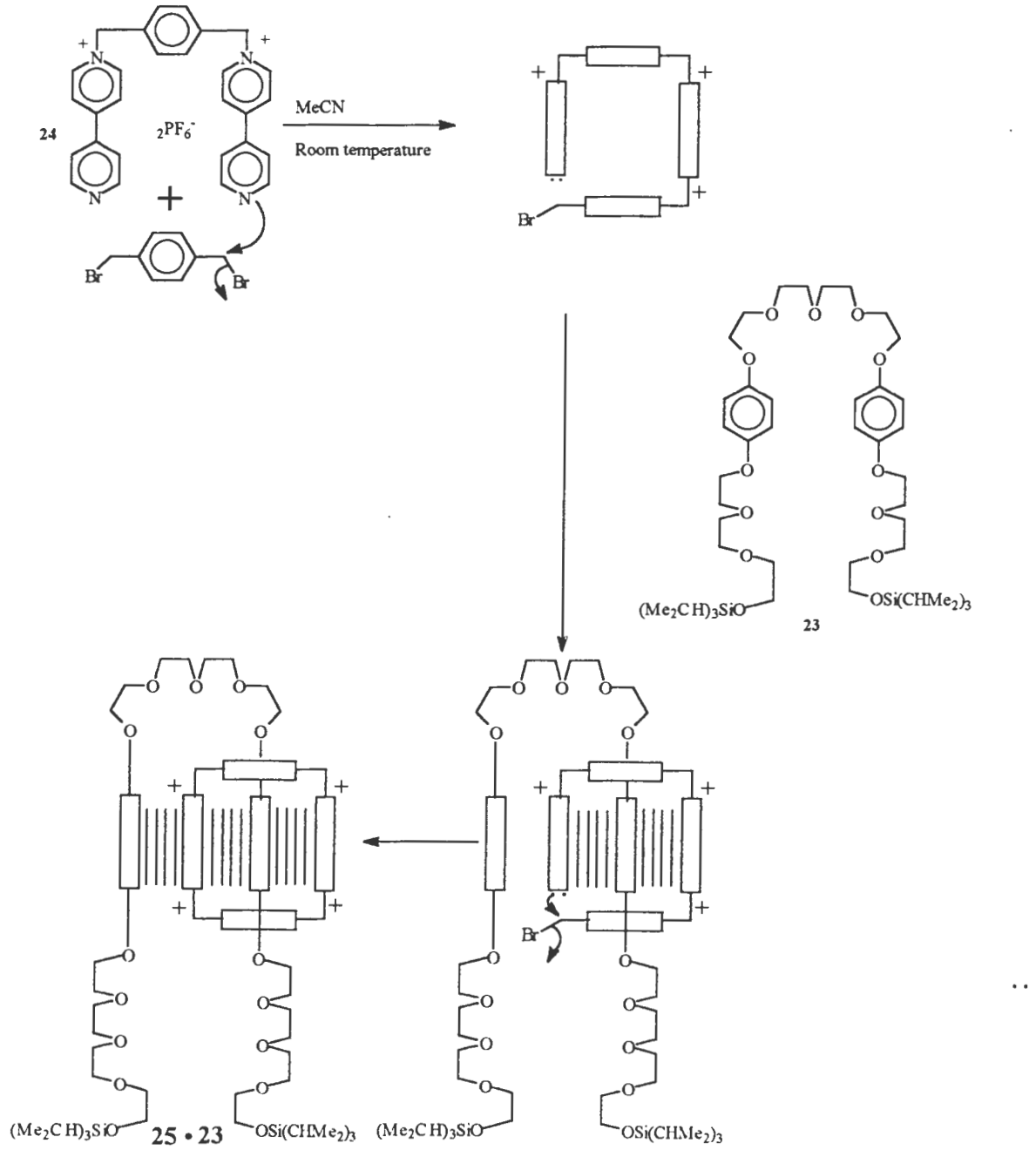

Figure 1.3.7. Mechanism of a *clipping procedure*.

The steps involved in the mechanism of the *clipping procedure*[9] are nitrogen-carbon bond formation between the dication, **24**, and bis(bromomethyl)benzene resulting in the formation of the trication which is then *clipped* onto the neutral chain, **23**, followed by a second nitrogen-carbon bond formation step to give ring closure thus generating the tetracationic cyclophane, in place to yield the rotaxane **25 23**.

The synthesis of the dication **24,** as the PF_6 salt is documented in the literature.[17]

The authors[14] note that the associative interactions responsible for the template synthesis of this rotaxane include; electrostatic dipole-dipole attractions between the dicationic bipyridinium units and the "solvating" polyether oxygen atoms; stabilizing dispersive forces including π/π stacking and charge transfer interactions between the π-electron rich hydroquinol rings and the π-electron deficient bipyridinium units and electrostatic "T-type" edge-to-face interactions involving the hydroquinol rings and the p-phenylene units in the cyclophane, **25**.

The ^1H NMR spectrum of the rotaxane **25 23** exhibits temperature dependence. The authors[14] identify this as being the result of a shuttling action of the cyclophane **25** as it moves from one π-electron rich donor site or "station" to the other. The authors[14] calculated the free energy barrier of the shuttling process from the temperature dependence of the shifts of the protons of the bipyridinium rings (ΔG=13.3 kcal mol^{-1}), from the temperature dependence of the shifts of the protons on the paraphenylene rings (ΔG=12.4 kcal mol^{-1}) and from the temperature dependence of the shifts of the protons of the hydroquinol rings (ΔG=13.2 kcal mol^{-1}). This process is shown in Figure 1.3.8. below.

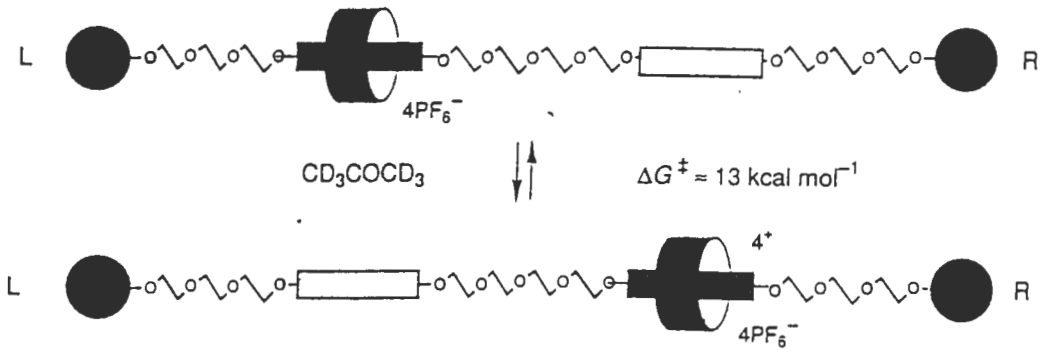

Figure 1.3.8. A molecular shuttle in action.

An alternative way to prepare a rotaxane is by a *threading prodedure*.[18, 19]

In the synthesis of the pseudorotaxane, **25·26** as shown below, "bluebox", **25**, is combined with a thread **26**, in acetonitrile solution to give the pseudorotaxane **25·26** as shown below. The product is known as a pseudorotaxane as it is not a true rotaxane due the the absence of bulky blocking groups on the ends of the thread which lock "bluebox" on the thread.

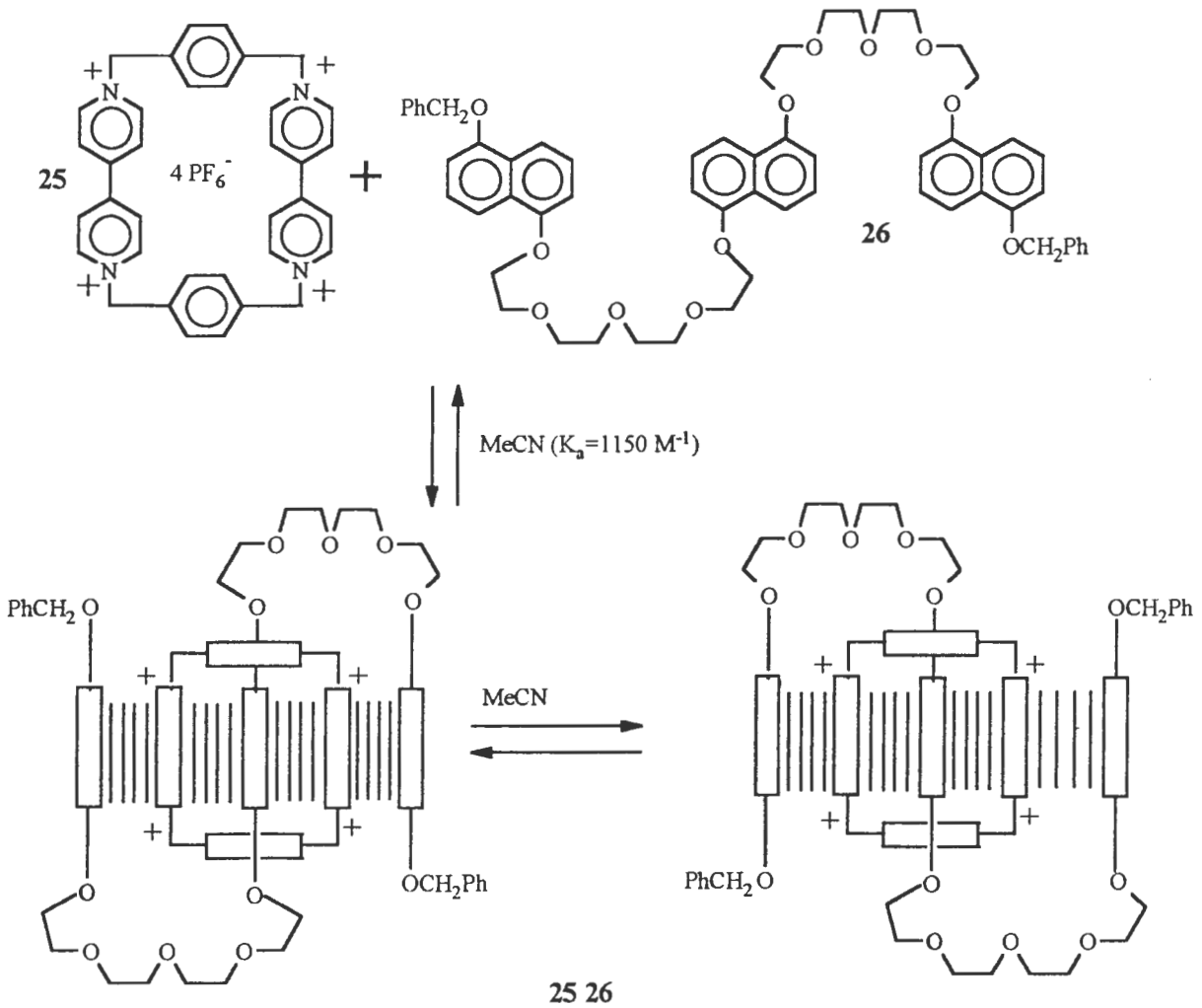

25 26

The 400 MHz ^{1}H NMR spectrum of the pseudorotaxane **25·26** showed line broadening at room temperature. However, on cooling to -30°C, the signals were resolved to show only one translational isomer undergoing a degenerate equilibration process involving switching of π-donor stations complexed by "bluebox", **25**. The authors[19] assigned the dynamic NMR behaviour of the pseudorotaxane **25·26** by considering chemical shift changes of the protons of the thread and those of "bluebox", **25**, as well use of homonuclear correlation spectroscopy.

The rotaxane **25·27** has been prepared by a *clipping procedure*, (as previously described) as well as by a *threading prodedure*.[18] In this approach the thread, without blocking groups, was threaded through "bluebox", **25**, by mixing the thread, **27**, and "bluebox", **25**, in acetonitrile solution. Bulky triisopropylsilyl end groups were then used to stopper the rotaxane by reacting the chain, as a diol, with triisopropylsilyltriflate in the presence of 2,6-dimethylpyridine base as shown below. This reaction was carried out in 22% yield.

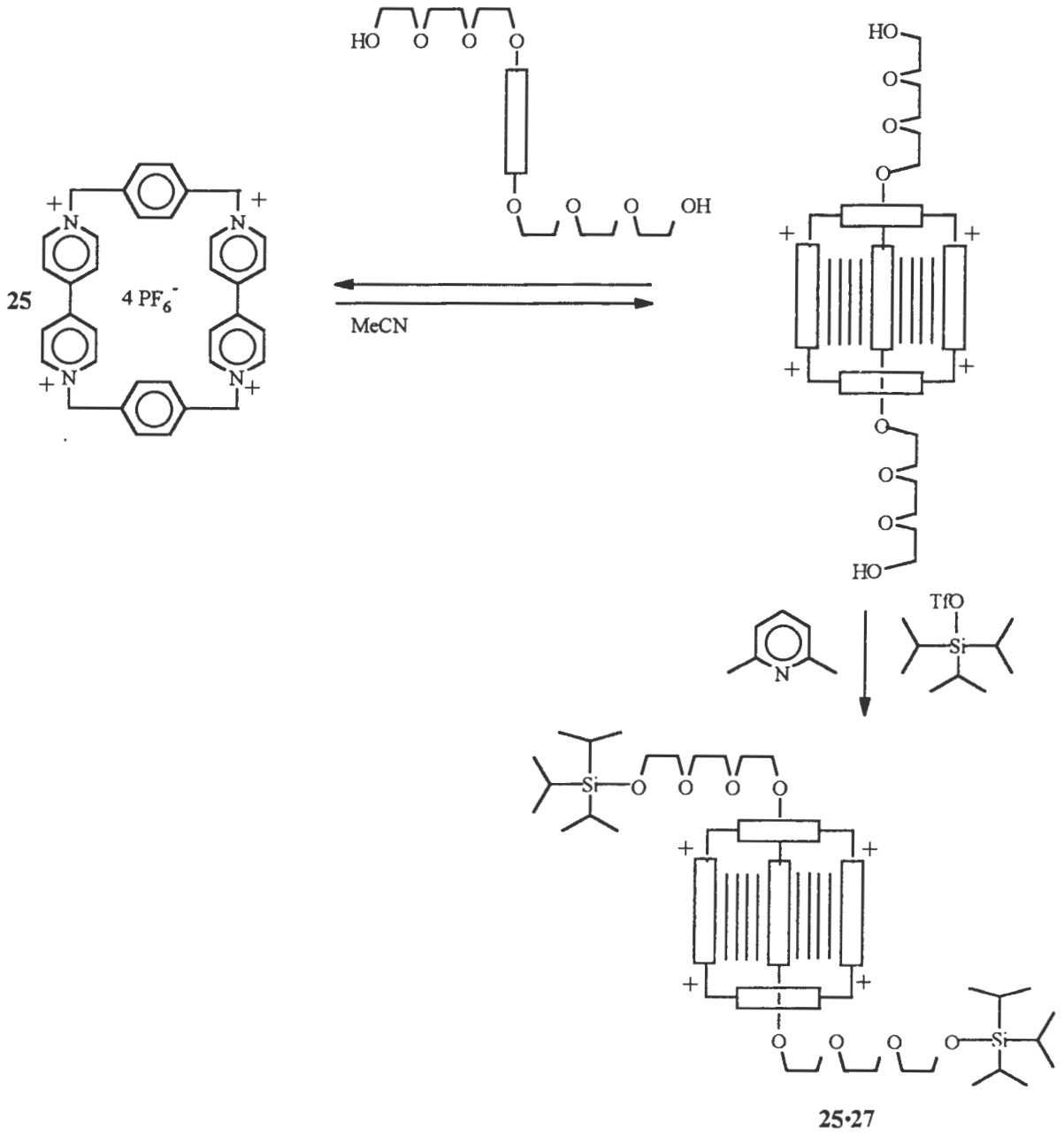

Figure 1.3.9. Synthesis of the rotaxane **25·27** by a *threading procedure*.

Subsequent developments in the synthesis of rotaxanes[20] resulted in the incorporation of the π-acceptor sites in the thread, thus using a charged thread whilst the macrocycle used to give the rotaxane is a crown ether incorporating π-donor sites. An example of such a rotaxane synthesis is given below using intially a *threading procedure* with the macrocycle bis-p-phenylene-34-crown-10 (BPP34C10) and a π-electron deficient thread containing two bipyridinium units (19% rotaxane yield).

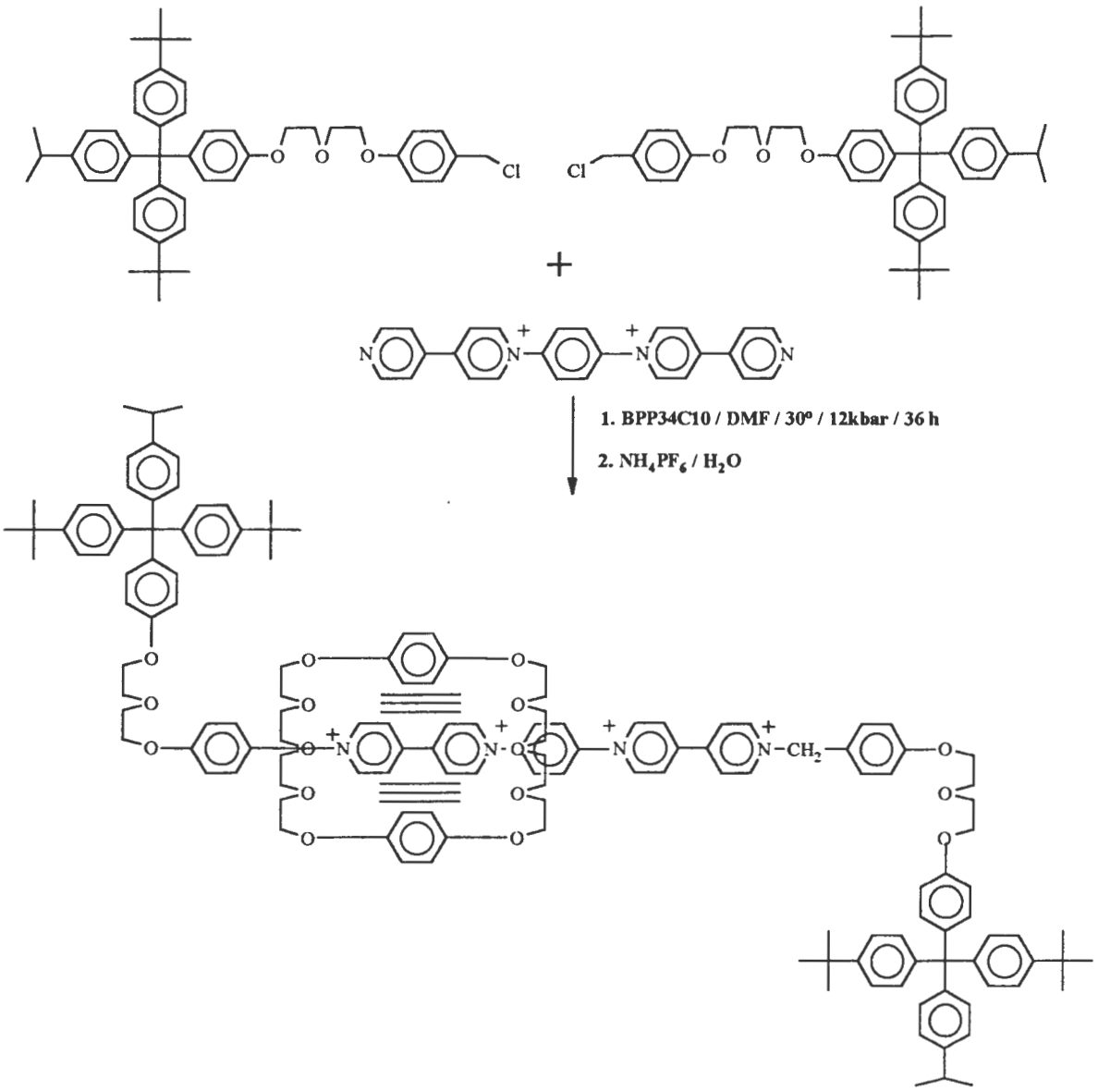

Figure 1.3.10. Synthesis of a rotaxane having a π-acceptor thread and π-donor macrocycle using a *threading procedure*.

A *slipping procedure* was then used to form a 3-rotaxane; the macrocycle, 1,5-dinaptho-38-crown-12 (1/5DN38C10) and the 2-rotaxane were preformed and then

encouraged to associate with one another under exactly the correct ammount of thermal energy. It is interesting to note that the cavity of 1,5-dinaptho-38-crown-12 (1/5DN38C10) is very slightly larger than that of bis-p-phenylene-34-crown-10 (BPP34C10). This was investigated by Stoddart and coworkers[20] and it was found that the yield of a *slipping procedure* was slightly higher for the larger of the two macrocycles.

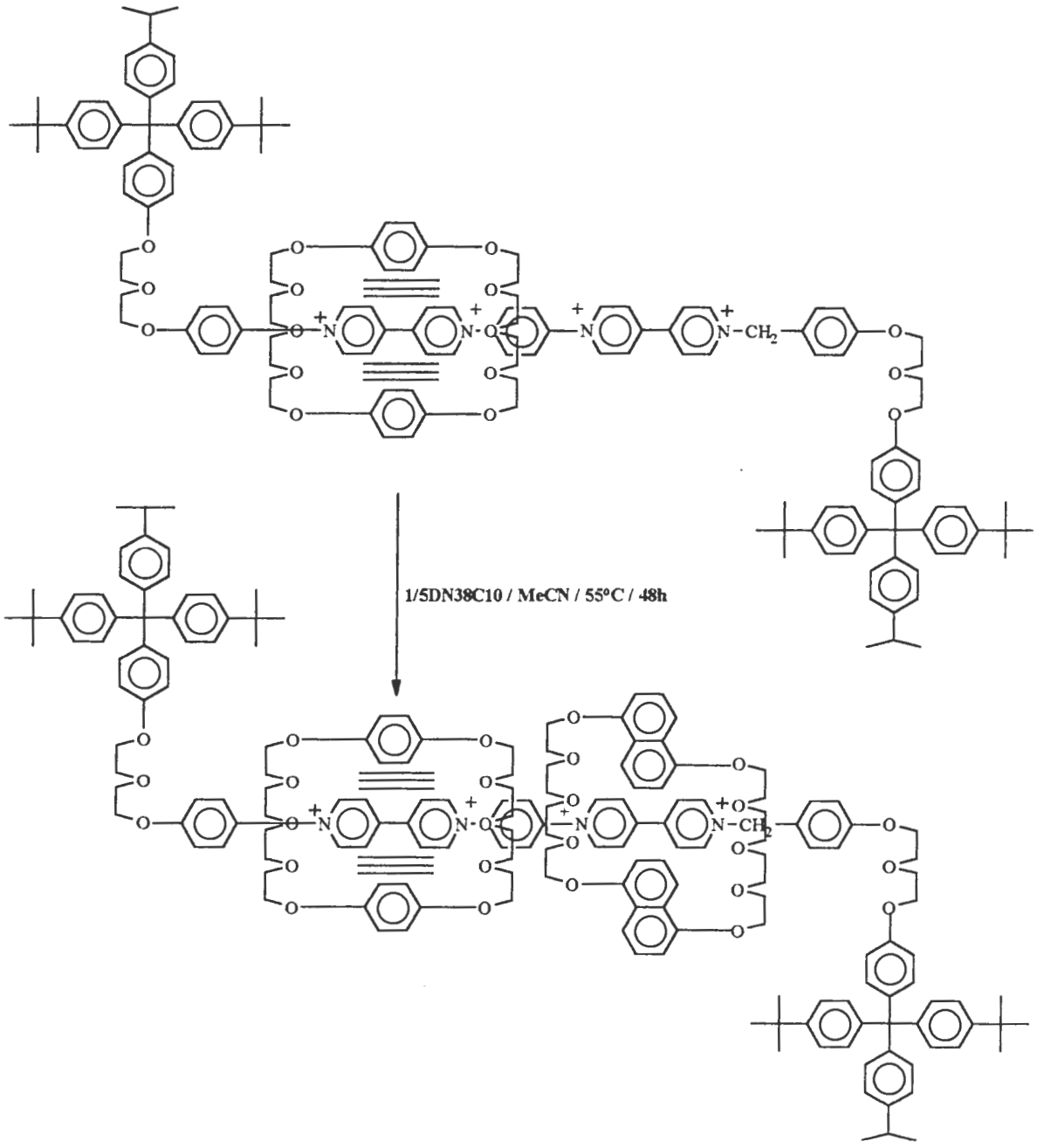

Figure 1.3.11. Synthesis of a 3-rotaxane from a 2-rotaxane by a *slipping procedure*.

These developments led to the synthesis of branched [n]rotaxanes, regarded as the first step towards dendritic rotaxanes[21].

1.4. The synthesis of multimetallic iron and ruthenium systems.

An early publication by King[22] described the preparation of $[(\eta^5\text{-}C_5H_5)Fe(CO)_2]_2(CH_2)_n$ for n = 3 to 6 using the reaction of the salt, $Na[(\eta^5\text{-}C_5H_5)Fe(CO)_2]$ and the respective α, ω-dibromoalkane as shown in equation 1.4.1 below.

Equation 1.4.1.

$$[CpFe(CO)_2]_2 \xrightarrow[THF]{Na\,/\,Hg} Na[CpFe(CO)_2]$$

$$2\,Na[CpFe(CO)_2] + Br(CH_2)_nBr \longrightarrow [CpFe(CO)_2]_2(CH_2)_n$$

King described the properties of these alkanediyl compounds as compatible with the σ-bonded structure of the trimethylene derivative shown below. King characterised these compounds by ^1H NMR, infrared spectroscopy, melting point and molecular mass determinations.

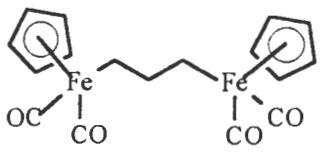

Moss and co-workers[23] subsequently confirmed King's early observation of the σ-bonded structure with the determination of the crystal structures of $[(\eta^5\text{-}C_5H_5)Fe(CO)_2]_2(CH_2)_3$ and $[(\eta^5\text{-}C_5H_5)Fe(CO)_2]_2(CH_2)_4$. The Fe-$CH_2$ bond distance was determined as 2.11 Å. Subsequently Moss and co-workers[24] reported the synthesis of $[(\eta^5\text{-}C_5H_5)Fe(CO)_2]_2(CH_2)_n$ for n = 7 to 12 from the dibromide precursors $Br(CH_2)_nBr$ as shown in equation 1.4.1. above. Comprehensive mass spectral fragmentation pathways were reported on the basis of metastable peaks as well as differential scanning calorimetry traces.

Moss and coworkers[25,26] investigated the reaction of μ(α, ω)-alkanediyl complexes of iron(II) with tertiary phosphines. Moss and Scott[25] reported that the reaction of tertiary phosphines with binuclear alkanediyl compounds proceeds in a stepwise fashion. A kinetic study showed rapid formation of the phosphine-substituted monoacyl species

followed by a sudden change in the reaction rate. The slower reaction of the phosphine- substituted monoacyl with a second equivalent of tertiary phosphine was attributed to the increased steric hindrance of the tertiary phosphine substituted monoacyl product. The rate of reaction was also found to be dependent on the length of the polymethylene bridge, reflecting the decrease in steric hinderance with increased distance between the metal atoms. These reactions are shown below in equation 1.4.2.

Equation 1.4.2.

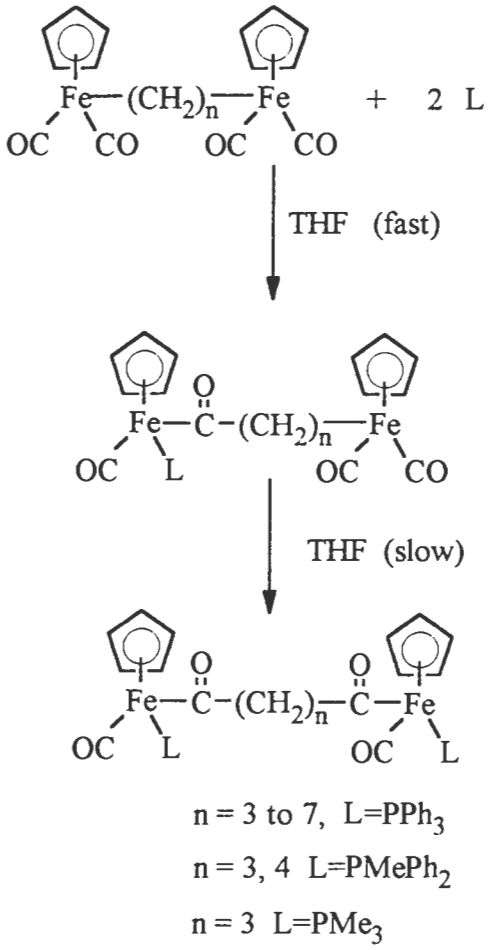

n = 3 to 7, L=PPh_3

n = 3, 4 L=$PMePh_2$

n = 3 L=PMe_3

The NMR spectrum of the disubstitued diacyl product showed a complex multiplet for the four CH_2CO protons. Low temperature NMR studies showed no change in the splitting of the methylene signals. Moss and Scott[25] explained that this splitting pattern resulted from diastereomeric shielding of these protons by the asymetric [CpFe(CO)(L)] groups (where L is the phoshine substituent). The protons in each CH_2CO group are non equivalent and geminal coupling could thus have given rise to the observed multiplet.

Liao[26] showed that $Cp(CO)_2Fe(CH_2)_6Br$ could be reacted with phenol in the presence of base to yield the organometallic alkyl-aryl ether as shown in equation 1.4.3.

Equation 1.4.3.

Moss and Liao[27,28] have since pioneered the synthesis of organometallic dendrimers

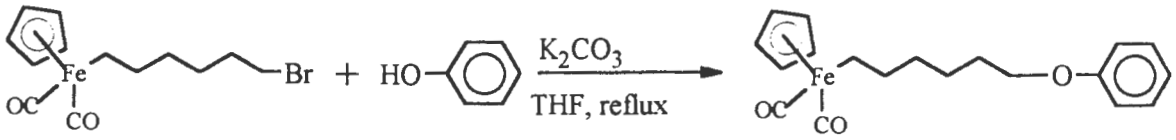

containing ruthenium-carbon σ-bonds. The synthesis of these dendrimers uses the reaction of $Cp(CO)_2Ru(CH_2)_3Br$ with 3,5-dihydroxybenzyl alcohol yielding the binuclear benzyl alcohol compound which is then converted to the benzyl bromide as shown below.

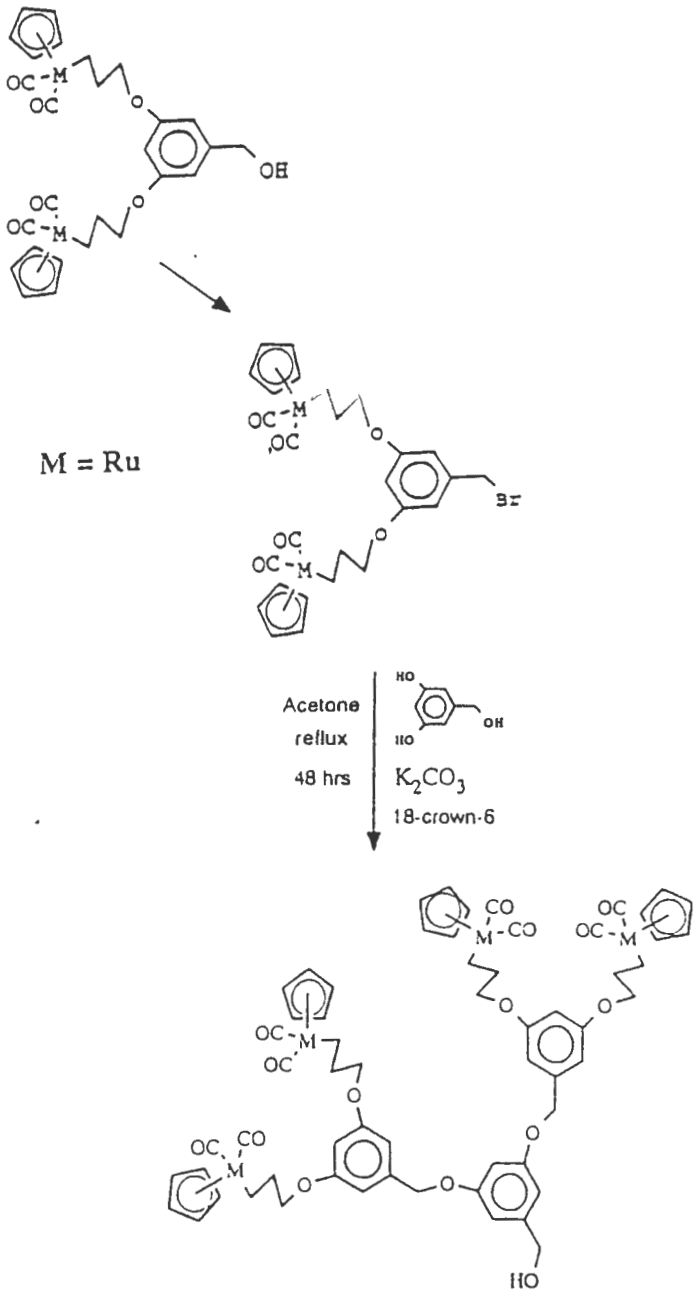

This benzyl bromide was then reacted with 3,5-dihydroxybenzyl alcohol to give the second generation dendritic wedge, which was then converted to the benzyl bromide. This was then further reacted with 3,5-dihydroxybenzyl alcohol to give the third generation dendrimer which was reacted with a trifunctional core to yield a dendrimer having 48 metal atoms[28].

1.5. The significance of an organometallic rotaxane.

In order to classify any specific rotaxane as being an example of an organometallic rotaxane, it is necessary to specify criteria by which organometallic, metalloorganic and organic rotaxanes may be differentiated since examples of all three of these types of rotaxanes may be found in the literature. A recent article[29] by Dagani, considering the relevance of organometallic chemistry in materials science, attempts to distinguish organometallic compounds from metal-organic compounds. The criteria suggested was that for a compound to be organometallic, the metal has to be bonded directly to carbon while for a compound to be metal-organic, the metal must be bound or coordinated to atoms other than carbon, such as oxygen or nitrogen. An organic rotaxane would thus be a rotaxane not containing a metal atom either coordinated or σ-bonded to a carbon atom of the structure.

An X-ray structure of (1,3-xylyl-18-crown-5)diphenylmagnesium[30], **15**, the first organometallic rotaxane found in the literature[30], is shown below. The authors[30] note that the magnesium shows unusual hexacoordination: the magnesium atom is bonded to the carbons of the two phenyl groups, strongly bonded to oxygen atoms 2 and 3 and less strongly bonded to oxygen atoms 1 and 4 as shown below. The Ph-Mg-Ph unit approaches being linear with the C(17)-Mg-C(23) angle of 163.8°. The phenyl groups are not coplanar, instead they are rotated 66° away from each other.

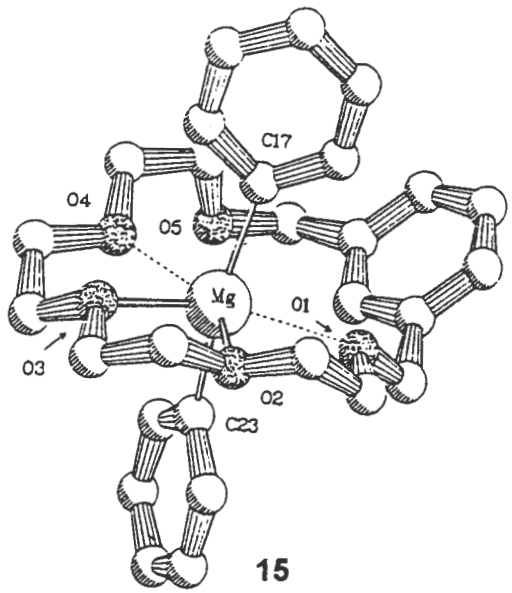

15

Figure 1.5.1. X-ray crystal structure of (1,3-xylyl-18-crown-5)diphenylmagnesium; an organometallic rotaxane.

In discussing the mode of formation of the organometallic rotaxane **15**, the authors[30] note that the cavity of the crown ether is too small to allow a phenyl group of diphenylmagnesium to directly penetrate the crown so the authors postulate that complex formation must therefore occur by dissociation of a phenyl anion, complexation of the resultant Ph-Mg^+ cation by the crown ether followed by recombination of the phenyl anion. To prove this proposed dissociative mechanism, the bridged diaryl magnesium metallocycle **16** was synthesized[31]. Combination of the metallocycle **16** with the crown ether, 1,3-xylyl-18-crown-5, in toluene resulted in the formation of the 2-catenane, **17**, thus proving the dissociative mechanism postulated by the authors[30].

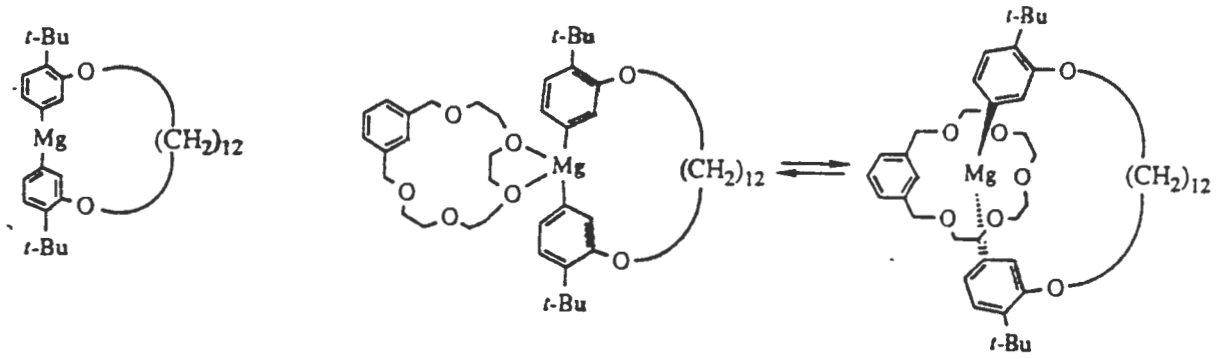

16 **17**

Figure 1.5.2. The bridged diaryl magnesium metallocycle **16** and the organometalic catenane **17** formed by combination of the metallocycle with the crown ether, 1,3-xylyl-18-crown-5.

Benniston and Harriman[32] have synthesized an organometallic rotaxane based on the tetracationic π-acceptor, "bluebox", and a π-donor ferrocene stoppered polyether thread. The thread, **18,** was prepared by the reaction of ferrocenyl carboxylic acid chloride and 1,4-bis[2-{2-(2-hydroxyethoxy)ethoxy}ethoxy]benzene using triethylamine base. The thread was recovered in 62% yield and the rotaxane was isolated in 10% yield. The structural assignments were made by Benniston and Harriman[32] on the basis of X-ray crystallography and ^{1}H NMR spectroscopy.

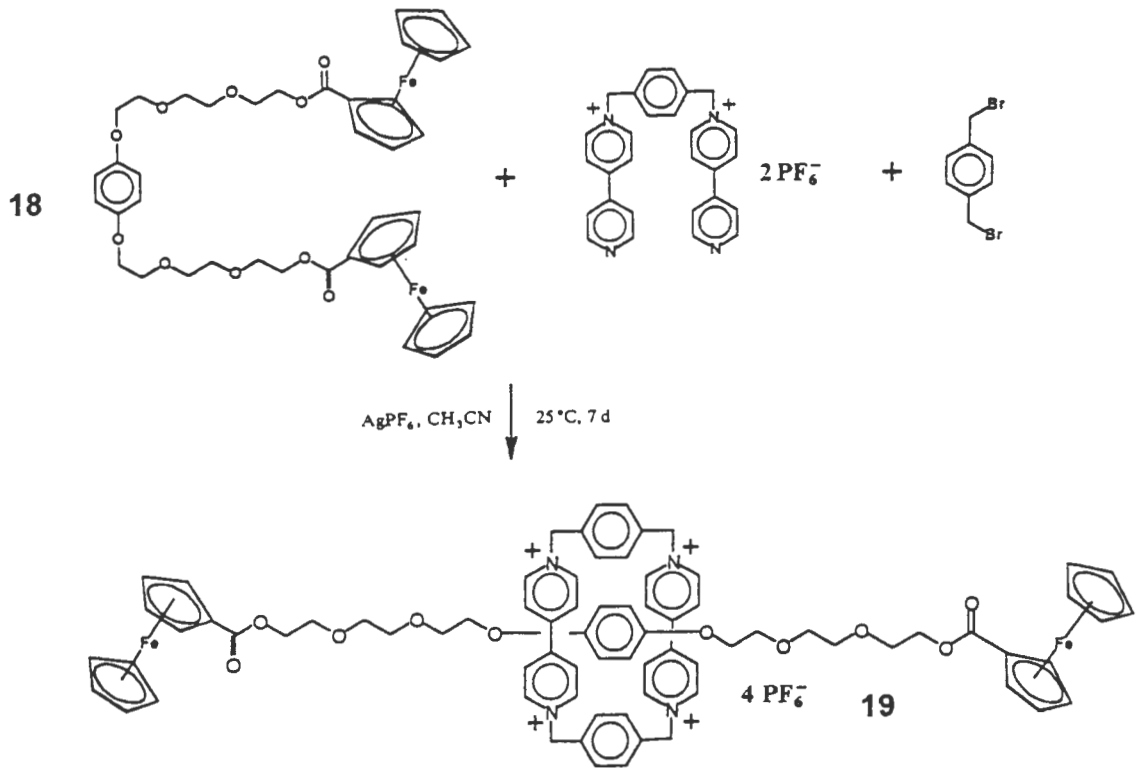

Figure 1.5.3. Synthesis of the organometallic rotaxane, **19**.

Cyclic voltametry studies made of the rotaxane in acetonitrile gave a one-electron redox potential of -0.53V vs the saturated calomel electrode (SCE) for reduction of the tetracationic cyclophane and 0.46 and 1.14V vs SCE respectively for oxidation of the ferrocene and dialkoxybenzene subunits.

Laser flash photolysis of **19** in acetonitrile solution with a 500 fs laser pulse at 437 nm resulted in a single electron transfer from the dialkoxybenzene to the cyclophane. Benniston and Harriman[32] suggested that the resultant radical ion pair is deactivated by charge recombination. However this process was in competition with oxidation of one of the ferrocene stopper groups by the oxidised dialkoxybenzene unit. Thus, the ground state system was reached by electron transfer to the π-radical cation of the cyclophane from the adjacent ferrocinium cation. This electron transfer is comparatively slow, Benniston and Harriman[32] explain that this slow process involves migration of the cyclophane along the thread in order to minimise electrostatic repulsion between the positively charged reactants thus **19** acts as a light-induced molecular shuttle. This photoprocess is shown on the following page.

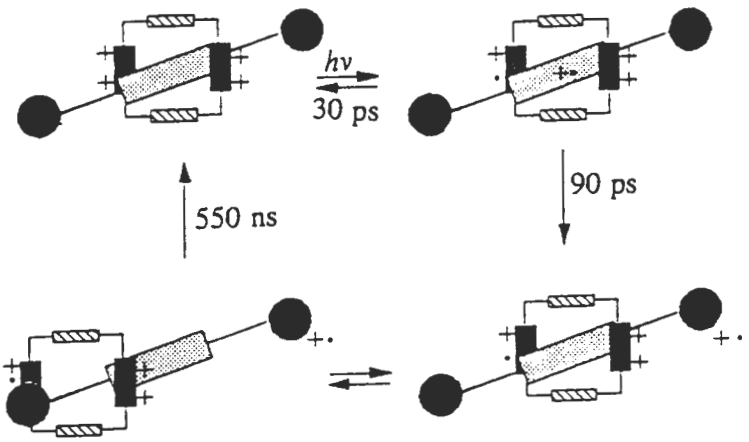

Figure 1.5.4. Laser flash photolysis of **19** and resultant photoprocess.

Further studies by Benniston and Harriman[33] used ^{1}H NMR to show that the rotaxane can exist in different conformations as shown in figure 1.5.5. below. The terminal ferrocene groups can associate with the cyclophane, resulting in folding of the thread to give a closed conformer. In solution, the ferrocene groups may remain free to give an open conformer and the cyclophane, itself, may migrate along the thread.

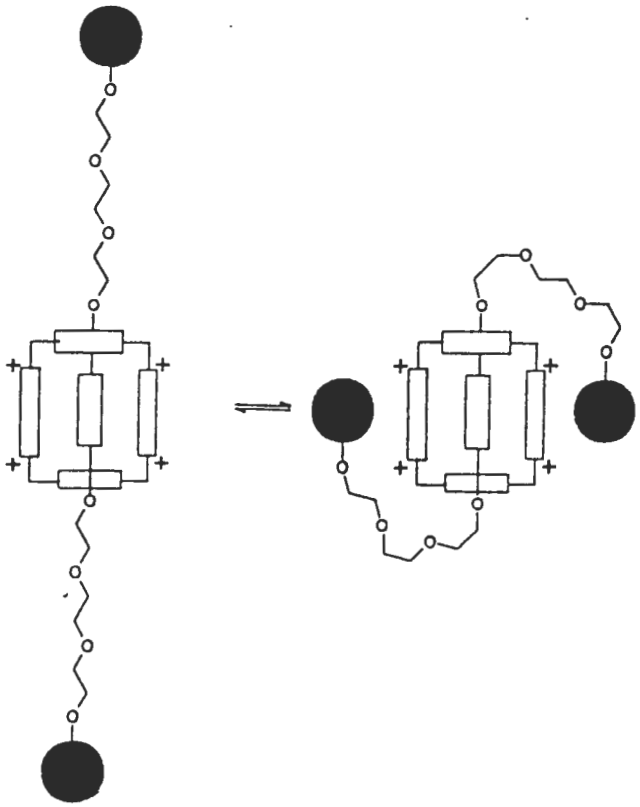

Figure 1.5.5. Open and closed conformations of **19.**

Benniston and Harriman[33] have synthesized a rotaxane, **20**, as shown below, with two π-donor stations which provide for increased migration of the cyclophane along the thread resulting in more complex conformations in solution. The major processes of interest are (i) the oscillation of the cyclophane along the thread, (ii) π-stacking of ferrocene groups with the cyclophane and (iii) π-stacking of the unoccupied π-donor station with the exterior of the cyclophane.

These processes were investigated[33] using low temperature ^{1}H NMR spectroscopy and the conformational exchange processes are shown in figure 1.5.6.

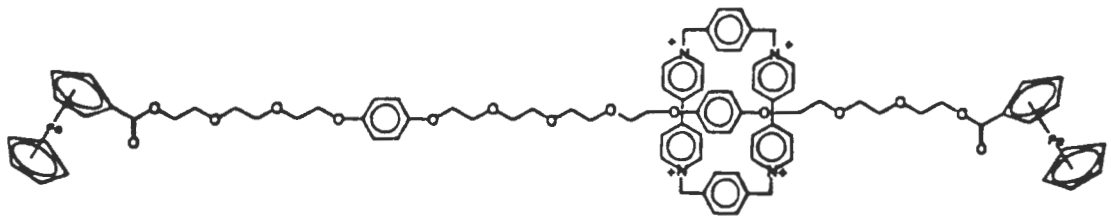

20

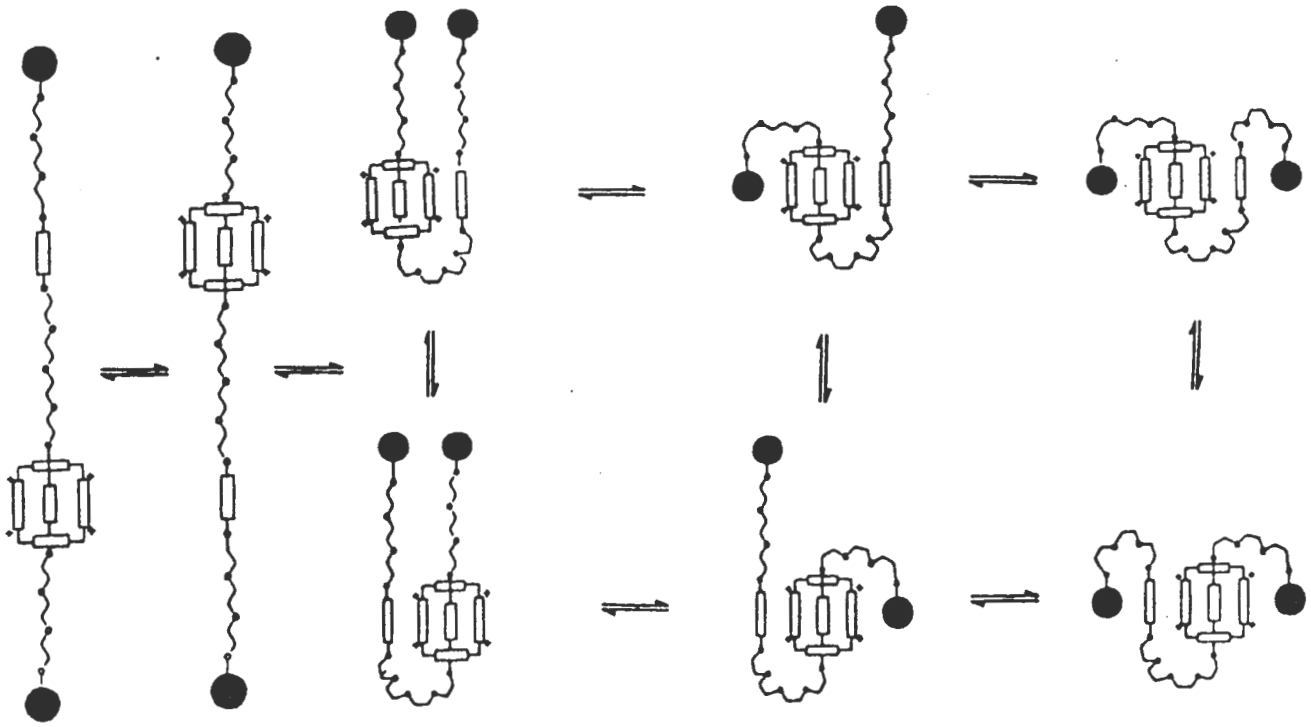

Figure 1.5.6. A rotaxane having two π-donor stations and the associated conformational processes of this molecule.

Benniston and Harriman[33] concluded, that for the one station rotaxane **19** the cyclophane lies preferentially over the central dialkoxybenzene donor. However the cyclophane has hindered migration along the one station thread due to the shortness of the thread and this movement of the cyclophane may be further hindered by the molecule adopting a closed conformation in which the stoppers associate with the cyclophane. For the two station rotaxane, **20**, the cyclophane migrates incoherently along the thread but prefers to reside over one of the dialkoxybenzene donors rather than on the thread itself. The terminal stoppers, because of their aromatic nature, tend to associate closely with the pyridinium ring of the cyclophane which give a closed conformation in which π-stacking extends throughout the molecule. All the structures are dynamic on the NMR time scale. The various conformational changes noted, occur simultaneously, so it is not feasible to try to assign rate constants or activation energies to any specific process.

Chapter 2

The synthesis of μ(1,n)alkanediyl compounds of iron containing a central π-electron donor.

2.1 Introduction.

The synthesis of μ(1,n)alkanediyl iron compounds starting from dihaloalkyl precursors is well documented.[34] The synthesis of binuclear cyclopentadienylirondicarbonyl compounds involves the reaction of the salt, $Na[CpFe(CO)_2]$, with a dihalide, $X(CH_2)_nX$, in THF solution according to equation 2.1

$$2\ Na[CpFe(CO)_2] + X-(CH_2)_n-X \xrightarrow{THF} [CpFe(CO)_2]-(CH_2)_n-[CpFe(CO)_2] + 2NaX \qquad 2.1$$

We used the above route to synthesise μ(1,n)alkanediyl compounds of iron containing a central π-electron donor from a dihalide containing a central hydroquinone group as described below.

2.2 Synthesis of the dihalide precursors.

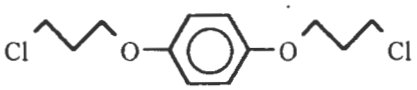

(1)
1,4-Bis (3-chloro-1-propoxy)benzene

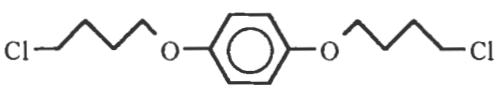

(2)
1,4-Bis (4-chloro-1-butoxy)benzene

The synthesis of the dihalides **1** and **2** is shown in equation 2.2.

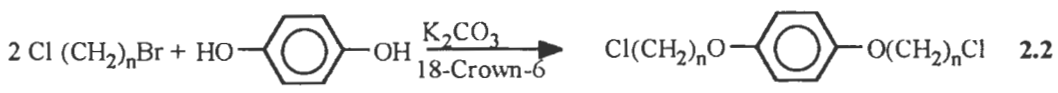

2.2

1: n = 3 (86%)

2: n = 4 (75%)

The synthesis of the dihalides **1** and **2** required hydroquinone to be alkylated with a 1-bromo-n-chloroalkane. In both instances the phenoxide nucleophile displaced the bromide chemoselectively, yielding primarily the dichloride. Thus, potential problems which could have arisen from polymerisation side reactions were avoided. Stoddart and coworkers[18] have used DMF as the reaction solvent for similar intermolecular S_N2 halide displacements. However, ultimately the combination of the lower boiling CH_3CN, and 18-crown-6 to solubilise the K_2CO_3, proved superior for our purposes. The reaction was monitored by thin layer chromatography and when deemed complete, the reaction was quenched by the addition of saturated aqueous ammonium chloride. The crude product was isolated by an ethyl acetate extraction and purified by silica gel chromatography (see experimental section for full details).

Characterization of the dihalides **1** and **2**:

The dihalides **1** and **2** were characterized by ^1H and ^{13}C NMR spectroscopy, infrared spectroscopy, mass spectrometry, elemental analysis and melting point.

2.2.1. ^1H NMR data for compounds **1** and **2**.

The ^1H NMR data for compounds **1** and **2** is summarised in table 2.2.1 below. Compound **1** showed an $A_2B_2X_2$ spin system while compound **2** showed an $A_2B_2M_2X_2$ spin system. The assignments were made by comparison of the spectra with those of similar halogenated alkyl aryl ethers and dihaloalkyl compounds.[35]

The ^1H NMR spectrum of **1** showed a signal at δ3.74 ppm which was assigned to the chloromethylene signal, by comparison with 1,3-dichloropropane, which shows a similar chloromethylene triplet at δ3.71 ppm. The synthesis of compound **1** from hydroquinone and 1-bromo-3-chloropropane yields mainly the dichloride **1**, however, a bromide is also a possible minor product through displacement of the less reactive chloride. The presence of a bromo-adduct, as a minor impurity, was identified by a small triplet in the ^1H NMR spectrum at δ3.60 ppm, similar in chemical shift to the bromomethylene triplet of 1,3-dibromopropane[35]. The signal at δ4.07 ppm was assigned to the oxymethylene signal by comparison with the spectrum of 3-phenoxypropyl bromide[35] which shows an oxymethylene triplet at δ4.05 ppm.

Compound **1** showed an upfield quintet at δ2.21 ppm which was assigned to the central methylene connecting the chloromethylene and oxymethlene groups, by comparison with 1,3-dichloropropane which shows a similar quintet at δ2.20 ppm. The ^{1}H NMR spectrum of **2** was assigned by similar comparisons and by analogy to **1**. The ^{1}H NMR spectrum of **1** is shown overleaf.

Table 2.2.1 ^{1}H NMR data for compounds **1** and **2**[a].

Compd.	δ_H-OC$_6$H$_4$O-	δ_H -OCH$_2$	δ_H -CH$_2$Cl	δ_H-CH$_2$-
1	6.84, s, (4H)	4.07, tr, (4H) ^{3}J= 5.88 Hz	3.74, tr, (4H) ^{3}J= 6.40 Hz	2.21, q, (4H) ^{3}J= 6.16 Hz
2	6.82, s, (4H)	3.95, tr, (4H) ^{3}J= 5.84 Hz	3.62, tr, (4H) ^{3}J= 6.31 Hz	1.94, m, (8H)

a: in $CDCl_3$ relative to TMS (δ_H= 0.00 ppm), tr = triplet, s = singlet, q = quintet, m = multiplet.

2.2.2 ^{13}C NMR data for compounds **1** and **2**.

The ^{13}C NMR data for compounds **1** and **2** is given in Table 2.2.2 below.

The chloropropoxy group of compound **1** gives three distinct carbon signals, while the chlorobutoxy group of compound **2** gives four distinct methylene signals. For both compounds there are two separate signals for the six carbons of the aromatic ring, a less intense downfield resonance for the two para related oxygen substituted and a more intense upfield resonance for the four hydrogen substituted carbons.

Table 2.2.2 ^{13}C NMR assignments for compounds **1** and **2**[b].

Compd.	δ_C CH$_2$	δ_C CH$_2$Cl	δ_C OCH$_2$	δ_C CH (Ar)	δ_C OC (Ar)
1	32.4	41.5	65.0	115.5	153.0
2	26.7, 29.3	44.7	67.6	115.4	153.1

b: in $CDCl_3$ relative to $CDCl_3$ (δ_C= 77.0 ppm)

Figure 2.2.1 The ^{1}H NMR spectrum of **1**.

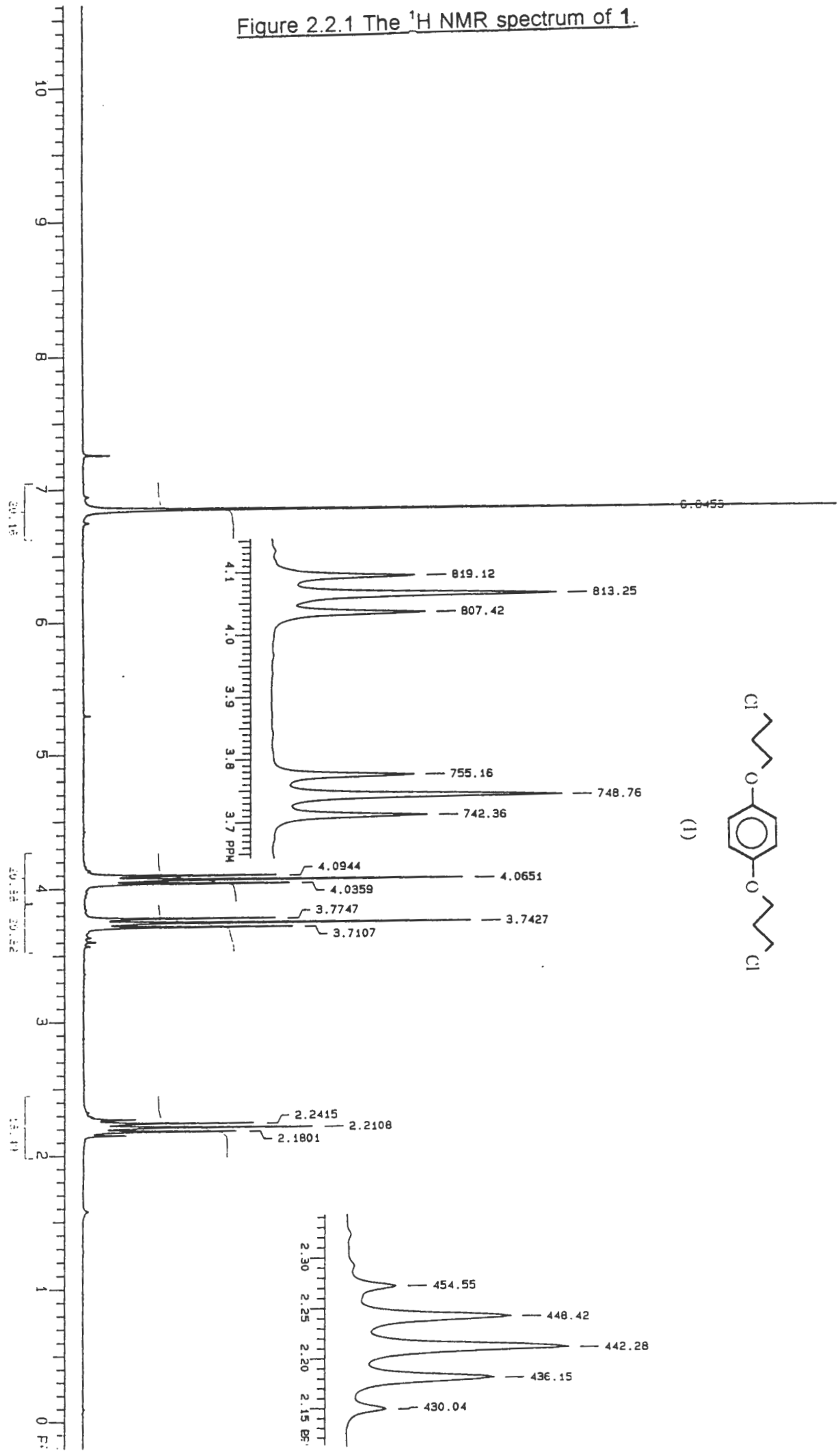

(1)

2.2.3. Mass spectrometry and elemental analysis.

The mass spectral fragmentation patterns for compounds **1** and **2** involve the loss of the chloroalkyl side chains and are shown below. The molecular ions of the dihalides **1** and **2** were seen at m/e = 262 and m/e = 290 respectively.

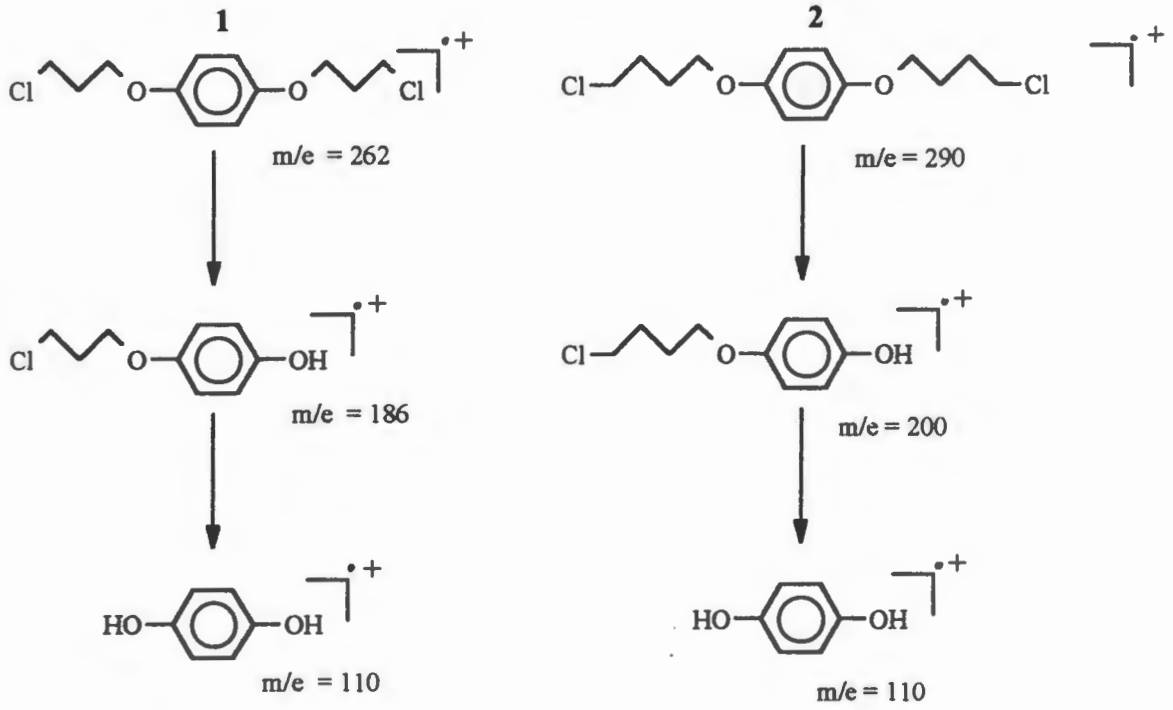

Figure 2.2.3. Mass spectral fragmentation patterns for **1** and **2**.

The elemental analysis results and melting points are tabulated in Table 2.3 below.

Table 2.3 Elemental analysis and melting points for the dihalides **1** and **2**.

Compound	Element	Calculated %	Found %	Melting point °C
1	C H	54.8 6.13	54.6 6.17	65 - 66
2	C H	57.7 6.92	57.2 6.97	75 - 77

2.3. Synthesis of μ(1,n)alkanediyl di-iron compounds having a central π-electron donor.

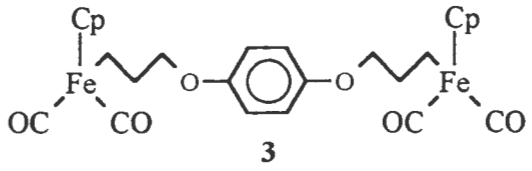

3

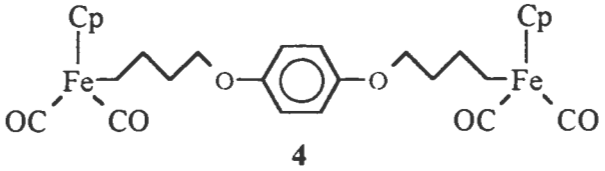

4

With the dihalides, **1** and **2**, in hand the above iron compounds were synthesised according to equation 2.3.

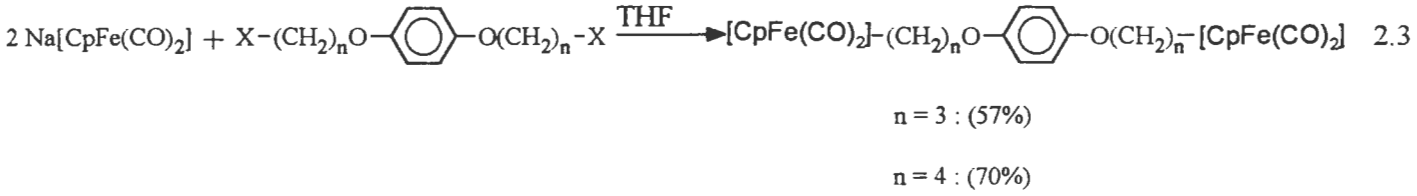

2.3

$Na[CpFe(CO)_2]$ was prepared by reducing the dimer, $[CpFe(CO)_2]_2$, over sodium amalgam.[34] The reaction of $Na[CpFe(CO)_2]$ with the relevant dihalide was initially kept at 0°C for one hour after which time the reaction mixture was allowed to equilibrate to room temperature; allowing a total reaction time of 12 hours. Both compounds **3** and **4** were isolated as golden yellow crystalline solids. Thin layer chromatographic investigations showed that the red coloured dimer, $[CpFe(CO)_2]_2$, could not be separated readily from the product using column chromatography. Thus compounds **3** and **4** were recrystallised from cold hexane with moderate yields. Yields: 57% for **3** and 70% for **4**.

Characterization of the diiron compounds **3** and **4**.

The new diiron products **3** and **4** were fully characterized by ^1H and ^{13}C NMR spectroscopy, infrared spectroscopy, mass spectrometry, elemental analysis and melting point.

2.3.1. ^{1}H NMR data for products **3** and **4**.

The ^{1}H NMR data for products **3** and **4** is summarised in Table 2.3.1 below.

The assignments for the diiron products **3** and **4** were made by comparison with the dihalide precursors and with reference to NMR data of haloalkyl complexes of iron[36], particularly $CpFe(CO)_2(CH_2)_3Br$.[36] The spectrum of the diiron product **3**, shows a pronounced upfield shift of the methylene group α to the iron, at δ 1.44 ppm, relative to the spectrum of the dihalide precursor **1.** The methylene β to iron, at δ 1.89 ppm, is also shifted upfield slightly. This observed upfield shift of the α and β methylene protons of this iron alkyl system, relative to the downfield methylene shifts of the more electronegative dihalide precursor, is indicative of the electropositive (shielding) nature of the iron(II) centre.

Similarly, the spectrum of **4** shows upfield shifts. However, the resonances for the methylene groups α and β to iron coalesce to form a broad multiplet resonating at δ 1.52 ppm while the signal of the methylene γ to iron is a distinct quintet at δ 1.78 ppm. The resonance of the methylene group γ to iron in $CpFe(CO)_2(CH_2)_4Br$[36] is part of a multiplet, indistinct from the α and β signals which in comparison to the diiron product **4** indicates that the aryloxy group of **4** has a far stronger inductive withdrawing effect than a bromine atom. Both compounds **3** and **4** show triplets for the aryloxy methylene signals and sharp singlets for the pentahaptocyclopentadienyl signals.

The ^{1}H NMR spectra of products **3** and **4** are given overleaf.

Table 2.3.1 ^{1}H NMR data for diiron products **3** and **4**.

Compd.	δ-OC$_6$H$_4$O-	δ_HC$_5$H$_5$	δ_H-OCH$_2$	δ_H-CH$_2$-	δ_H-CH$_2$-Fe
3	6.82, s, (4H)	4.76, s, (10H)	3.84, t, (4H) ^3J =6.7 Hz	1.89, m, (4H)	1.44, m, (4H)
4	6.83, s, (4H)	4.74, s, (10H)	3.91, t, (4H) ^3J= 6.4 Hz	1.78, q, (4H) ^3J= 6.2 Hz	1.52, m, (8H)

Figure 2.3.1 ^{1}H NMR spectrum of the diiron product **3.**

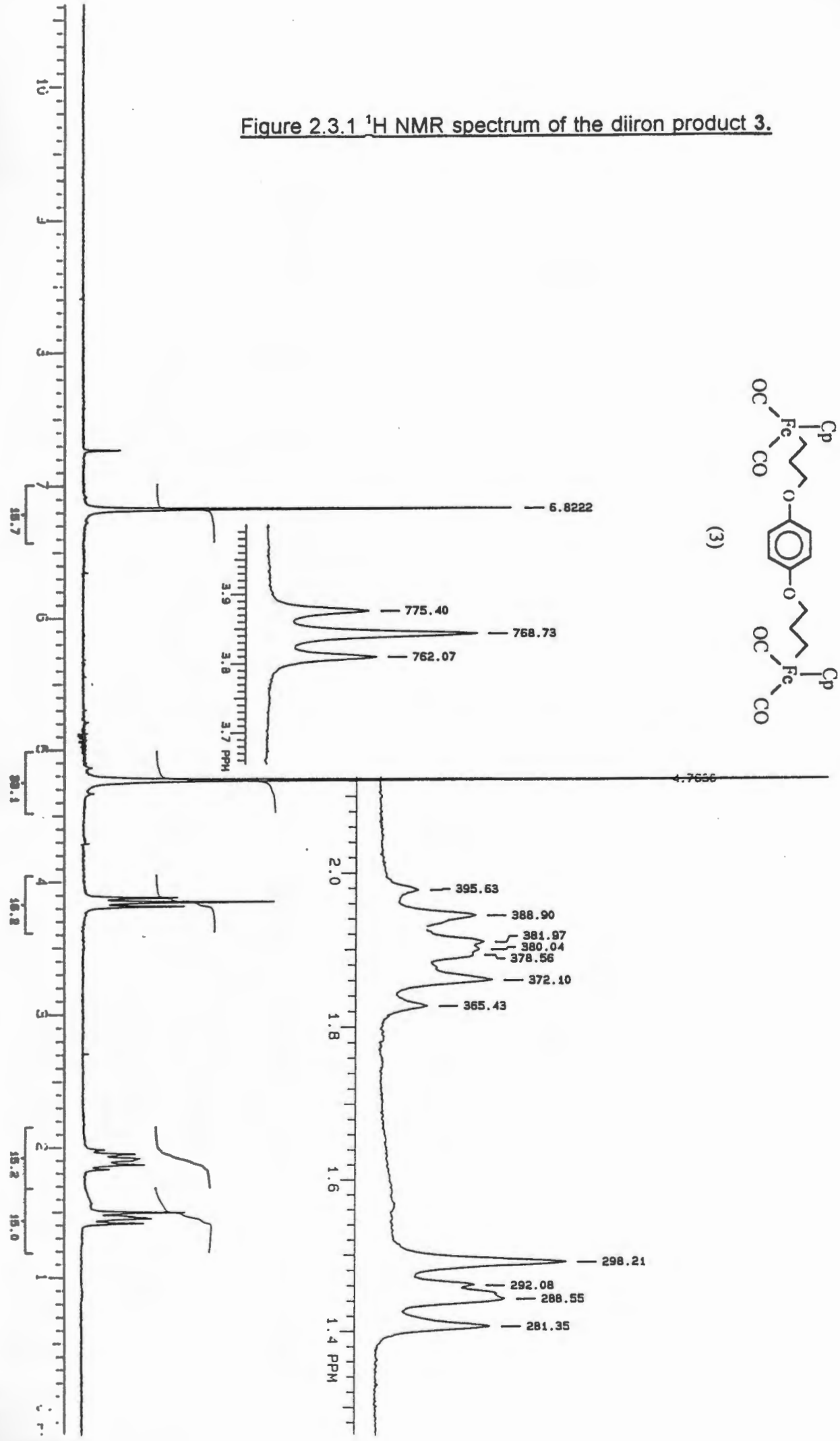

Figure 2.3.2. ^{1}H NMR spectrum of the diiron product **4**.

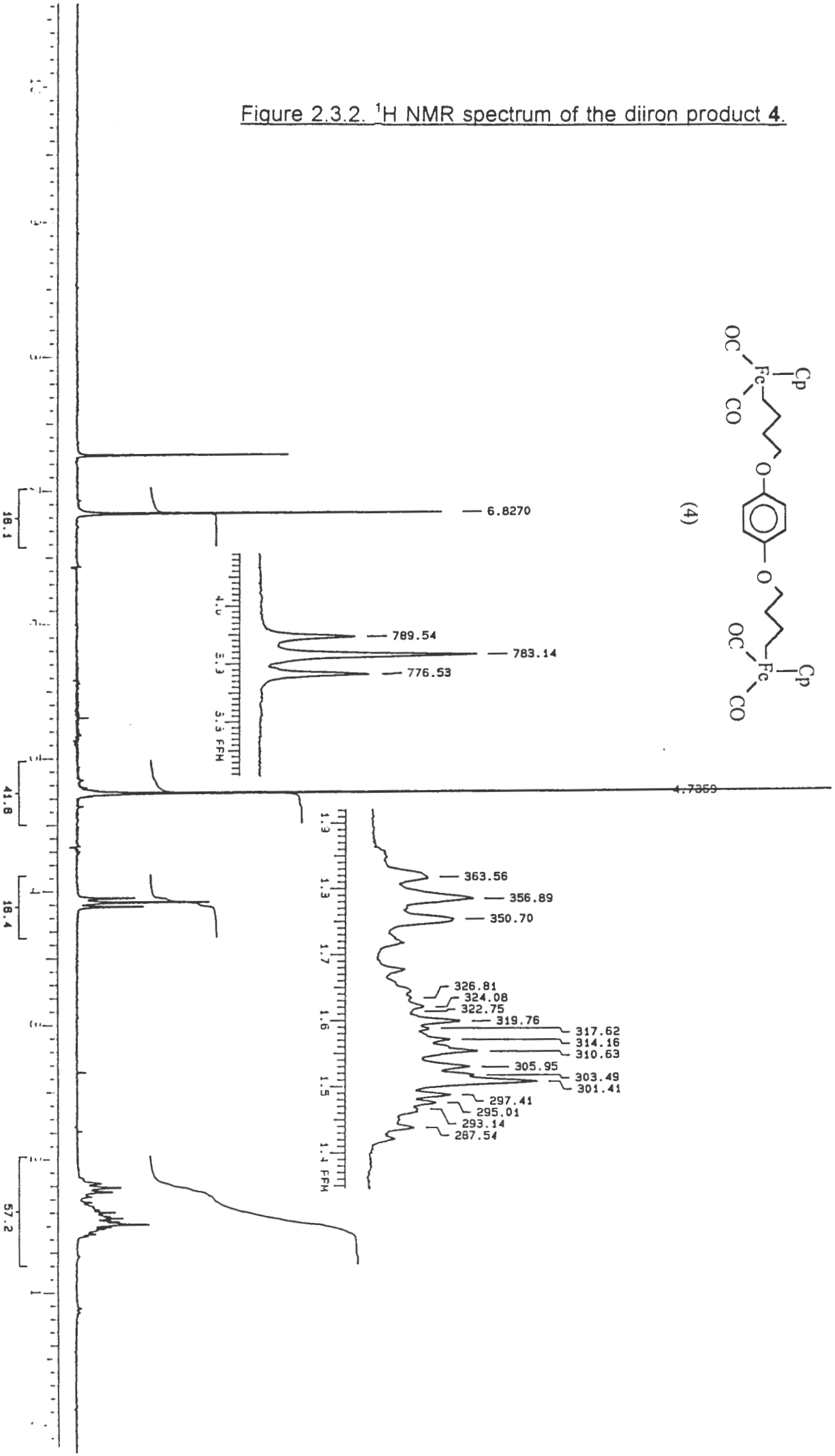

2.3.2 ^{13}C NMR data for compounds **3** and **4**.

The ^{13}C NMR data for compounds **3** and **4** is summarised in Table 2.3.2.

The ^{13}C NMR spectra of **3** and **4** were assigned by comparison with spectra of halogenoalkyl complexes of iron[37] and spectra of the dihalide precursors **1** and **2**. Inductive release from iron causes the carbon of the methylene group α to iron to resonate upfield while the shifts of the remaining carbons are analogous to those of the dihalide precursors. This agrees with the observed shielding effect of the iron centre observed in the ^{1}H NMR spectrum.

Table 2.3.2 ^{13}C NMR data for diiron products **3** and **4**.

Compd.	$\delta_C\underline{C}H_2Fe$	$\delta_C\underline{C}H_2$	$\delta_C O\underline{C}H_2$	$\delta_C\underline{C}_5H_5$	$\delta_C\underline{C}H$ (Ar)	$\delta_C\underline{C}O$ (Ar)	$\delta_C\underline{C}O$
3	-2.4	37.3	71.5	85.4	115.4	153.2	217.3
4	2.8	34.2, 34.3	68.3	85.3	115.5	153.2	217.6

2.3.3 Mass spectrometry.

The mass spectra of compounds **3** and **4** exhibit peaks characteristic of compounds containing the $[CpFe(CO)_2]$ group[37]. In both cases the highest m/e peak observed was $[M-2CO]^+$. The fragmentation pattern of **3** is shown below.

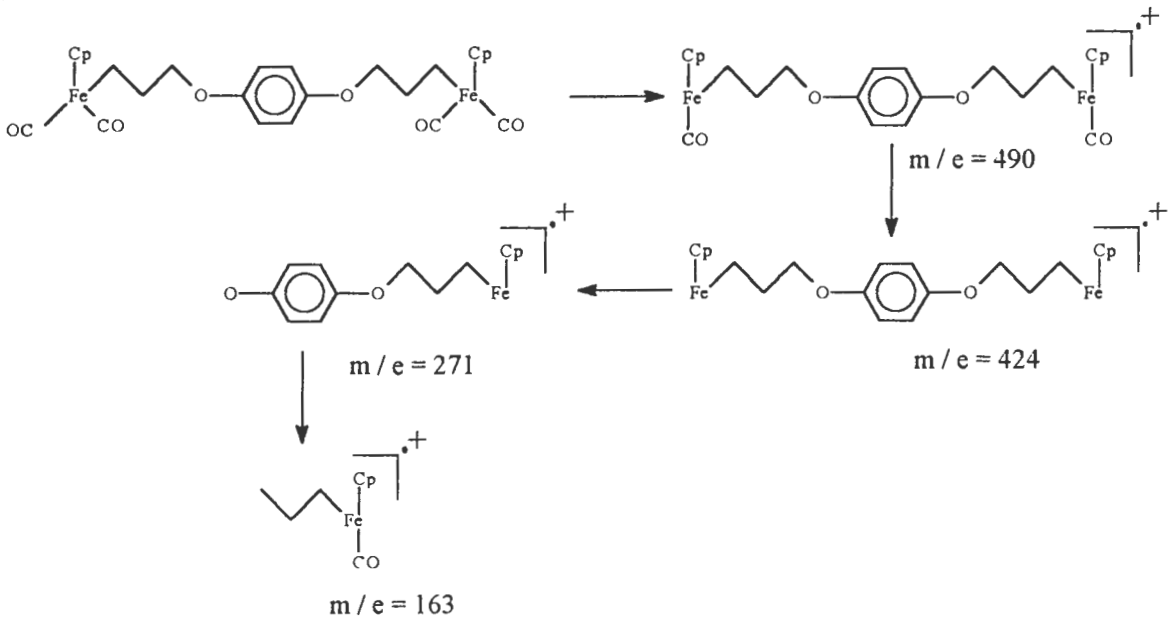

Figure 2.3.3. Mass spectral fragmentation pattern of **3**.

2.4. Synthesis of bis(triphenylphosphine)diacyldiiron systems[38]; derivatization of **3**.

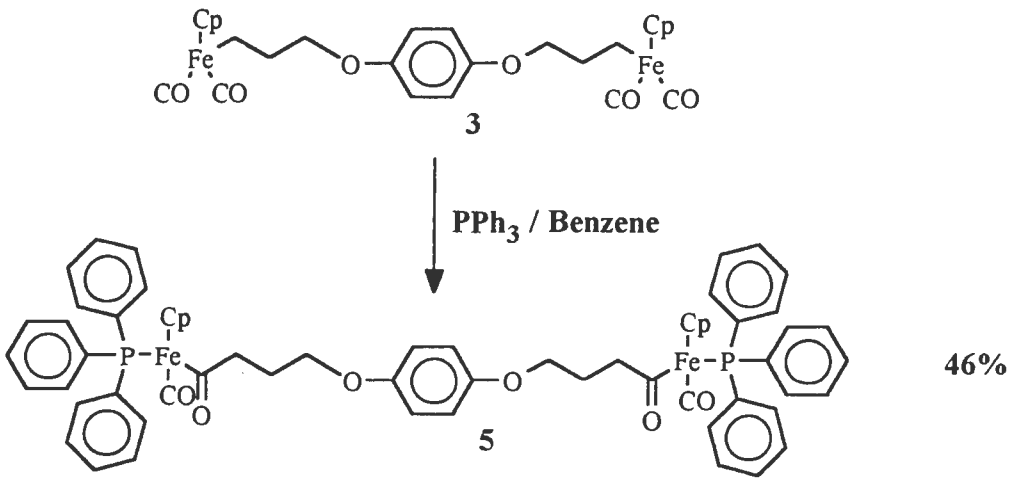

Equation 2.4. Synthesis of **5**.

Compound **3** was reacted with 2.0 equivalents of triphenylphosphine for 6 hours in refluxing benzene (equation 2.4.). The solvent was removed under reduced pressure which yielded a viscous brown oil which was chromatographed on an alumina column. Gradient elution initially eluted unreacted starting materials (established by thin layer chromatography) followed by a polar yellow band. The product **5** was isolated in 46% yield and characterized as the bis(triphenylphoshine)diacyldiiron compound **5**.

Characterization of the bis(triphenylphosphine)diacyldiiron product **5**.

Product **5** was characterized by ^{1}H and ^{13}C NMR spectroscopy, infrared spectroscopy, elemental analysis and melting point.

Each iron atom of **5** is chiral, and together with the mirror plane of symmetry, results in the possibility of obtaining two diastereomers, one of which is meso and the other racemic. Similar chiral iron acyl complexes have been studied and have found use as chiral auxilliaries in organic synthesis[39]. Consideration of the spectral data suggests that **5** exists as two unique diastereomers which we were unable to separate. The stereochemistry of similar bis(triphenylphosphine)diacyldiiron systems were noted by Davidson and Martinez[40] to consist of diastereomerically related pairs of enantiomers. A and A' are enantiomeric and are diastereomeric with B/B' which are a meso compound. This meso compound is proven to be meso using a mirror plane as shown in Figure 2.4.1 below.

Figure 2.4.1.

Diagrammatic representation of the two possible diastereoisomers (A, A', and B) of compound **5** and the internal symmetry plane showing that B is a meso compound.

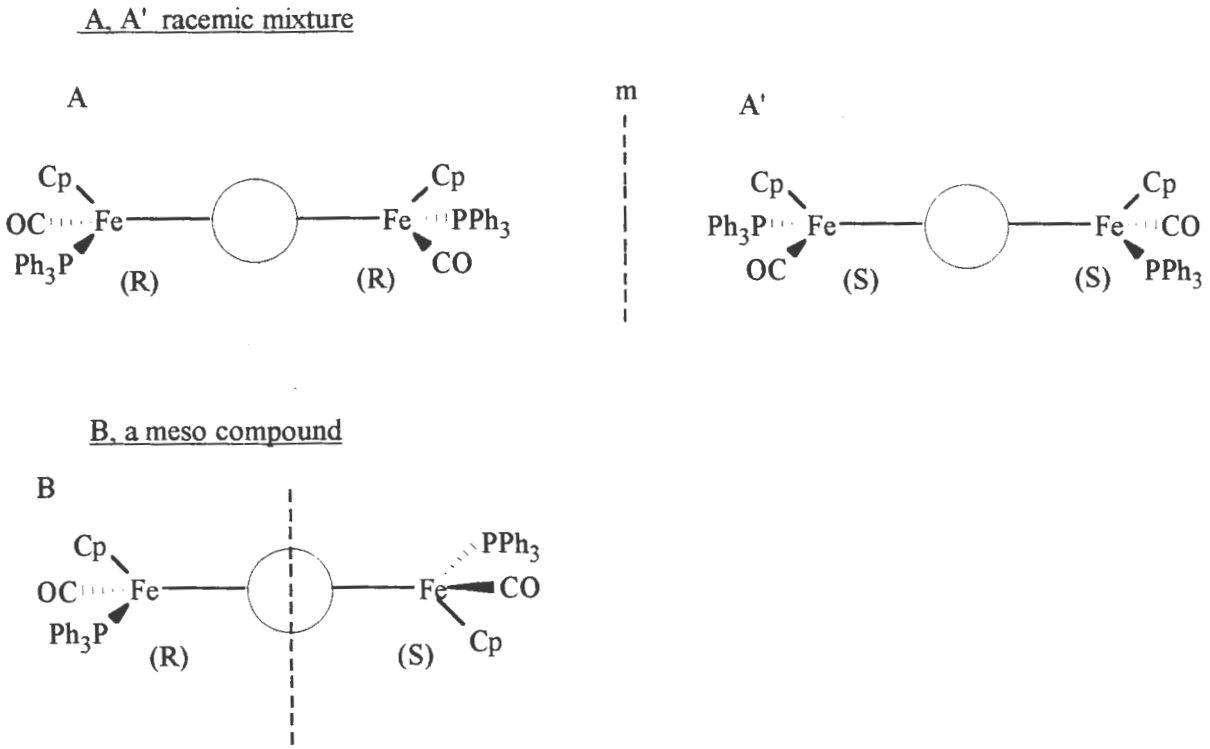

2.4.1 ^{1}H NMR spectroscopy:

The ^{1}H NMR data is summarised in table 2.4.1.

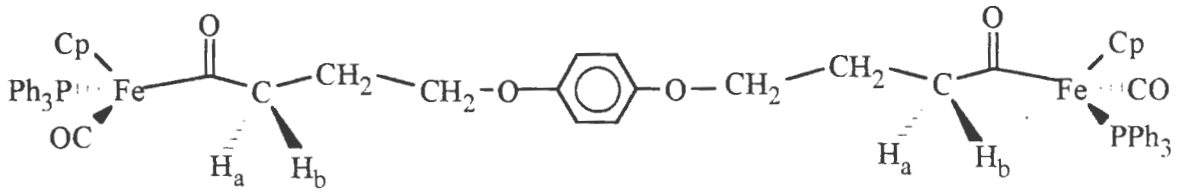

The most important resonances in the ^{1}H NMR spectrum of **5** are the set of diastereotopic signals at δ 2.71 ppm and δ 3.05 ppm for the protons α to the carbonyl group ($H_a$and H_b) as shown above. Both resonances appear as a doublet of triplets

resulting from geminal coupling (J = 17 Hz) and vicinal coupling (J = 7 Hz) as shown in the splitting diagram below. From a synthetic standpoint, it may be assumed that each resonance corresponds to a 50 : 50 mixture of the two diastereomers (racemic and meso), since the possibility of remote asymmetric induction is small. Further evidence for this view is found in the ^{13}C NMR spectrum and is discussed in the following section.

Figure 2.4.2. Splitting diagram for H_a / H_b couplings.

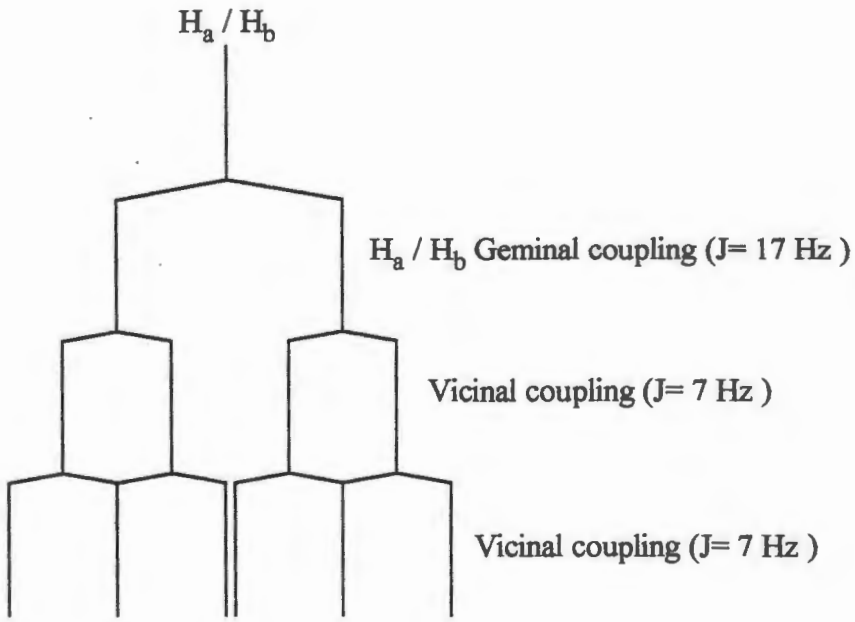

Table 2.4.1 ^1H NMR data for product **5**.

Compd.	$\delta_H P(C_6\underline{H}_5)_3$	δ_H-$OC_6\underline{H}_4O$-	$\delta_H C_5\underline{H}_5$	$\delta_H OC\underline{H}_2$	δ_H-$C\underline{H}_2CO$	δ_H-$C\underline{H}_2$-
5	7.45, m, (30H)	6.72, s, (4H)	4.49, s, (10H)	3.55, m, (4H)	2.71, dt, (2H) 3.05, dt, (2H)	1.55, m, (4H)

Figure 2.4.3. ^{1}H NMR spectrum of the bis(triphenylphosphine)diacyldiiron product, **5**.

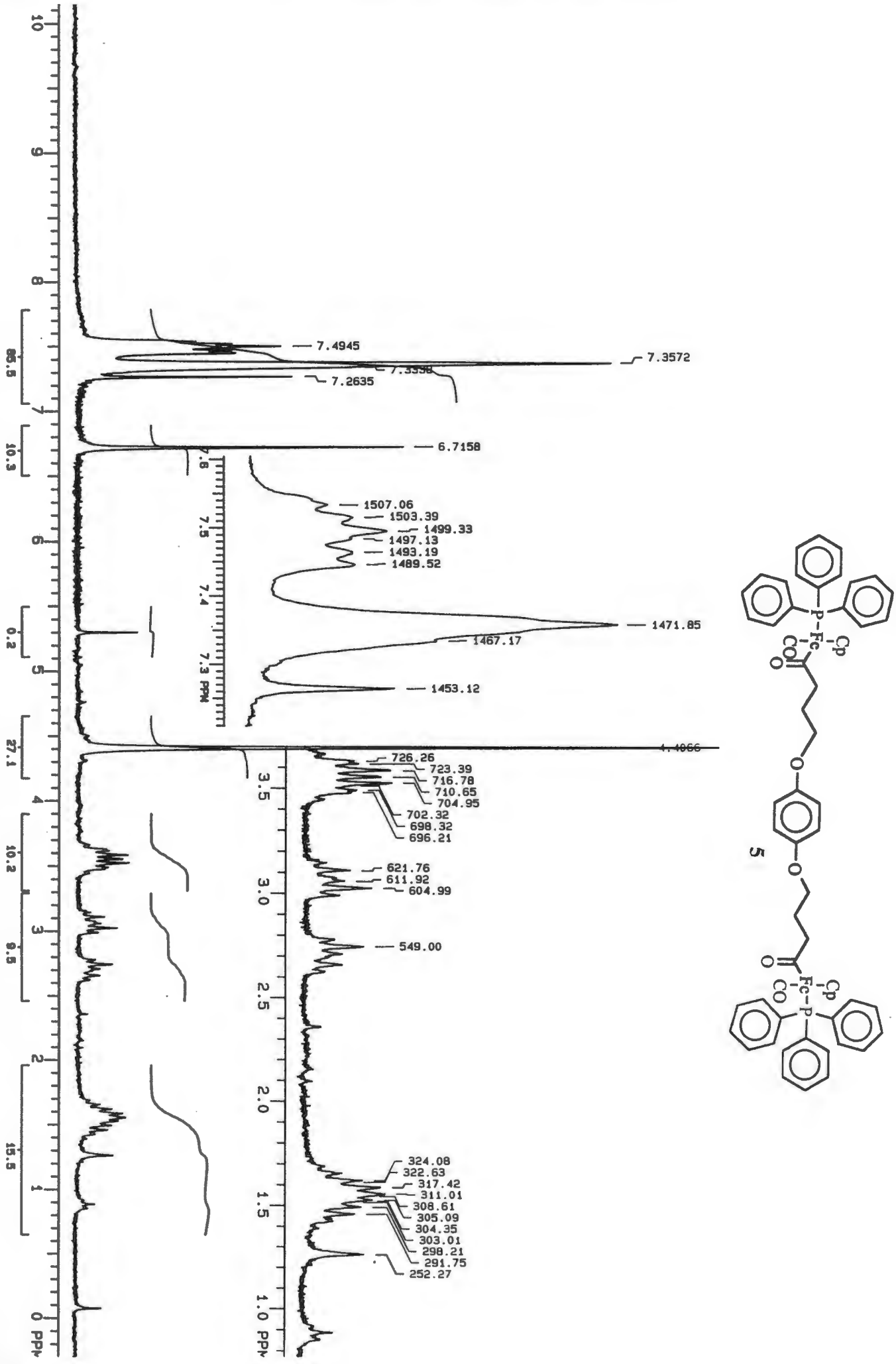

2.4.2 ^{13}C NMR spectroscopy:

The ^{13}C NMR spectrum of **5** was assigned by comparison with the spectrum of **3**, the diiron precursor. The ^{13}C NMR spectrum of **5** shows evidence for the existence of two diastereomers; the methylene α to the iron acyl group gives two separate resonances, at δ 61.67 ppm and δ 61.78 ppm. The carbonyl signals are inconclusive since there appears to be two separate resonances however only one of these two resonances is sufficiently intense to be above the detection limit. The triphenylphosphine signal shows three doublets due to carbon-phosphorous coupling and one singlet; the carbon-phosphorous coupling constant decreases with carbon to phosphorus distance. The triphenylphosphine signal is assigned as follows: δ_C136.4($^1J_{C\text{-}P}$43Hz,), 133.3($^2J_{C\text{-}P}$9.9Hz, ortho carbon), 128.0($^3J_{C\text{-}P}$9.6Hz, meta carbon), 129.7 (para carbon).

Table 2.4.2 ^{13}C NMR data for product **5**.

Compd	$\delta_C\underline{C}H_2$	$\delta_C\underline{C}H_2CO$	$\delta_CO\underline{C}H_2$	$\delta_C\underline{C}_5H_5$	$\delta_C\underline{C}H(Ar)$	$\delta_CP(Ph_3)$	$\delta_C\underline{C}O(Ar)$	$\delta_C\underline{C}O$
5	24.86	61.67, 61.78	68.04	85.19	115.30	127.92 - 136.86	153.01	220.23

Chapter 3

The synthesis of Organometallic Polyethers:

3.1. Introduction.

Polyether threads having a central π-donor are well known in the rotaxane literature.[41] The synthetic challenge was to establish a procedure by which iron-carbon sigma bonds could be linked to polyethers to give a stable organometallic polyether thread suitable for the synthesis of an organometallic rotaxane using organometallic systems such as those outlined in section 1.4 of Chapter 1. A potential problem of which we were aware, was that the iron nucleophile, in the form of the salt, $Na[CpFe(CO)_2]$, may cleave the polyether thread by displacing the phenoxide thus forming a β-alkoxy iron species. Thus, from the outset, we were aware that the leaving group to be used in the metalation step should be highly labile so that the iron nucleophile would chemoselectively displace the leaving group and not cleave the polyether thread.

3.2. Initial Experiments.

Initially, a model alkylation was carried out using the known[41] polyether diol thread, **6**, 1,4-bis[2-(2-hydroxyethoxy)ethoxy]benzene. Bromination of this diol gave the dibromide **7**, 1,4-bis[2-(2-bromoethoxy)ethoxy]benzene in 86% yield as shown in the reaction scheme 3.2.1 overleaf This dibromide, **7**, was isolated as a glassy matrix.

Reaction of $Na[CpFe(CO)_2]$ with this dibromopolyether in THF at 0°C, shown in scheme 3.2.1 overleaf, gave a non-polar organometallic product which was chromatographed on alumina and eluted readily as a yellow band with an eluent of 10% dichloromethane in hexane.

The ^1H NMR spectrum showed no phenyl signal indicating that the polyether thread had been cleaved by the iron nucleophile.

It was therefore decided to reconsider the way in which we linked the iron-carbon sigma bond to the polyether thread to optimise the possibility of efficient coupling.

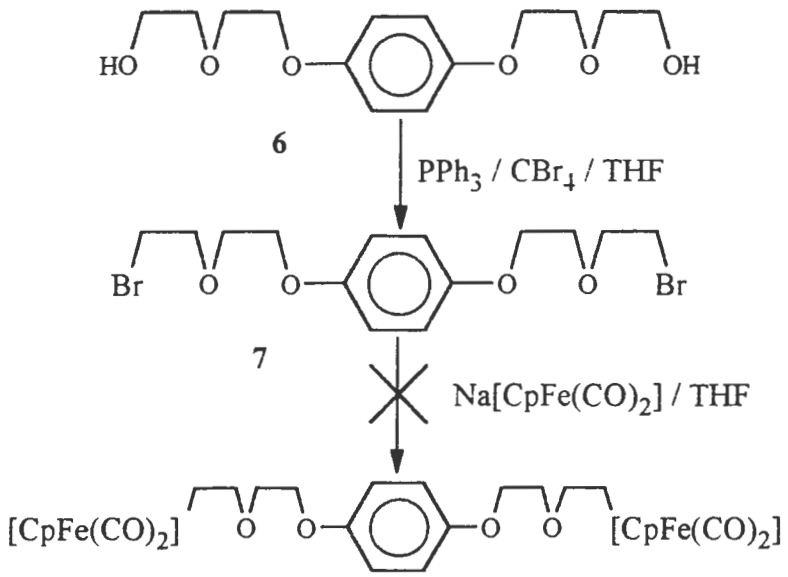

Scheme 3.2.1. Synthesis of **7** and reaction with $Na[CpFe(CO)_2]$.

Characterization of the dibromide **7**.

The dibromide, **7**, isolated as a crystalline solid, was characterised by ^1H NMR, ^{13}C NMR, high resolution mass spectrometry, infrared spectroscopy and melting point.

3.2.1. ^1H NMR data for the dibromide **7**.

The ^1H NMR data for the dibromide **7** is summarised in table 3.2.1 below.

The ^1H NMR spectrum was assigned by comparison with the spectrum of the diol precursor which is documented.[8] The ^1H NMR spectrum showed a characteristic bromomethylene triplet at δ 3.49 ppm. The polyoxymethylene groups gave two multiplets, one at δ 3.87 ppm and the other at δ 4.09 ppm. The multiplet at δ 4.09 ppm was assigned to the phenoxymethylenes as shown by the integration. The phenyl signal is seen as a sharp singlet.

Table 3.2.1. ^1H NMR data for the dibromide **7**[a] in $CDCl_3$ solution.

Compd.	δ_H CH_2	δ_H OCH_2	δ_H Ar
7	3.49, tr, (4H) ^3J= 6.0 Hz	3.87, m, (8H) 4.09, m, (4H)	6.85, s, (4H)

a: in $CDCl_3$ relative to TMS (δ_H= 0.00 ppm), tr = triplet, s = singlet, q = quintet, m = multiplet.

3.2.2 ^{13}C NMR data for dibromide **7**.

The ^{13}C NMR data for the dibromide **7** is summarized in table 3.2.2.

Six resonances were observed. An upfield resonance at δ_C 30.2 ppm was assigned to the bromomethylene carbons; three resonances were assigned to the oxymethylene carbons of the polyether group in the vicinity of δ_C 70 ppm; two separate resonances were assigned to the aromatic ring. The four hydrogen substituted carbons resonated at δ_C 115.7 ppm while the two oxygen substituted carbons resonated at δ_C 153.1 ppm.

Table 3.2.2. ^{13}C NMR data for dibromide **7**[b] in $CDCl_3$ solution.

Compd.	$\delta_C\underline{C}H_2$	$\delta_C0\underline{C}H_2$	$\delta_C\underline{C}H$ (Ar)	$\delta_C\underline{C}O$ (Ar)
7	30.2	68.2, 69.8, 71.4	115.9	153.1

b: in $CDCl_3$ relative to $CDCl_3$ (δ_C= 77.0 ppm)

3.2.3. Mass Spectrometry.

The molecular ion of the dibromide **7** was observed at m/e = 412. The fragmentation pattern, as shown below, involved the loss of the bromoethoxyethyl fragments. The subsequent fragmentation of the bromoethoxyethyl fragment was also evident in the mass spectrum with a peak observed at m/e = 107 for the bromoethyl fragment.

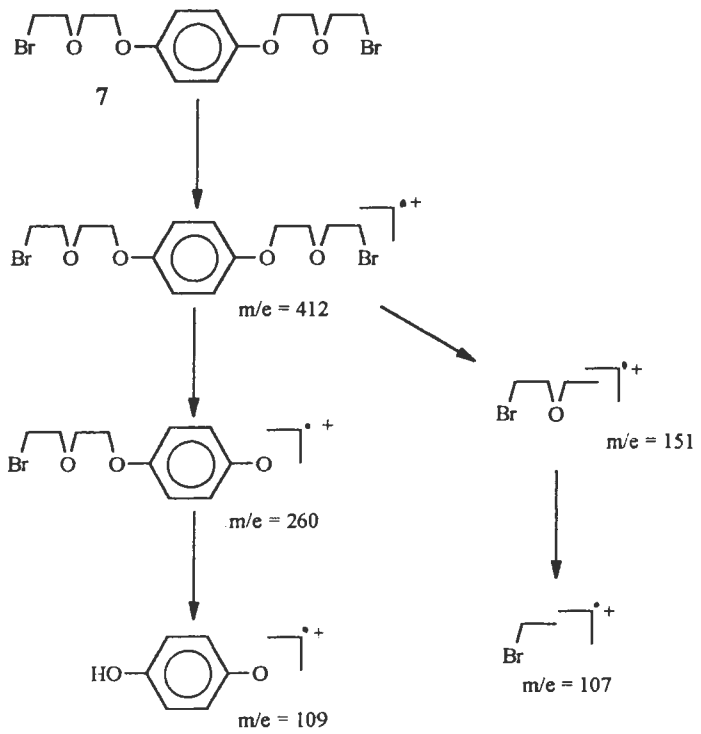

Scheme 3.2.3. Mass spectral fragmentation pattern of **7**.

3.3. A proposal of a synthetic route to organometallic polyethers.

The next step was to consider the stability of the organometallic system with which we were dealing, and since iron propyl species are known[42] to be stable, it was decided to use a propyl spacer between the cyclopentadienylirondicarbonyl moiety and the polyether thread. Thus, starting from the known polyether, 1,4-bis[2-(2-hydroxyethoxy)ethoxy]benzene **6**, a two step allylation / hydroboration-oxidation synthesis as shown in the reaction scheme 3.3.1 below, yielded the diol **9**, bearing terminal hydroxyl groups separated from the polyether group by a propyl spacer.

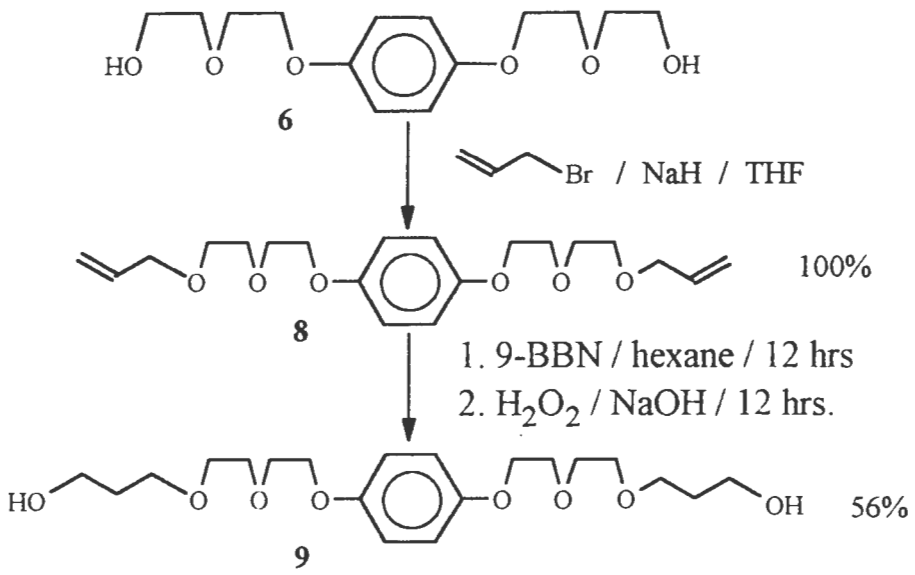

Scheme 3.3.1

The polyether diol thread, **6**, was readily allylated using allyl bromide / sodium hydride base in refluxing THF to yield the bis-allyl derivative **8**, as shown above. Purification was accomplished by column chromatography on silica gel followed by rigorous drying under high vacuum for 48 hours to remove all residual solvent. The product formed a dull yellow coloured wax. This wax form of the bis-allyl product readily reverts to a viscous oil form at 10^0C.

Hydroboration of the bis-allyl product **8** was undertaken using a 0.5M hexane solution of 9-borabicyclo[3.3.1]nonane (9-BBN) in preference to other hydroborating agents such as borane-dimethyl sulphide or borane-tetrahydrofuran as the highly sterically hindered 9-BBN gave only the anti-Markovnikov addition product regioselectively.

The inductive withdrawing effect of the oxygen of the polyether group in the allylic position to the double bond may have resulted in both anti-Markonikov and Markovnikov addition of borane to the double bond with the less hindered boranes. Regioselectivity studies[43] of analogous substituted olefins have been conducted. For instance, the addition of borane-tetrahydrofuran to 3-ethoxypropene gives 81% anti-Markovnikov addition and 19% Markovnikov addition product. Further, it was specified[43] that the regioselectivities of borane-dimethylsulfide and borane-tetrahydrofuran are identical. Thus, with such poor site selectivity, it was deemed best to use a sterically controlled hydroboration.

Characterization of the bis-allyl product **8** and the diol **9**.

The diol was characterized by ^{1}H NMR, ^{13}C NMR, mass spectrometry, infrared spectroscopy and elemental analysis while the bis-allyl product was characterised by ^{1}H NMR, ^{13}C NMR, high resolution mass spectrometry, infrared spectroscopy and melting point.

3.3.1.1. ^{1}H NMR data for the product **9**.

The ^{1}H NMR data for diol, **9,** is summarised in Table 3.3.1.

The assignments of diol, **9,** were made with reference to the documented spectrum of the diol precursor, **6**. The spectrum showed a characterisetic group of multiplets in the vicinity of 3.8 ppm due to the oxymethylene groups of the polyether side chains. The ^{1}H NMR spectrum of the diol **9** shows a slightly distorted triplet at δ 4.05 ppm which can be assigned to the phenoxymethylene group. Further assignments of each of the oxymethylene signals would require long range homonuclear correlation spectroscopy experiments. The phenyl resonance was observed as a sharp singlet since the para-substituted polyether groups are equivalent. The hydroxyl group of the diol **9** appeared as a very broad singlet at δ 2.68 ppm and the hydroxypropyl methylene β to the hydroxyl group appeared as a characteristic well-defined quintet at δ 1.79 ppm resulting from vicinal coupling with ^{3}J = 5.7 Hz. The ^{1}H NMR spectrum of the diol, **9**, is included for reference and is labelled as Figure 3.3.1.

Table 3.3.1. ^{1}H NMR data for product **9** in $CDCl_3$ solution.

Compd.	$\delta_H OC_6\underline{H}_4O$	$\delta_H O\underline{CH}_2$	$\delta_H O\underline{H}$	$\delta_H C\underline{H}_2$
9	6.81, s, (4H).	4.07 - 3.60 (24H)	2.68, br s, (2H)	1.79, q, ^{3}J=5.7 Hz, (4H).

Figure 3.3.1. ^{1}H NMR spectrum of the diol product **9**.

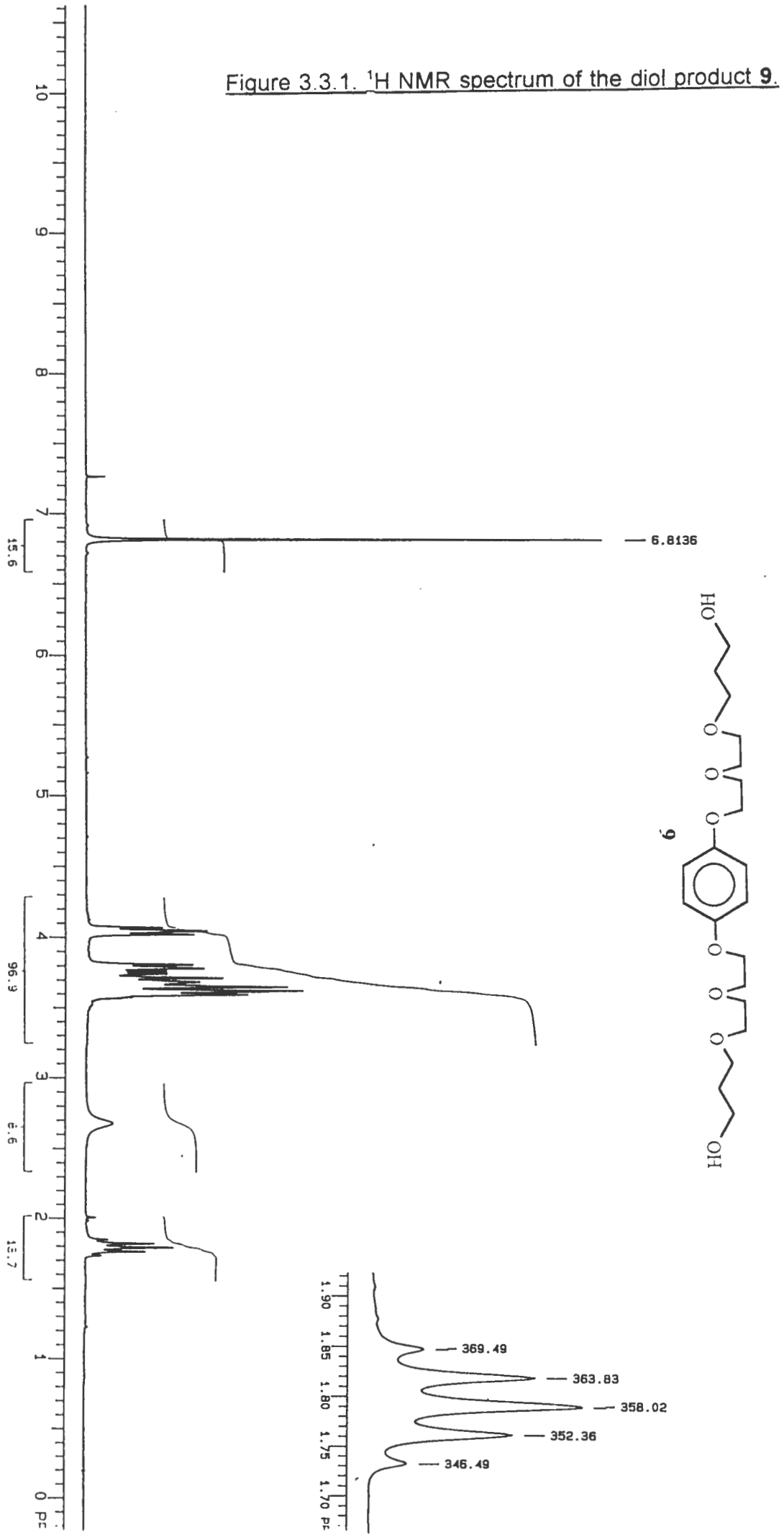

3.3.2.1. ^{1}H NMR data for the product **8**.

The ^{1}H NMR data for product **8** is summarised in Table 3.3.2. below.

The assignment of product **8** was made with reference to the documented spectrum of the diol precursor,**6**, from which **8** was synthesized.

The spectrum of this bis-allyl polyether was characterized by a group of multiplets in the vicinity of 3.8 ppm arising from the oxymethylene groups of the polyether side chains. The phenyl resonance appeared as a sharp singlet since the para-substituted polyether groups are equivalent. Two separate olefinic resonance were observed, one at δ 5.20 ppm, integrating for 4 protons and the other at δ 5.89 ppm, integrating for 2 protons. These resonances were assigned to H_a / H_b and H_e respectively as shown in Figure 3.3.2.1. An interesting multiplet was observed in the ^{1}H NMR spectrum of the bis-allyl product **8** at δ 5.89 ppm. The allyl group with designated protons and line diagram are shown in Figure 3.3.2.1. along with the relevant portion of the spectrum. The spectrum shows four overlapping triplets. A calculation of the coupling constants involved, revealed three different types of coupling present. The first coupling resulted from large (H_b / H_e) *trans*-olefinic coupling with (J=17.3 Hz). The second coupling, (H_a / H_e), involved *cis*-olefinic coupling with ($J_{a,e}$=10.3 Hz), thus conforming to known vicinal olefin couplings.[44] The last two couplings involved H_c / H_e vicinal couplings.

The ^{1}H NMR spectrum of the bis-allyl product, **8**, is included for reference and is labelled Figure 3.3.2.

Table 3.3.2. ^{1}H NMR data for the bis-allyl product, **8**.

Compd.	$\delta_H OC_6\underline{H}_4O$	$\delta_H OC\underline{H}_2$	$\delta_H C{=}C\underline{H}$
8	6.83, s, (4H)	4.09 - 3.58 (20H)	5.89, m, (2H) 5.19, m, (4H)

Figure 3.3.2.1. Line diagram and resonance for the allyl group of **8** at 5.89 ppm.

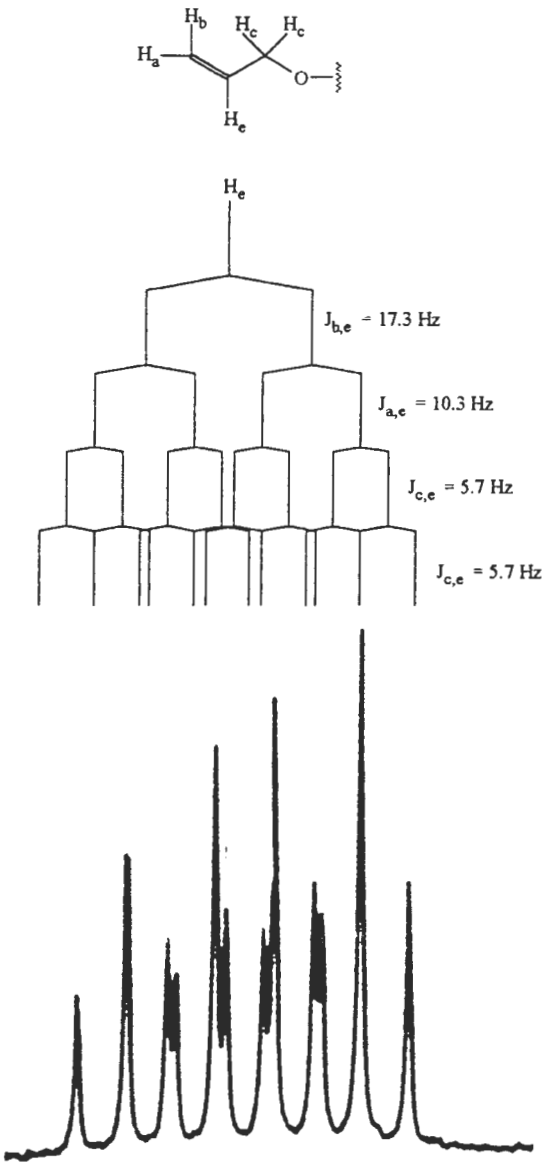

Figure 3.3.2. ^{1}H NMR spectrum of bis-allyl product **8.**

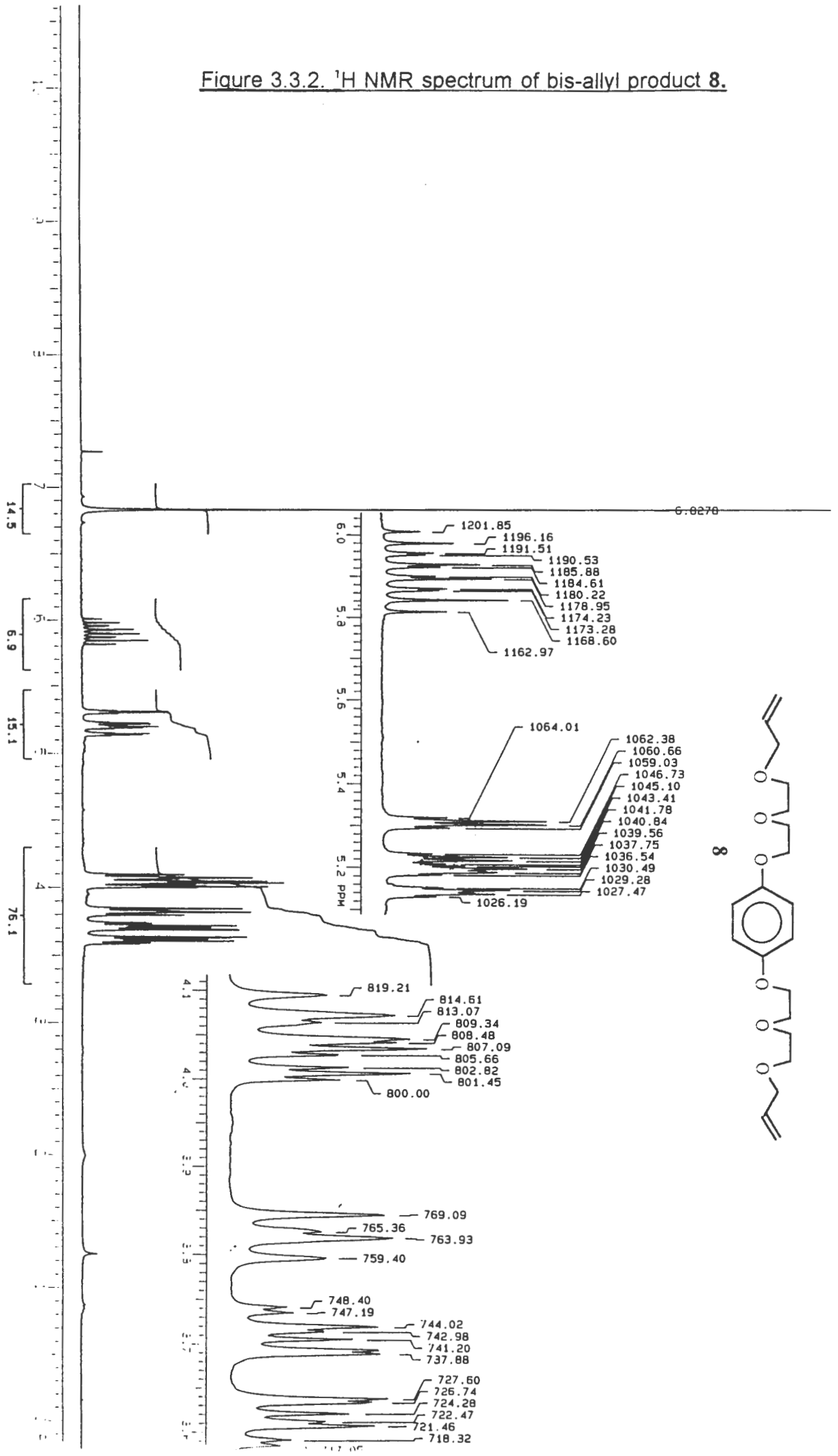

3.3.2.2. ^{13}C NMR data for the products **8** and **9**.

The ^{13}C NMR data for both products is summarised in Table 3.3.2.

The ^{13}C NMR spectra of products **8** and **9** each showed five characteristic oxymethylene carbon resonances of the polyether groups in the region 68 ppm to 72 ppm. Two separate resonances were observed for each aromatic group; one downfield resonance at δ 153.0 ppm for the two oxygen substituted aromatic carbons and one upfield resonances at δ 115.5 ppm for the four hydrogen substituted aromatic carbons.

The spectrum of the bis-allyl product **8** showed two olefin resonances; the terminal olefinic methylene carbon resonated at δ 134.6 ppm while the substituted olefinic methylene carbon resonated at δ 117.0 ppm as expected from spectra of model compounds.[44] The spectrum of the diol, **9**, showed the hydroxyl substituted methylene carbon resonance at δ 61.3 ppm while the methylene group β to the hydroxyl group resonated at δ_c 31.9 ppm.

Table 3.3.2.2. ^{13}C NMR data for products **8** and **9**.

Compd.	$\delta_c\underline{C}H_2$	$\delta_c\underline{C}H_2OH$	$\delta_cO\underline{C}H_2$	$\delta_c\underline{C}H$ (Ar)	$\delta_c\underline{C}O$ (Ar)	$\delta_cC=C$
8	------	---------	72.2, 70.7, 69.8, 69.4, 68.0	115.5	153.O	134.6, 117.0
9	31.91	61.32	70.6, 70.2, 70.0, 69.8, 68.0	115.5	153.0	---------

3.3.3. Mass Spectrometry.

Parent ions were observed for both products **8** and **9**. Fragmentation involved the loss of the polyether side chains as shown below.

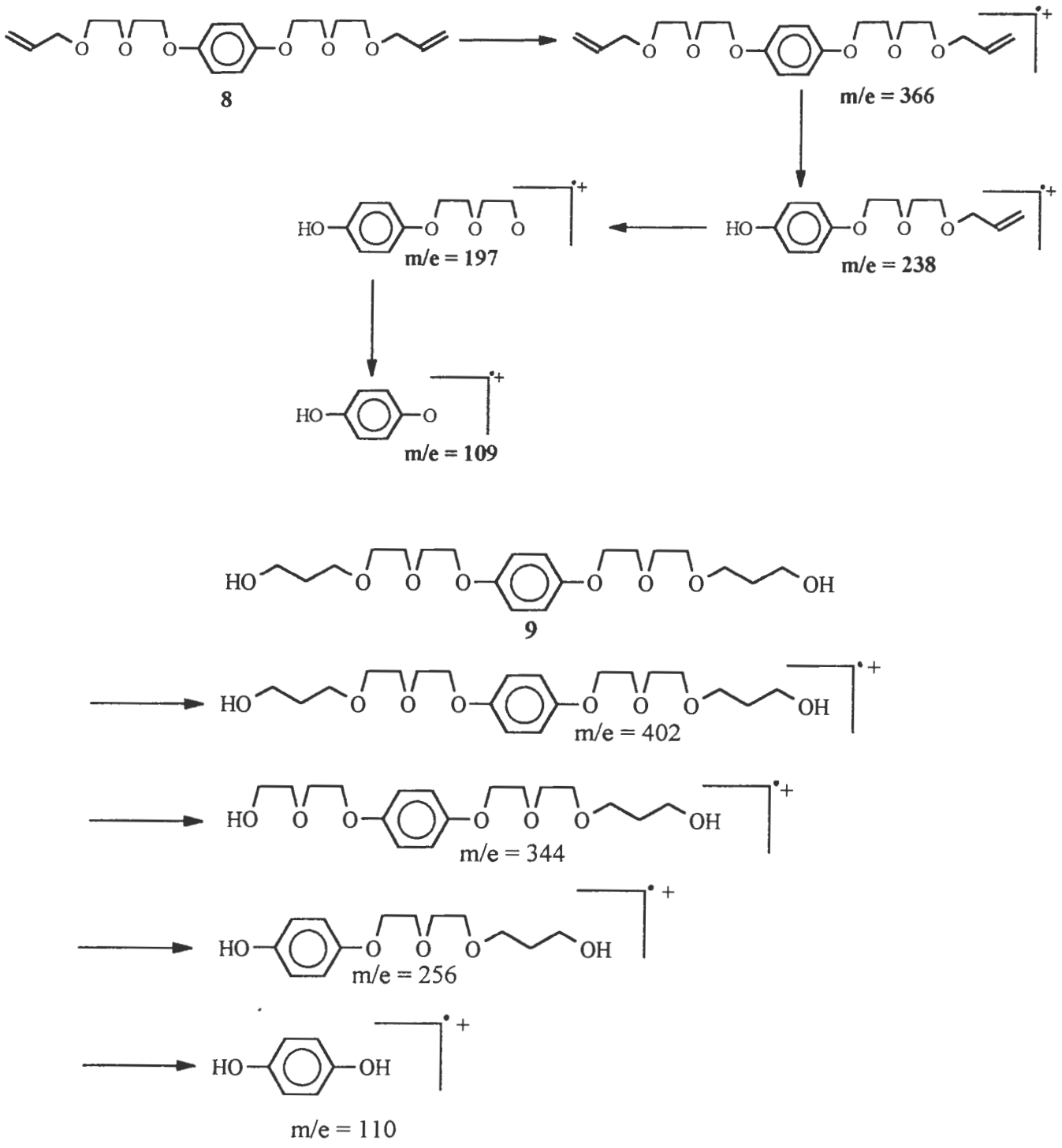

Scheme 3.3.3. Mass spectral fragmentation patterns for **8** and **9**.

3.3.4. Preparation of the the bis-tosylpolyether **10** and dibromopolyether **11**.

A one step transformation of the primary hydroxyl groups of the diol **9** gave a polyether with leaving groups separated from the polyether functionality by a propyl spacer.

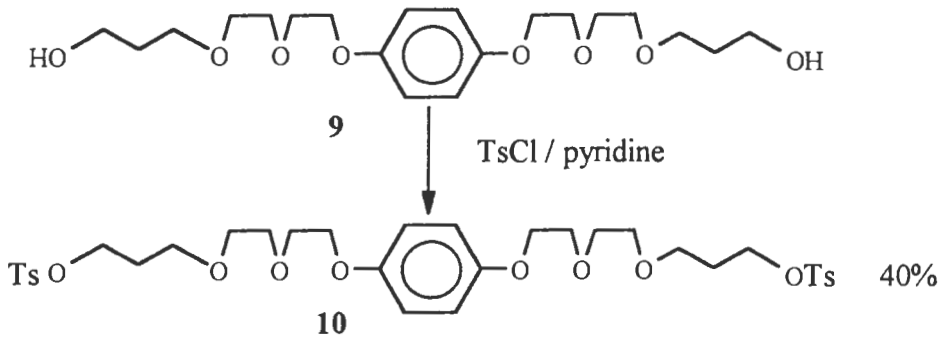

Equation 3.3.4.1.

Initially, the bis-tosylpolyether, **10**, was prepared for metalation, since the tosylate leaving group is particularly labile. However, **10** could not be induced to crystallise or to form a wax. The stability of **10** was found to be poor since purification by chromatography on silica resulted in a low yield and separation of tosyl chloride from **10** was problematic. Instead, a bromination reaction yielded the dibromopolyether, **11**, in good yield, as shown in equation 3.3.4.2. below. Product **11** could be readily purified by chromatography and formed a wax at -30 °C.

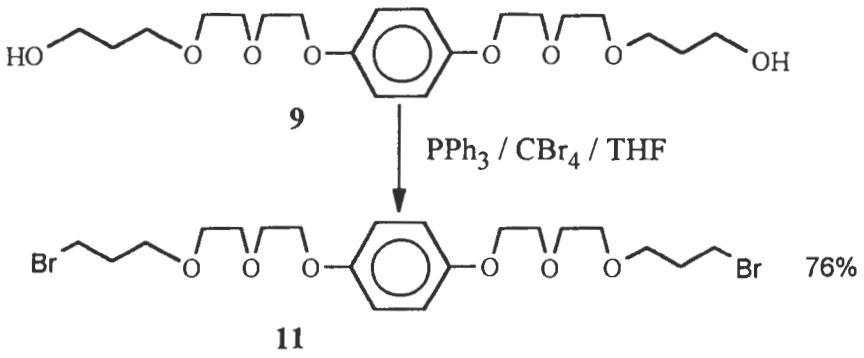

Equation 3.3.4.2.

Characterization of the bis-tosylpolyether **10** and dibromopolyether **11**.

Product **10** was fully characterised by ^{1}H NMR and ^{13}C NMR spectroscopy, infrared spectroscopy and high resolution mass spectrometry. Product **11** was fully characterised by ^{1}H NMR and ^{13}C NMR spectroscopy, infrared spectroscopy, mass spectrometry and elemental analysis.

3.3.4.1. ^{1}H NMR data for the products **10** and **11**.

The ^{1}H NMR data for product **11** is summarised in Table 3.3.4.1.

The assignment of the ^{1}H NMR spectrum of the dibromopolyether, **11**, was made by comparison with the ^{1}H NMR spectrum of the diol, **9**. The spectrum of **11** shows the characteristic polyether resonances in the region 3.8 ppm to 4.1 ppm arising from the oxymethylene groups of the polyether. The phenyl resonance is observed as a sharp singlet since the para substituted groups are equivalent. The bromopropyl methylene, β to the bromo substituent is a characteristic well-defined quintet at 2.09 ppm resulting from vicinal coupling, with ^3J = 6.1 Hz. The bromopropyl methylene α to the bromo substituent falls in the polyether region and could not be discerned from the oxymethylene signals.

Table 3.3.4.1-^{1}H NMR data for the product **11.**

Compd.	$\delta_H OC_6\underline{H}_4O$	$\delta_H OC\underline{H}_2$ / $\delta_H C\underline{H}_2Br$	$\delta_H C\underline{H}_2CH_2Br$
11	6.84, s, (4 H)	3.80 - 4.10 (24 H)	2.09, q, (4H) ^3J = 6.1 Hz

Similarly, the ^{1}H NMR spectrum of the bis-tosylpolyether, **10**, was assigned by comparison with the ^{1}H NMR spectrum of the diol, **9,** and these assignments are summarised in Table 3.3.4.2 below. The polyether resonances were observed in the region 3.4 ppm to 4.2 ppm and amongst these resonances was the methylene group α to the tosylate substituent. The toluenesulfonyl group showed an AB system, giving two aromatic doublets; at 7.32 ppm (^3J = 8.0 Hz, aromatic protons adjacent to the methyl group) and at 7.77 ppm (^3J = 8.3 Hz, aromatic protons adjacent to the sulphonyl group). The aromatic methyl substituent appeared as a sharp singlet at 2.42 ppm. The methylene group β to the tosyl group gave a well defined quintet at 1.90 ppm resulting from vicinal coupling with ^3J = 6.1 Hz. The phenyl resonance appeared as a sharp singlet at 6.82 ppm.

Table 3.3.4.2-^{1}H NMR data for the product **10.**

Compd.	$\delta_H C_6H_4$ (Ts)	$\delta_H OC_6\underline{H}_4O$	$\delta_H OC\underline{H}_2$	$\delta_H C\underline{H}_2CH_2OTs$	$\delta_H C\underline{H}_3$ (OTs)
10	7.77, d, (4H) 7.32, d, (4H)	6.82, s (4H)	3.4 - 4.2 (24H)	1.90, q, (4H) ^3J = 6.08 Hz	2.42, s, (6H)

Figure 3.3.4.1. ^{1}H NMR spectrum of the dibromopolyether, **11**.

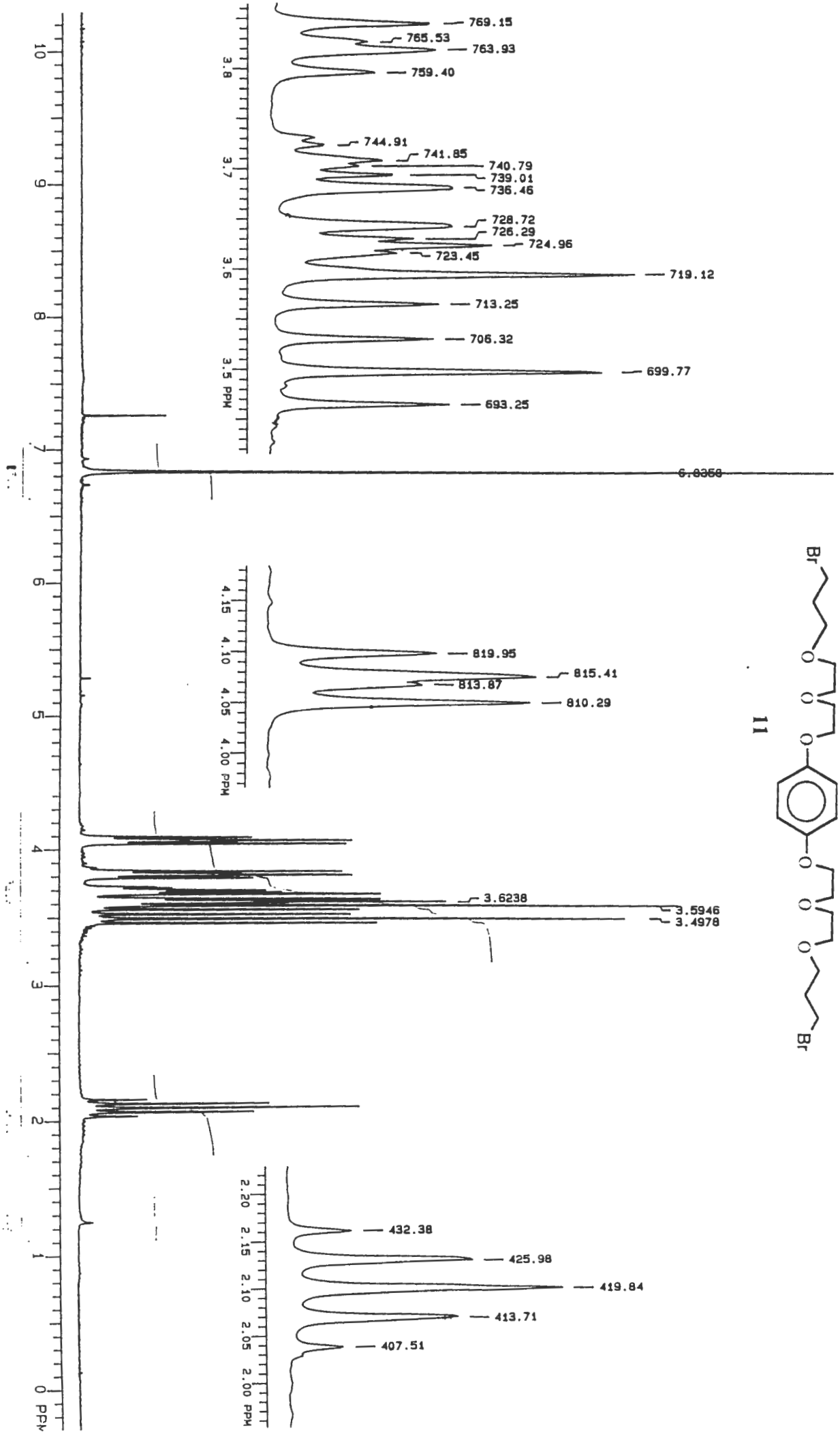

Figure 3.3.4.2. ^{1}H NMR spectrum of the bis-tosylpolyether, **10**.

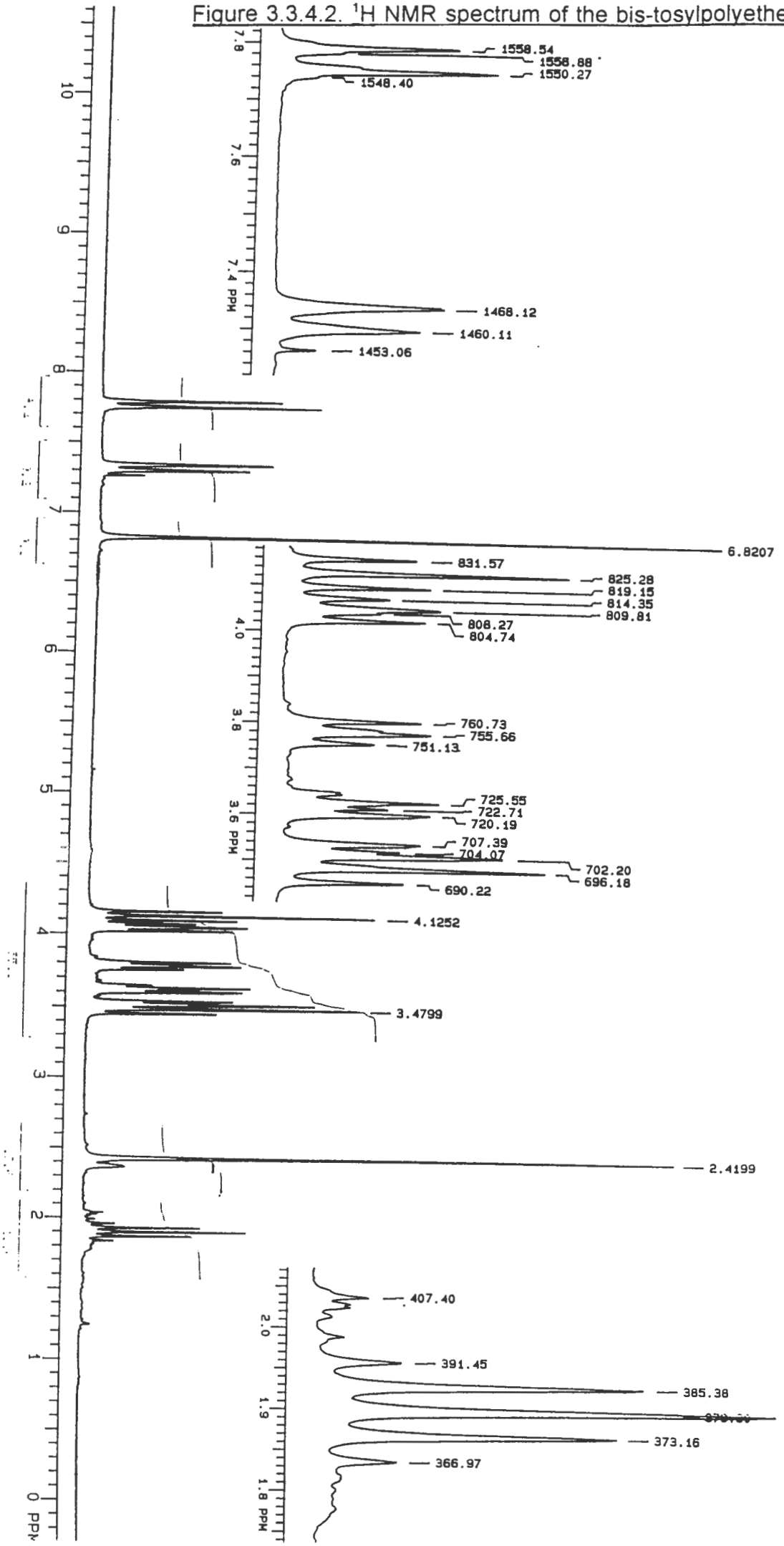

3.3.5 ^{13}C NMR data for the products **10** and **11**.

The ^{13}C NMR spectra of products **10** and **11** both showed the characteristic oxymethylene resonances of the polyether methylenes in the region 67 ppm to 74 ppm. The ^{13}C NMR spectrum of the bis-tosylpolyether, **10**, gave two resonances in the region 20 ppm to 35 ppm (21.8 ppm, 26.4 ppm). These resonances (assigned by comparison with the spectra of the diol and that of tosyl chloride) are due to the methyl group of the tosyl substituent, and the β methylene of the propyl spacer group respectively. The tosyl substituent gave four resonances in the aromatic region, two of which (130.2 ppm and 126.9 ppm) are fairly intense resonances and are therefore assigned to the C-H carbons of the tosyl group while the remaining weak resonances (146.8 ppm and 141.6 ppm) are assigned to the aromatic carbons bearing the sulfonyl and methyl groups respectively. The phenyl group gives rise to the two charateristic resonances (115.5 ppm and 153.0 ppm) as observed for all the other polyethers discussed so far; these are similarly assigned to the C-H carbons of the aromatic ring and the C-O carbons of the aromatic ring respectively.

Table 3.3.5.1 ^{13}C NMR shifts for the bis-tosylpolyether, **10**.

Compd	C-O (Ar)	C-H (Ar)	OTs (Ar)	OCH_2	CH_2CH_2OTs	Me (Ts)
10	153.1	115.6	127.9, 139.8, 133.1, 144.7	70.6, 70.3, 69.8, 68.0, 67.7, 66.6	29.3	21.6

The dibromopolyether, **11**, gave two resonances in the region 25 ppm to 35 ppm (32.7 ppm and 30.6 ppm) which were assigned to carbons α and β to the bromine atoms. The five polyether carbons were observed in the region 67 ppm to 72 ppm as before. The phenyl group gave two characteristic resonances at 153.0 ppm and 115.5 ppm assigned to the C-O carbons of the aromatic ring and the C-H carbons of the aromatic ring respectively.

Table 3.3.5.2 ^{13}C NMR shifts for the dibromopolyether, **11**.

Compd.	C-O (Ar)	C-H (Ar)	OCH_2	CH_2CH_2Br	CH_2Br
11	153.0	115.5	70.7, 70.3, 69.8, 68.6, 68.0	32.7	30.6

3.3.6. Metallation of the dibromopolyether, **11**, and of the bis-tosylpolyether, **10**.

Both the bis-tosylpolyether, **10**, and the dibromopolyether, **11**, were successfully metallated by reaction with two equivalents of $Na[CpFe(CO)_2]$ in THF at -78°C for one hour followed by a further hour at room temperature to yield the diironpolyether, **12**, as shown below(equation 3.3.6.1.). The only difference between the two approaches being that the dibromopolyether was far easier to use and gave a superior yield. The diironpolyether, **12**, was isolated as a light sensitive yellow-coloured viscous oil which could not be crystallised.

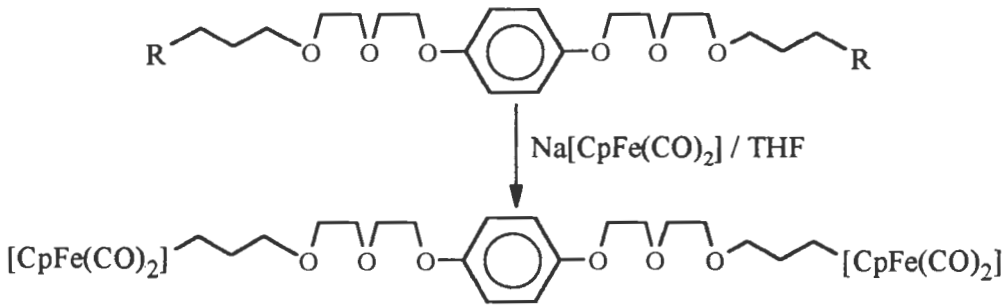

12 R = OTs yield = 44%
R = Br yield = 92%

Equation 3.3.6.1

To enhance the stability of **12** and to increase the bulk of the end groups, **12**, was reacted with 2.5 equivalents of PPh_3 to yield **13** via phosphine substitution and carbonyl insertion, (equation 3.3.6.2.), similar to the preparation of **5** as described in Chapter 2.

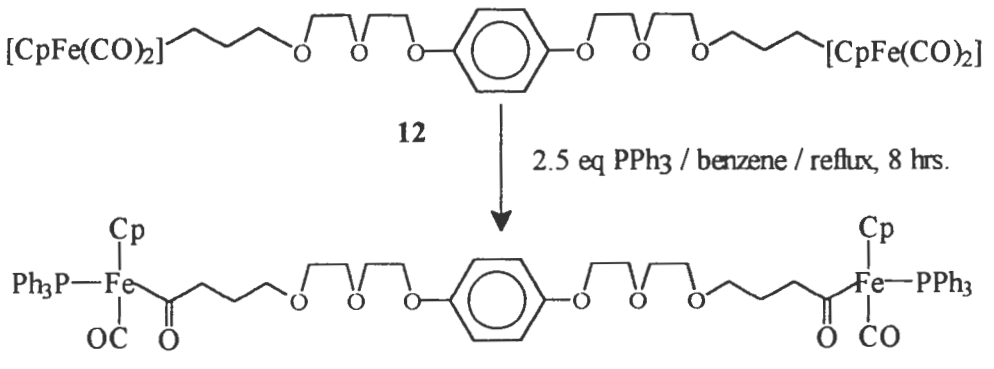

13

Yield = 71 %

Equation 3.3.6.2.

3.3.6.1. ^{1}H NMR data for the diironpolyether, **12**.

The ^{1}H NMR spectrum of the diironpolyether was readily assigned by comparison with the spectra of **3**, as described in Chapter 2 of this thesis, and also by comparison with the spectra of the dibromopolyether, **11**, and diol, **9.** The ^{1}H NMR data is summarised in Table 3.3.6.1 below. The propyl spacer between the polyether chain and the iron atom gives rise to three methylene resonances, the first of which was a complex mutliplet at 1.34 ppm arising from the methylene α to the iron atom. The second resonance, a complex multiplet at 1.74 ppm which resembled a quintet, was assigned to the methylene group β to the iron atom. The steric bulk of the cyclopentadienyliirondicarbonyl substituent resulted in the protons of the α and β methylene groups being magnetically non equivalent due to restricted rotation between possible conformers and thus the resonances of the α and β methylenes appeared as multiplets. The methylene group γ to the iron atom appeared as a well defined triplet at 3.40 ppm with ^3J = 6.9 Hz, resulting from vicinal coupling. Similarly the resonances for the polyether methylenes were multiplets resulting from magneticly non-equivalent protons due to restricted rotation of the polyether chain. The cyclopentadienyl resonance was observed as a sharp singlet at 4.72 ppm. The phenyl signal was observed as a sharp singlet at 6.72 ppm. A dichloromethane solvent peak was observed at 5.29 ppm.

Table 3.3.6.1. ^{1}H NMR data for the diironpolyether, **12**.

Compd	δ_H $OC_6\underline{H}_4$	δ_H Cp	δ_H OCH_2	$\delta_H C\underline{H}_2CH_2CH_2Fe$	δ_H $C\underline{H}_2CH_2Fe$	δ_H $C\underline{H}_2Fe$
12	6.84, s, (4H)	4.73, s, (10H)	3.5 - 4.2, m, (20H)	3.40, t, (4H) ^3J = 6.9 Hz	1.74, m, (4H)	1.34, m, (4H)

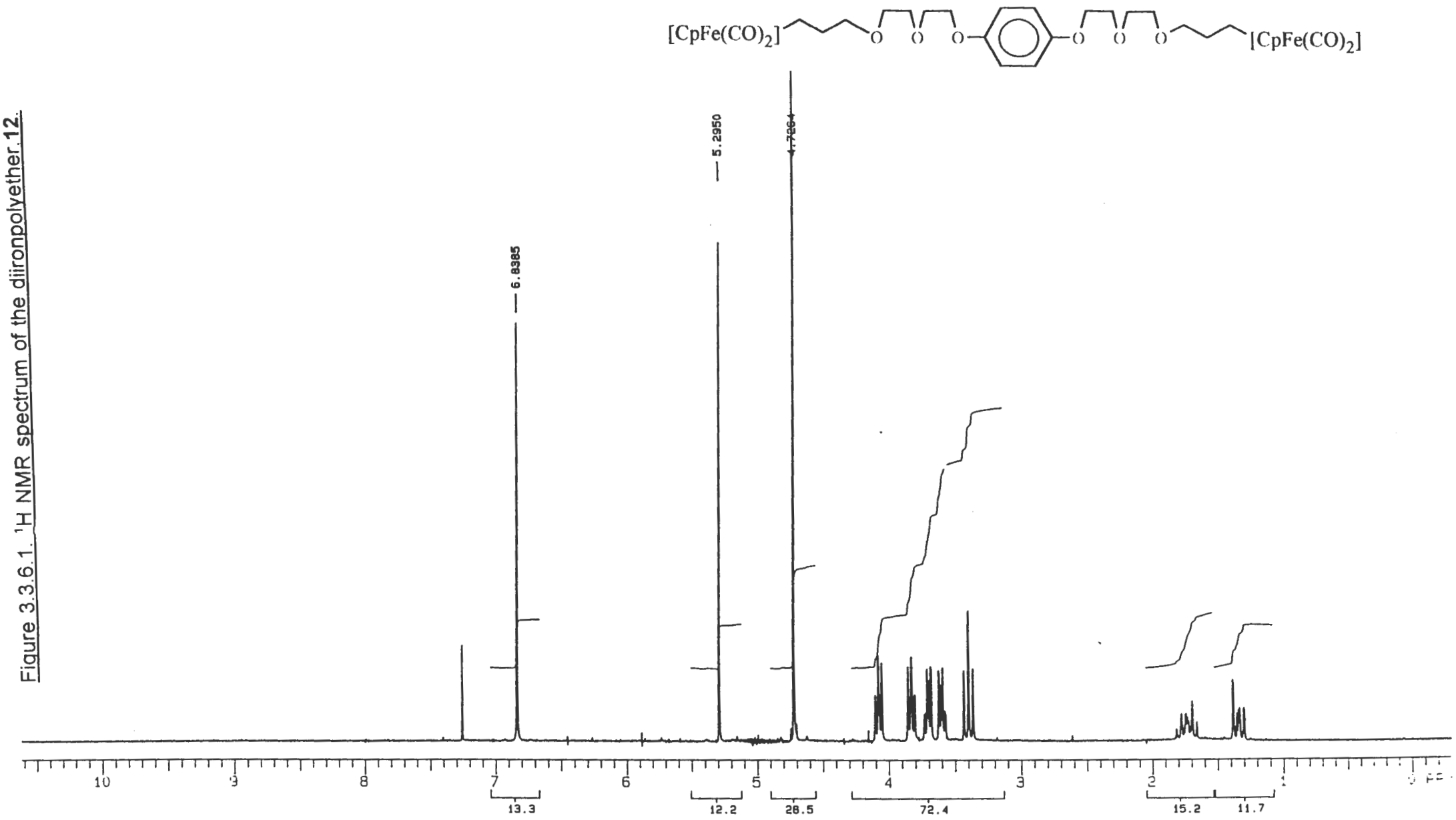

Figure 3.3.6.1. ^{1}H NMR spectrum of the diironpolyether **12**.

3.3.6.2. ^{13}C NMR data for the diironpolyether, **12**.

The ^{13}C NMR spectrum of **12** was assigned by comparison with the ^{13}C NMR spectra of **3** as described in Chapter 2 of this thesis and also by comparison with the ^{13}C NMR spectra of the dibromopolyether, **11**, and diol, **9.** These assignments are summarised in Table 3.3.6.2. below. The carbons of the methylene groups α and β to iron resonated at 2.1 ppm and 37.7 ppm respectively. The polyether methylene carbons appeared as five distinct resonances between 68 ppm and 75 ppm. The cyclopentadienyl carbon resonance was observed at 85.4 ppm. The carbons of the phenyl group gave rise to the two characteristic resonances (115.6 ppm and 153.1 ppm) as observed for the other polyethers discussed so far; these were similarly assigned to the C-H carbons of the aromatic ring and the C-O carbons of the aromatic ring respectively. The carbonyl ligands on the iron atom were observed as a single resonance at 217.4 ppm.

Table 3.3.6.2. ^{13}C NMR shifts for the diironpolyether, **12**.

Compd.	CO	C-O (Ar)	C-H (Ar)	Cp	OCH_2	CH_2CH_2Fe	CH_2Fe
12	217.4	153.1	115.6	85.3	74.5, 70.8, 70.0, 68,8 68.0	37.7	-2.1

Figure 3.3.6.2. ^{13}C NMR spectrum of the diironpolyether,**12**.

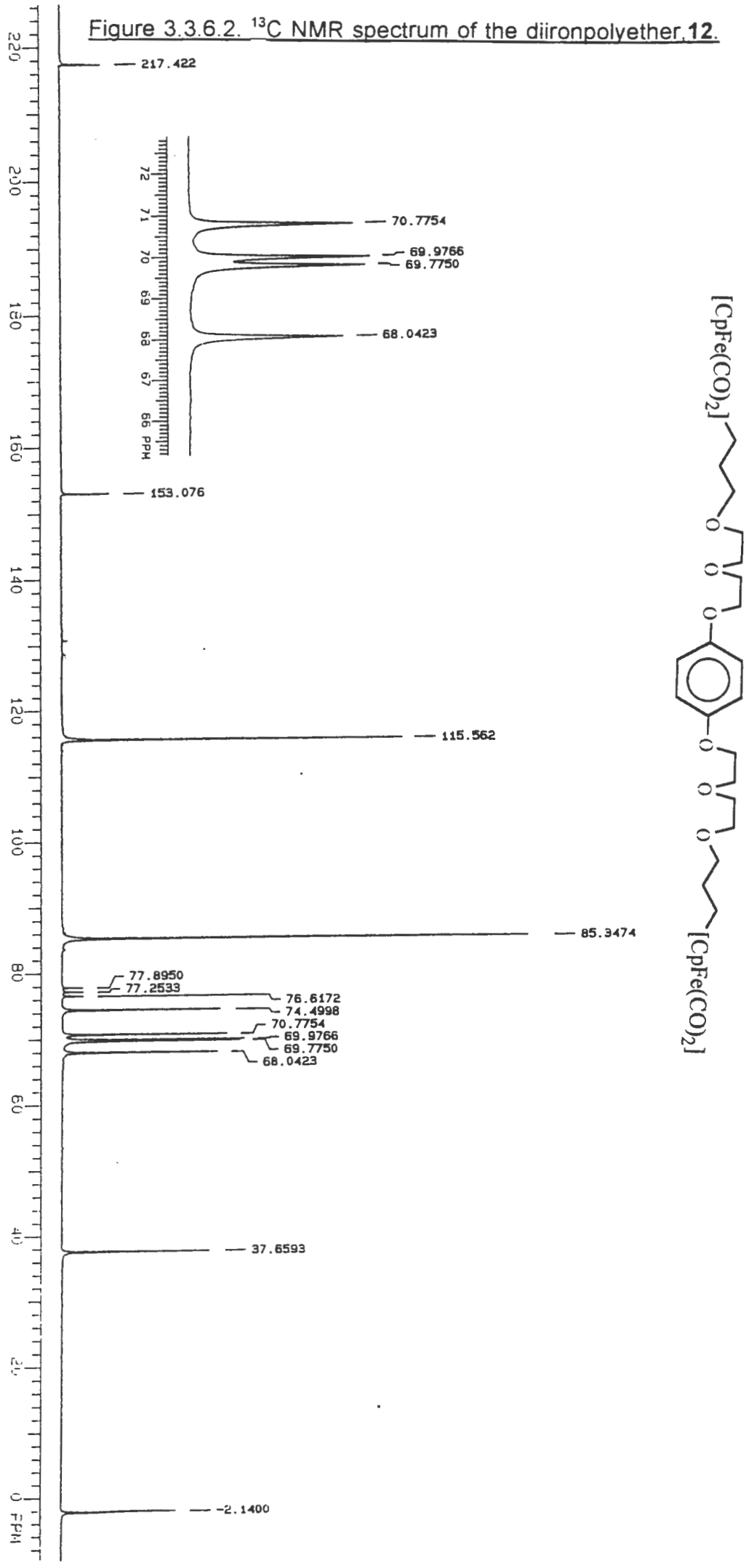

3.3.7. ^{1}H NMR data for the bis(triphenylphosphine)diacyldiiron polyether, **13**.

The ^{1}H NMR spectrum of the bis(triphenylphosphine)diacyldiironpolyether, **13**, was assigned by comparison with the NMR spectra of the diironpolyether, **12**, and that of the bis(triphenylphosphine)diacyldiiron product, **5**, as dicussed in Chapter 2 of this thesis. The ^{1}H NMR spectrum of **13** shows the characteristic polyether resonances in the region 3.4 - 4.1 ppm. The phenyl resonances were observed at 6.82 ppm and the resonances of the bulky triphenylphosphine groups were observed as a large complex multiplet at 7.3 ppm. The Cp signal was resolved into two separate signals, indicating non-equivalence, attributed to the presence of two diastereomers in these molecular systems as discussed in Chapter 2 of this thesis. The diastereotopic methylene protons α to the carbonyl appeared as two distinct signals at 2.94 ppm and 2.60 ppm. Similarly, the protons of the methylene group β to the carbonyl gave separate multiplet resonances, at 1.50 ppm and 1.32 ppm. The protons of the methylene γ to the carbonyl appeared as a complicated multiplet at 3.14 ppm (i.e. polyether like). Thus the difference in chemical shift of the diastereotopic methylene protons decreases as the distance from the iron atom increases. The polyether signals were observed as four distinct multiplets in the region 3.4 ppm to 4.2 ppm. The sharp singlet at 5.30 ppm is a dichloromethane solvent peak. This analysis assumes that each diastereomer gives the same NMR spectrum, a reasonable assumption since the two chiral centres are so far apart.

Table 3.3.7. ^{1}H NMR data for the bis(triphenylphosphine)diacyldiironpolyether, **13**.

Compd	$\delta_H PPh_3$	$\delta_H OC_6H_4O$	$\delta_H Cp$	$\delta_H OCH_2$	$\delta_H \gamma$-CH_2	$\delta_H \beta$-CH_2	$\delta_H \alpha$-CH_2
13	7.3, m, (30H)	6.83, s, (4H)	4.41, s, 4.40, s, (10H)	3.4 - 4.2 (16H)	3.14, m, (4H)	1.50, m, 1.32, m, (4H)	2.94, m, 2.60, m, (4H)

Figure 3.3.7. ^{1}H NMR spectrum of **13**.

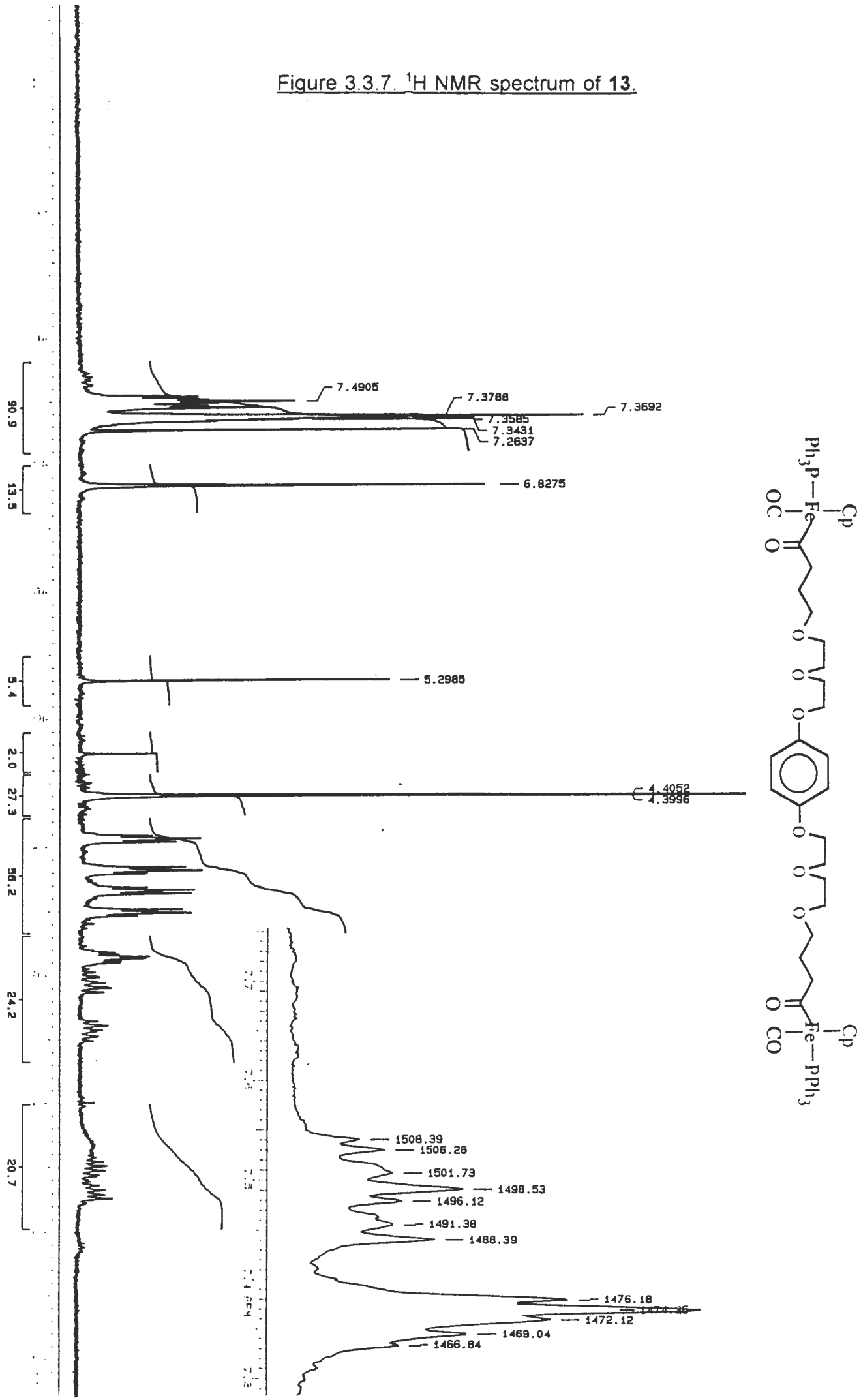

3.3.8. ^{13}C NMR data for the bis(triphenylphosphine)diacyldiironpolyether, **13**.

The ^{13}C NMR spectrum of **13** was assigned by comparison with the ^{13}C NMR spectra of the bis(triphenylphosphine)diacyldiiron product **5** and that of the diironpolyether, **12**. The carbon of the methylene group α to the iron-acyl carbonyl group gave two resonances, 62.0 and 62.1 ppm, for the two diastereomers. This doubling up of the α methylene carbon resonance indicated the presence of two distinct diastereomers. The small chemical shift difference (0.11 ppm) is exactly comparable to the shift difference observed in the ^{13}C NMR spectrum of **5** as discussed in section 2.4.2 of this thesis. The methylene group β to the the carbonyl gave a single resonance at 25.0 ppm while methylene group γ to the carbonyl resonated at 68.1 ppm. The polyether resonances appeared as a group of four resonances between 68.8 ppm and 70.9 ppm. The Cp group resonated at 85.2 ppm. The phenyl ring gave two resonances, an intense resonance at 115.6 ppm for the four hydrogen bearing carbons of the aromatic ring and a less intense resonance at 153.0 for the two oxygen bearing carbons. The signal of the bulky triphenylphosphine group was seen as a group of resonances in the region 127.9 to 136.9 ppm. Two weak carbonyl resonances appeared at 221 ppm. These were assigned to the acyl group and the carbonyl ligand on the iron atom.

Table 3.3.8. ^{13}C NMR shifts for the bis(triphenylphosphine)diacyldiironpolyether, **13**.

Compd.	CO	C-O (Ar)	C-H (Ar)	PPh_3
13	220.9	153.1	115.6	127.9 -136.9

Compd.	Cp	OCH_2	α-CH_2	β-CH_2	γ-CH_2
13 (cont'd.)	85.2	70.9, 70.7, 70.0, 69.8	62.0, 62.1	25.0	68.1

Figure 3.3.8. ^{13}C NMR spectrum of **13**.

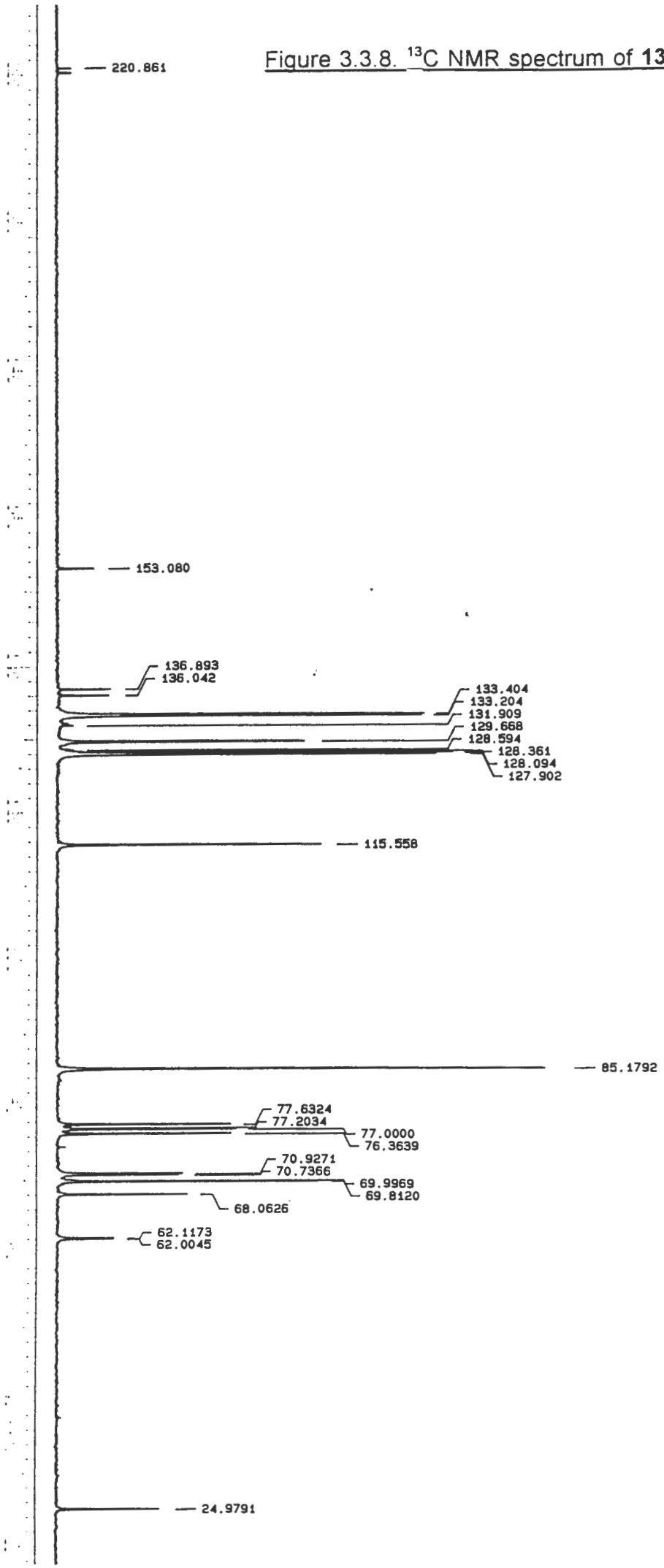

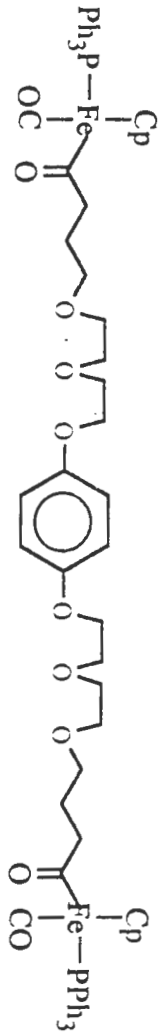

3.4. Attempted Rotaxane synthesis.

This synthesis was done according to the clipping method as explained in Section 1.3 of Chapter 1 of this thesis.
A sample of "horseshoe" was prepared according to the method used by Stoddart and coworkers[18] and the ^1H NMR spectrum is included and labelled as figure 3.4.2.

The experiment was carried out by dissolving 3 equivalents of **13** in CH_3CN; to this was added one equivalent of "horseshoe" and one equivalent of dibromoxylene. After two days, two equivalents of $AgBF_4$ were added and after another three days two more equivalents of $AgBF_4$ and a further equivalent of dibromoxylene was added. The reaction was allowed to stir for two more days. The reaction was monitored by thin layer chromatography.

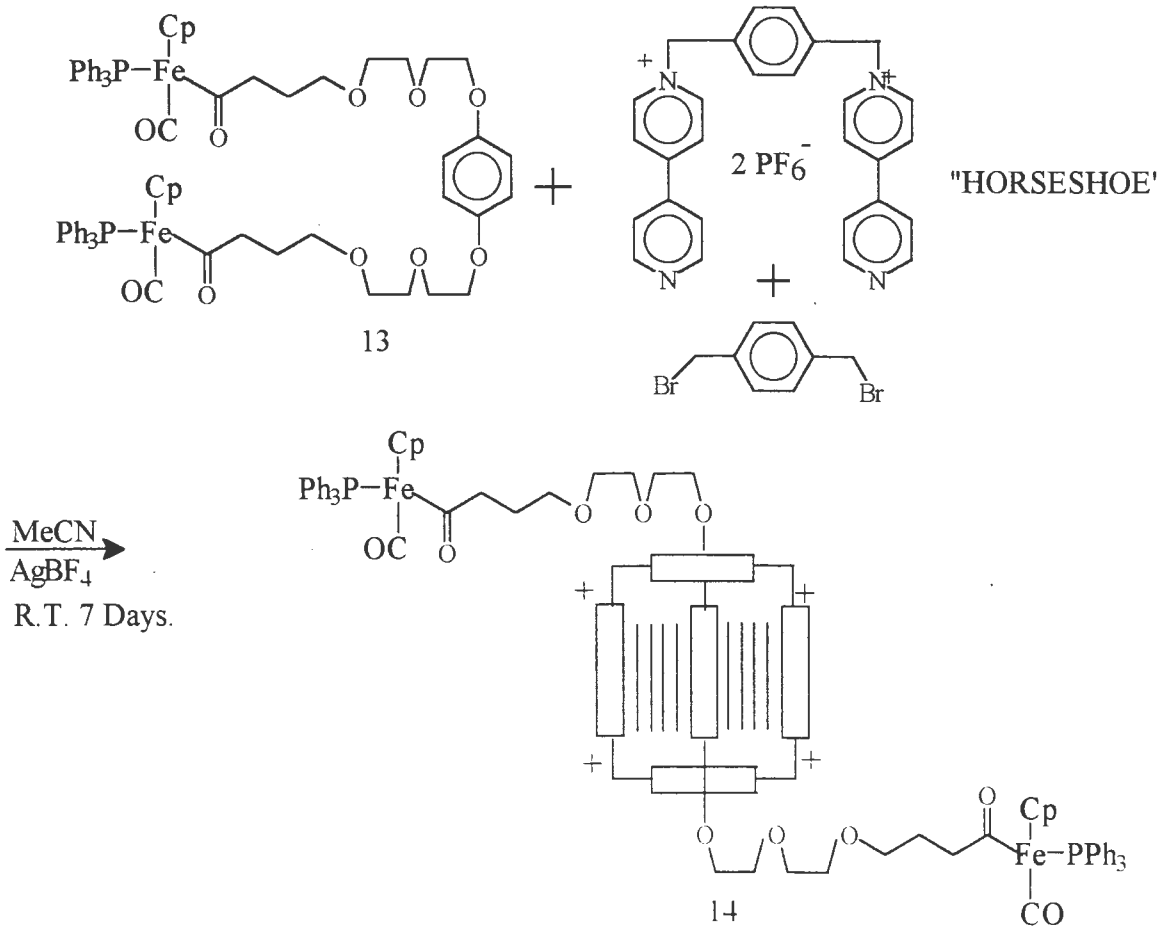

Scheme 3.4.1. Clipping reaction using the thread, 13, and horseshoe.

.Three fractions were isolated from this reaction by chromatography. They were, in order of increasing polarity:

1. excess **13**, 62%, relative to the initial ammount of **13** added;

2. yellow solid identified as "bluebox" (cyclobis(paraquat-p-phenylene)), 30% relative to the initial ammount of "horseshoe";

3. reddish gum, (63mg, 15%) investigated as the possible rotaxane, **14**.

The ^{1}H NMR spectrum of the reddish gum (see figure 3.4.1.) showed elements of the desired rotaxane, **14**. The signals for "bluebox", as part of a rotaxane could be assigned as follows:

i) δ_H 5.93 (4H, s) and δ_H 5.92 (4H, s) assigned to the methylene protons, (H_3, see 4.3., page 82, experimental section), which connect the phenylene to the pyridinium ring.

ii) The protons of the pyridinium ring β to the charged nitrogen, (H_2), gave two doublets: δ_H 8.71 (4H, d, ^3J = 5.5 Hz) and δ_H 8.70 (4H, d, ^3J = 5.4 Hz).

iii) The protons of the pyridinium ring α to the charged nitrogen atom (H_1) gave two doublets: δ_H 9.48 (4H, d, ^3J = 7.2 Hz) and δ_H 9.45 (4H, d, ^3J = 7.2 Hz).

The expected signal of the phenylene group of "bluebox" was not found as it is obscured by the massive triphenylphosphine signal in the region 7.4 to 7.8 ppm; the large triplet observed at 7.07 ppm is assigned to NH_4PF_6.

The presence of **13** in **14**, is evident from:

i) The large multiplet δ_H 7.60 (28H, m) assigned to the triphenylphosphine groups of **13**;

ii) δ_H 4.42 (10H, s) assigned to the cyclopentadienyl groups bonded to the iron atom;

iii) The large broad polyether methylene signals between 3.4 ppm and 4.1 ppm.

Support for **13** being encircled by "bluebox" comes from the comparison of ^{1}H chemical shift values. For instance, Benniston and Harriman[33] give the shifts of threaded "bluebox" in the case of rotaxane, **20**, (shown in section 1.5., page 30, Chapter 1 of this thesis) as:

i) δ_H 5.97 (8H, s.) assigned to the methylene protons, (H_3);

ii) δ_H 8.16 - 8.19 (8H. m) assigned to the pyridinium protons β to the charged nitrogen atom, (H_2),

iii) δ_H 9.31 - 9.33 (8H, m), assigned to the pyridinium protons α to the charged nitrogen atom, (H_1),

iv) δ_H 7.98 (4H, s) and δ_H 8.03 (4H, s) assigned to the phenylene protons.

In the case of "bluebox" on its own, without a guest, the shifts are given by Stoddart and coworkers[10a] as:

i) δ_H 5.74 (8H, s) assigned to the methylene protons (H_3);

ii) δ_H 8.16 (8H, d) assigned to the pyridinium protons β to the charged nitrogen (H_2);

iii) δ_H 8.86 (8H, d) assigned to pyridinium protons α to the charged nitrogen atom (H_1);

iv) δ_H 7.52 (8H, s) assigned to the phenylene protons .

The product, **14**, shows two singlets for the methylene protons at δ 5.93 ppm, two doublets for the α pyridinium protons and two doublets for the β pyridinium protons. A plausible explanation for the doubling up of ^{1}H NMR signals is that **13** exists as two unique diastereomers due to the chiral iron atoms. Each diastereomer therefore gives a unique rotaxane which thus results in the observed doubling up of the ^{1}H NMR signals. This evidence further suggests that **13** is encircled by "bluebox".

The shift data is given in table 3.4.1 below for an easy comparison.

Table 3.4.1. Comparative shift data.

Compd.	H_1	H_2	H_3
14	9.47	8.71	5.93
20[33]	9.31 - 9.33	8.16 - 8.19	5.97
"bluebox"[10a]	8.86	8.16	5.74

The observed ^{1}H NMR shifts for **14** are more in agreement with Benniston and Harriman's[33] rotaxane, **20**, suggesting that **13** is actually encircled by "bluebox". Furthermore, the polarity of **14** (slightly less polar than bluebox) and the slight orange-yellow colour of the spot observed on thin layer chromatography suggest that **13** was encirled by "bluebox" yielding the rotaxane **14**.

Unfortunately, further purification of the sample of **14** by chromatography did not give a better ^{1}H NMR spectrum.

The high yield of bluebox, 52mg (30%), indicated that **13** templates the synthesis of "bluebox" from "horseshoe" since in the absence of a polyether thread, at standard room temperature and pressure in dry CH_3CN, the highest observed yield of bluebox synthesised from horseshoe and dibromoxylene is 12%[18].

Figure 3.4.1. ^{1}H NMR spectrum of **14** in (DMSO-d_5).

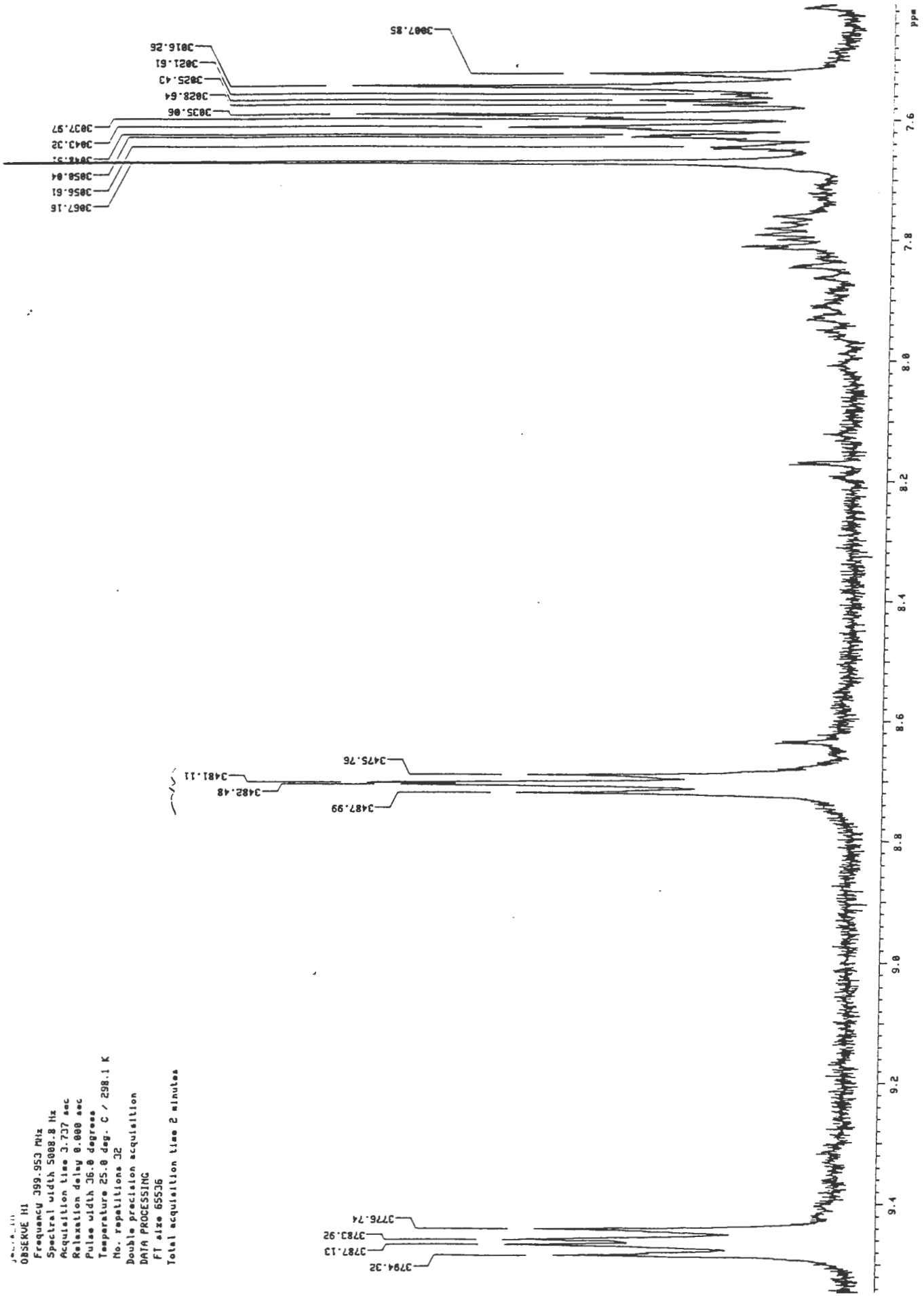

Figure 3.4.1. ^{1}H NMR spectrum of **14** in (DMSO-d_6) continued.

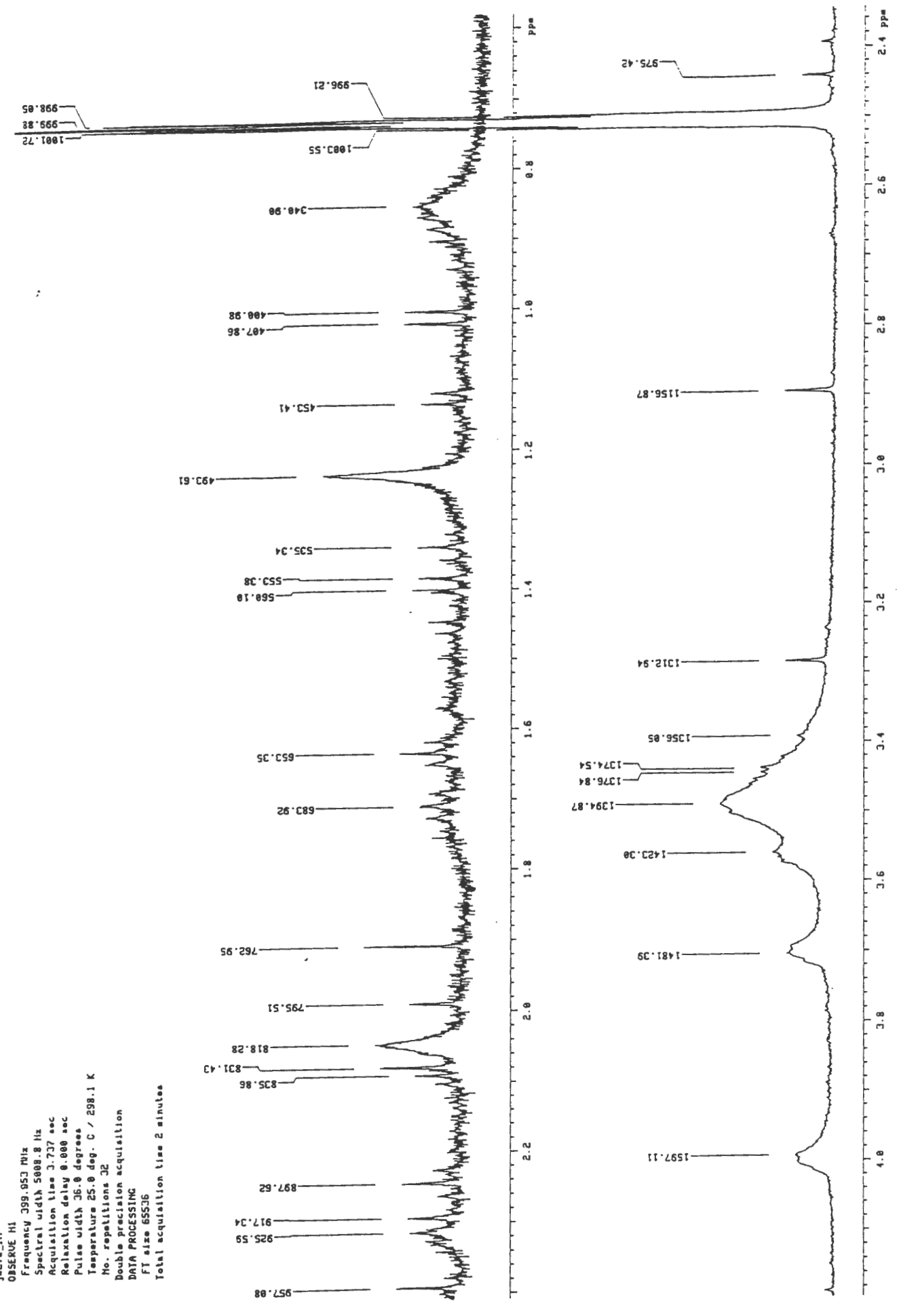

Figure 3.4.1. ^{1}H NMR spectrum of **14** in (DMSO-d_6) continued.

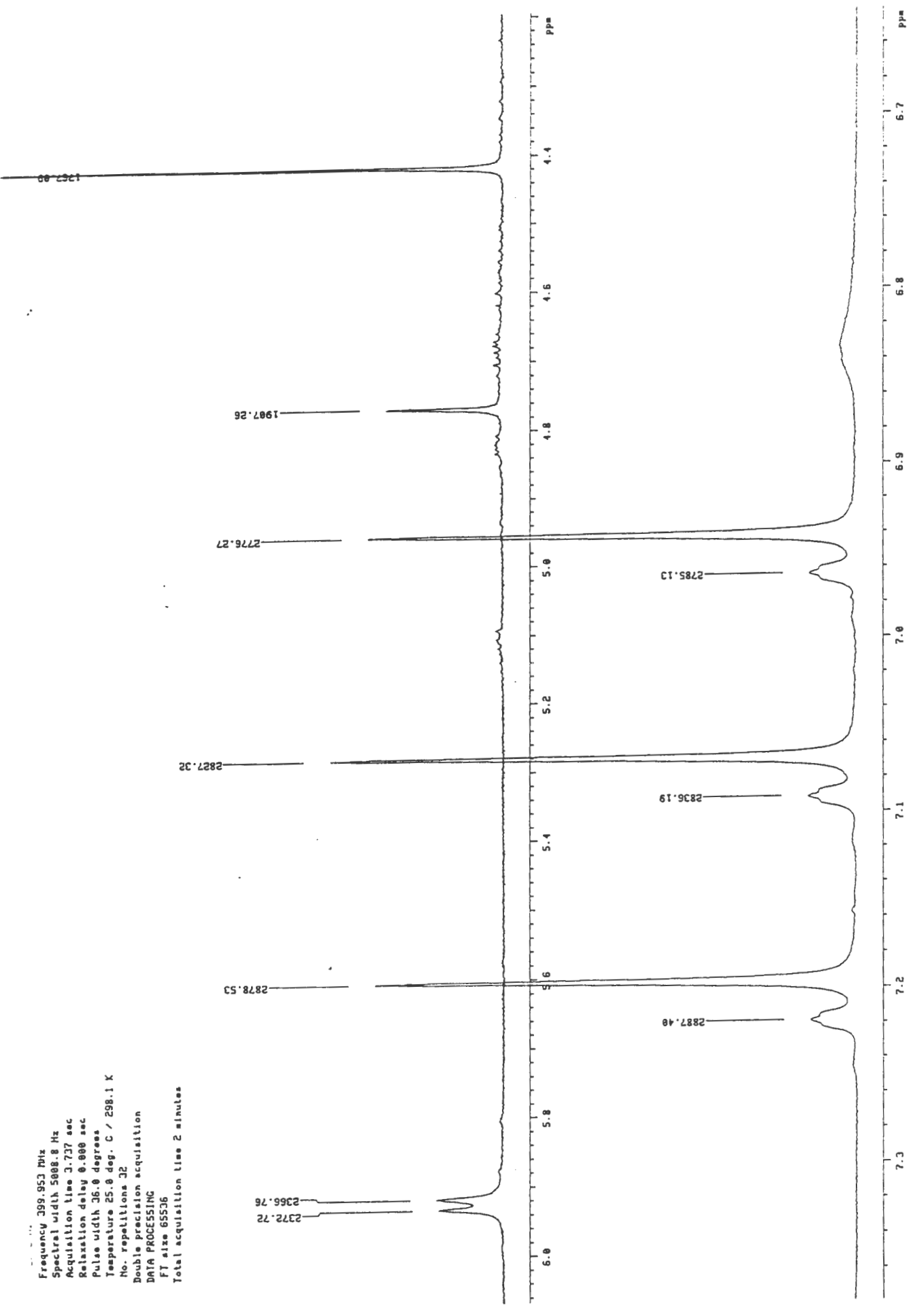

Figure 3.4.1. ^{1}H NMR spectrum of **14** in (DMSO-d_6).

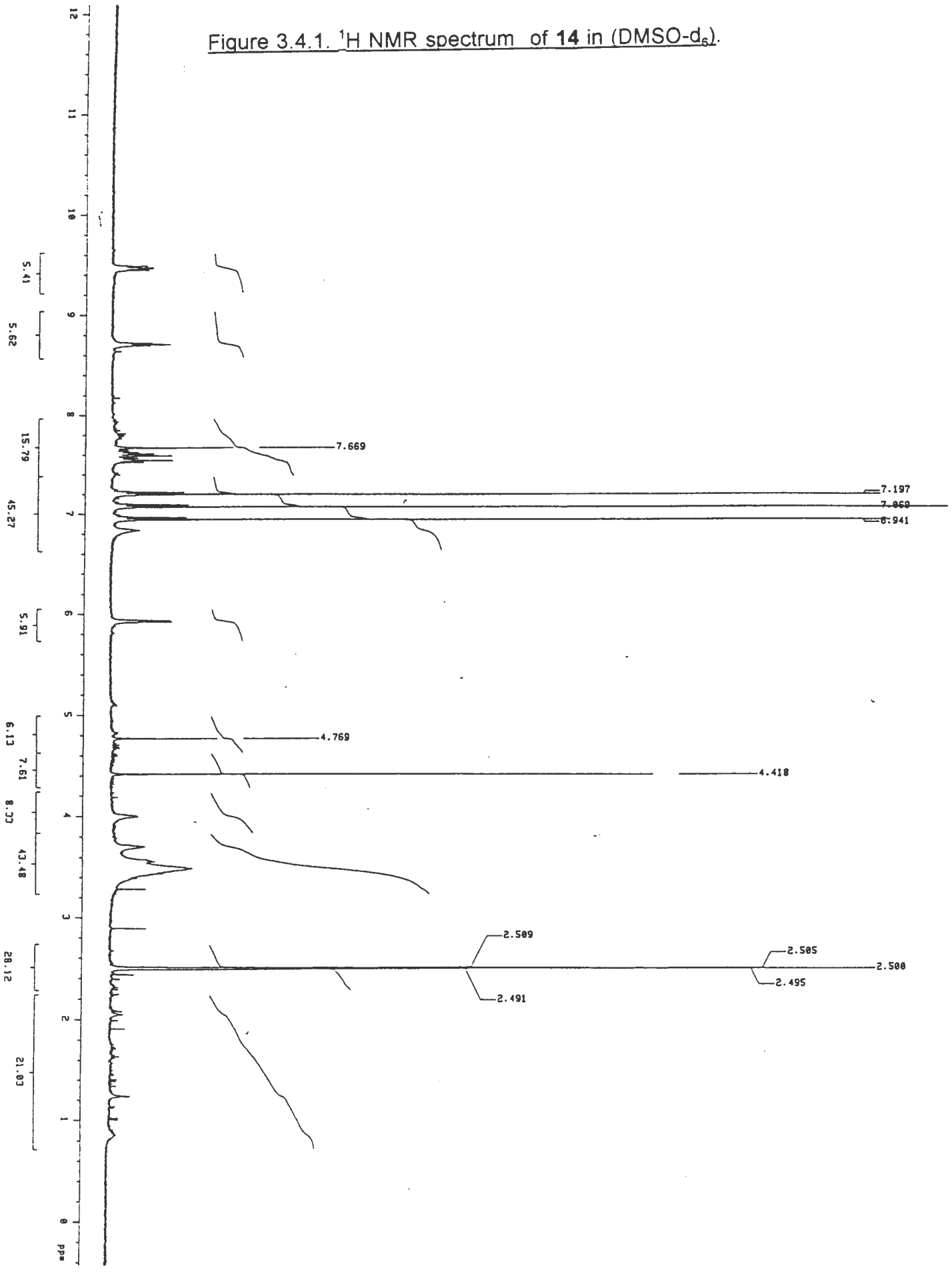

Figure 3.4.2. ^{1}H NMR spectrum of the sample of "Horseshoe" in (DMSO-d_6).

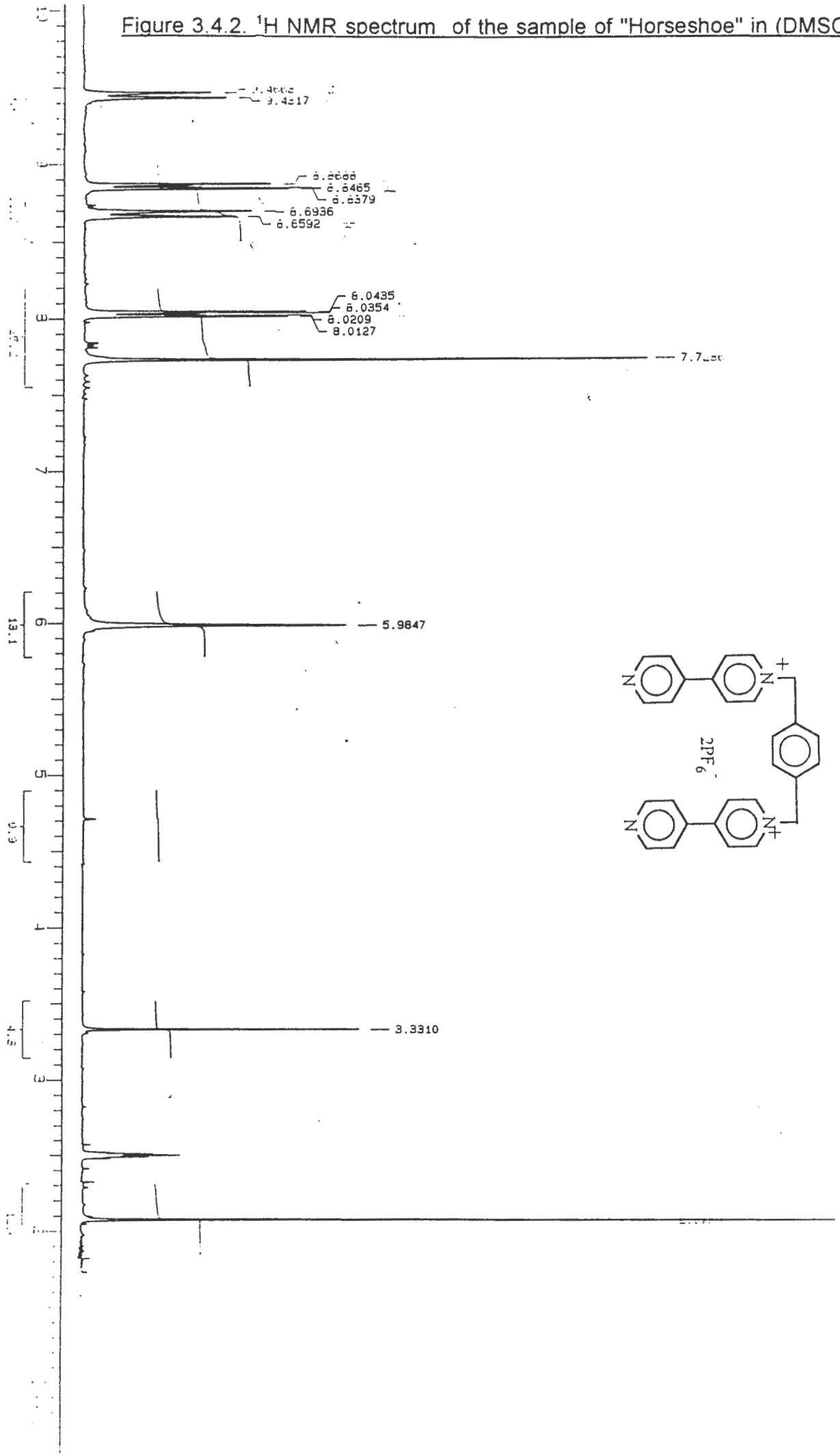

3.5 Conclusion.

The synthetic work completed for this thesis has established a route to organometallic polyethers suitable for rotaxane synthesis. The attempted synthesis of a rotaxane using iron-organometallic blocking groups produced a compound whose ^{1}H NMR data supports a rotaxane structure; however this compound could not be obtained analytically pure.

The only organometallic system used was based on iron; an analogous ruthenium polyether analogue may be synthesised by the same route. Such a ruthenium analogue would be more stable, and more likely to lead to the isolation and definitive characterisaton of a rotaxane. An attempt to prepare a rotaxane using the diiron polyether, **12** resulted in immediate decomposition of **12**, thought to be the result of oxidation of the iron centres with reduction of the tetracationic cyclophane, bluebox. To improve the stability of the iron-organometallic system, use of the triphenylphosphine substituted iron-acyl system was considered leading to the synthesis of **13**. The recovery of 62% of **13**, from the clipping reaction is indicative of the stability of this system and the isolation of 52mg of the tetracationic cyclophane, "bluebox", shows that the thread templated the formation of bluebox.

Use of the synthetic methods established in this research may be expected to lead to the synthesis of a new class of organometallic rotaxanes having metal - carbon σ-bonds. This in turn could lead to interesting research centred around the oxidation state of the metal centres and the influence thereof on "bluebox" and its shuttling processes[33].

Chapter 4

Experimental.

General.

All reactions were performed under an atmosphere of high purity nitrogen using Schlenk tube techniques unless otherwise stated.

$[CpFe(CO)_2]_2$ was purchased from Strem Chemicals Inc. and was used without further purification. PPh_3, $Br(CH_2)_3Cl$, $Br(CH_2)_4Cl$, hydroquinone, allyl bromide, carbon tetrabromide, 9-borabicyclo[3,3,1]nonane, tosyl chloride, dibromoxylene and 4,4'-bipyridine were bought from Aldrich Chemical Company, Inc.

The solvents used were generally analytical grade and were purified as follows:
THF, hexane and benzene were purified by distilling under a nitrogen atmosphere from Na / benzophenone; dichloromethane was distilled over $CaCl_2$ and CH_3CN was distilled over CaH_2.

Silica gel (70 - 230 mesh) was purchased from Merck. Aluminium oxide (70 - 230 mesh) was purchased from Merck. The aluminium oxide was deactivated as follows: a 50% slurry of the aluminium oxide in water was prepared and allowed to stand for two hours at room temperature. The water was then decanted and the aluminium oxide allowed to dry in an oven at 120°C for 24 hours.

^1H and ^{13}C NMR were recorded on a Varian VXR 200 (200.057 MHz and 50.31 MHz respectively) or a Varian unity 400 MHz (399.951 MHz and 100.579 MHz respectively) spectrometer. Tetramethyl silane was used as an internal reference and chemical shifts are given in δ downfield of TMS (δ 0.00). Routine ^1H NMR spectra were recorded on a Varian EM 360 (60 MHz) spectrometer.

Mass spectra were recorded on a VG micromass 16F mass-spectrometer at 70eV with an accelerating voltage of 4kV or at the mass-spectrometry unit of the Cape Technikon. Elemental analyses for C and H were carried out using a Heraeus CHN-rapid combustion analyser.

All reactions were monitored by thin layer chromatography using Merck t.l.c. aluminium sheets, silica gel 60 F_{254}, layer thichness 0.2 mm. Detection was done using an ultra violet lamp.

Melting points were determined on a Kofler hotstage microscope (Reichert Thermovar) and are uncorrected.

4.1. Experimental details for Chapter 2.

4.1.1. Synthesis of 1,4-bis[3-chloropropoxy]benzene, **1**.

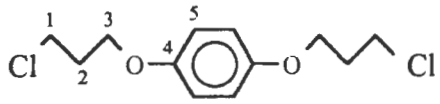

1

A 250 cm^3 2-necked flask was fitted with a reflux condenser with nitrogen inlet tap and charged with hydroquinone (2.75g, 25mmol), 3-bromo-1-chloropropane (7.85g, 50 mmol), K_2CO_3 (7.0g, 50mmol), 18-crown-6 (0.1g) and acetonitrile (80cm^3). The reaction was followed using thin layer chromatography (Tlc R_f = 0.63 in 20% ethyl acetate / 80% hexane.) After refluxing for 48 hours, the reaction was quenched with 50 cm^3 of saturated aqueous ammonium chloride and the product extracted with ethyl acetate (3X100 cm^3). The combined extracts were dried with magnesium sulphate, filtered and the solvent removed under reduced pressure. The crude product, isolated as an off-white solid, was purified by chromatography on 80g of silica gel. Initially, hexane was used as the eluent and the solvent polarity was increased in increments of 5% ethyl acetate until the product eluted (20% ethyl acetate / 80% hexane). The product-containing fractions were combined, the solvent removed and the product isolated as a white solid (5.63g, 86%). Further purification was accomplished by multiple recrystallisations from hot hexane to give needle-like crystals, m.p. 66-67°C.

IR ν_{max} (CCl_4): 2965 cm^{-1}, 2927, 1508, 1230, 807, 760 cm^{-1}.

MS, m/z: 262 (M^+, 44%), 186 (16%), 110 (100%), 109 (48%), 77 (12%), 41 (67%), 28 (52%).

δ_H (200MHz) 2.21 (4H, q, ^3J = 6.12Hz, $H_{2'}$), 3.74 (4H, tr, ^3J = 6.40 Hz, $H_{1'}$), 4.07 (4H, tr, ^3J = 5.89Hz, $H_{3'}$), 6.84 (4H, s, $H_{5'}$).

δ_C (50MHz) 32.4 (C_2), 41.5 (C_1), 65.0 (C_3), 115.5 (C_5), 153.0 (C_4).

Found: C, 54.6; H, 6.17; $C_{12}H_{16}O_2Cl_2$ requires C, 54.8 H, 6.13%.

4.1.2. Synthesis of 1,4-bis[4-chlorobutoxy]benzene, **2**.

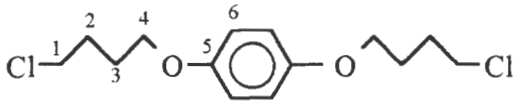

2

A 2-necked 100 cm^3 flask was fitted with reflux condenser and nitrogen inlet tap and charged with hydroquinone (1.1g, 10 mmol.), 4-bromo-1-chlorobutane (2.5 ml, 2.2mmol.), K_2CO_3 (1.21g, 22 mmol.), 18-crown-6 (0.05g) and acetonitrile (80cm^3). The reaction was followed by thin layer chromatography (Tlc R_f = 0.68 in 20% ethyl acetate / 80% hexane.) After refluxing for 48 hours, the reaction was quenched with 25 cm^3 of saturated aqueous ammonium chloride and the product extracted with ethyl acetate (3X50cm^3). The combined extracts were dried with magnesium sulphate, filtered and the solvent removed under reduced pressure. The crude product was isolated as an off-white solid and purified by chromatography on 40g of silica gel using gradient elution as explained for **1** previously. Further purification was similarly accomplished by multiple recrystallisations from hot hexane to give needle shaped crystals, (2.18g, 75%), m.p. 75-77°C.

IR ν_{max} (CCl_4) 2965, 2927, 1508, 1230, 807, 760 cm^{-1}.

MS, m/z: 290 (M^+, 41%), 200 (12%), 110 (100%), 109 (26%), 91 (100%), 81 (17%), 55 (100%), 29 (64%), 28 (53%), 27 (43%).

δ_H (200MHz) 1.94 (8H, m, H_2 & H_3), 3.62 (4H, tr, ^3J = 6.31 Hz, H_1), 3.95 (4H, tr, ^3J = 5.89 Hz, H_4.), 6.84 (4H, s, H_6.).

δ_C (50MHz) 26.7 (C_2), 29.3 (C_3), 44.7 (C_1), 67.6 (C_4), 115.4 (C_6), 153.1 (C_5).

Found: C, 57.7; H, 6.92; $C_{14}H_{20}O_2Cl_2$ requires: C, 57.2 H, 6.97.

4.1.3. Synthesis of 1,4-bis-(cyclopentadienyldicarbonyliron-3-propoxy)benzene, **3**.

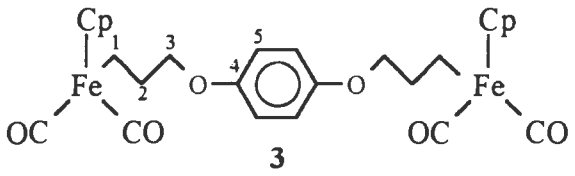

3

A 0.75 M solution of $Na[CpFe(CO)_2]$ was prepared by vigorously stirring $[CpFe(CO)_2]_2$ (1.33g, 3.75 mmol) in THF ($10cm^3$) over sodium amalgam (4 cm^3 Hg / 0.4g Na) for three hours during which time the colour of the solution changed from red to pale brown.

The dihalide, 1,4-bis[3-chloro-1-propoxy]benzene, **1**, (0.328g, 1.25 mmol), was dissolved in the minimum amount of THF and cooled to 0°C in a Schlenk tube equipped with a septum and nitrogen inlet tap. $Na[CpFe(CO)_2]$ (2.5 mmol, 3.75 cm^3 of the 0.75 M solution) was syringed slowly, over a period of 5 minutes, into the cooled dihalide solution. The reaction was kept at 0°C for one hour after which time the ice bath was removed and the reaction allowed to equilibrate to room temperature and left to stir for a further 8 hours at room temperature. The product was isolated by removing the THF under reduced pressure, the resultant green residue was extracted with dichloromethane (3 x 20 cm^3) and the extract filtered and solvent removed to give a viscous oil which crystallised rapidly. The product was purified by recrystallisation from hot hexane with a few drops of dichloromethane added to increase solubility, and isolated as bright yellow crystals (0.39g, 57%). (m.p. 140 - 142°C).

IR ν_{max} (CCl_4) 3024, 2937, 2006, 1949, 1506, 1229, 758 cm^{-1}.

MS, m/z: 490 (M^+-2CO, 18%); 368 (10%); 326 (27%); 247 (14%); 206 (10%); 186 (19%); 177 (15%); 149 (20%);121 (100%); 97 (6%).

δ_H (200MHz) 1.44 (4H, m, H_1), 1.89 (4H, m, H_2), 3.84 (4H, tr, ^3J = 6.7Hz, H_3), 4.76 (10H, s, Cp), 6.82 (4H, s, H_5).

δ_C (50MHz) -2.4 (C_1), 37.3 (C_2), 71.5 (C_3), 85.4 (Cp) 115.4 (C_5), 153.2 (C_4), 217.3 (carbonyls).

Found: C, 57.2; H, 4.87; $C_{26}H_{26}O_6Fe_2$ requires C, 57.2; H, 4.80%.

4.1.4. Synthesis of 1,4-bis-(4-cyclopentadienyldicarbonyliron-1-butoxy)benzene, **4**.

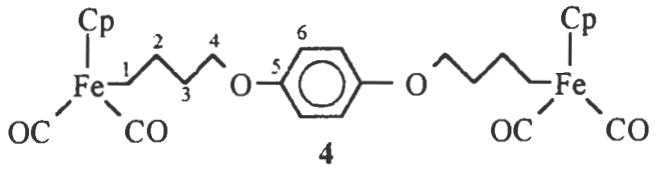

4

A 0.75 M solution of $Na[CpFe(CO)_2]$ was prepared as described above. The dihalide, 1,4-bis-[4-chloro-1-butoxy]benzene, **2**, (0.363g, 1.25 mmol.) was dissolved in the minimum amount of THF and cooled to 0°C in a Schlenk tube equipped with a septum and nitrogen inlet tap. $Na[CpFe(CO)_2]$ (2.5 mmol, 3.75 cm^3 of the 0.75 M solution) was slowly syringed into the dihalide solution over 8 minutes. The reaction was kept at 0°C for one hour followed by a further 8 hours at room temperature. The product was isolated by removing the THF under reduced pressure, the resultant green residue was extracted with dichloromethane (3 x 20 cm^3) and the extract filtered and solvent removed. The product was purified by recrystallisation from hot hexane with a few drops of dichloromethane added and isolated as golden yellow crystals (0.503g, 70%). (m. p. 140 - 143°C)

IR ν_{max} (CCl_4) 3025, 2942, 2007, 1951, 1506, 1226, 753 cm^{-1}.

MS, m/z: 518(M^+-2CO, 10%), 452 (17%), 340 (19%), 274 (31%), 110 (28%), 55 (21%), 28 (100%).

δ_H (200MHz) 1.52 (8H, m, H_1 & H_2), 1.78 (4H, q, ^3J = 6.2Hz, H_3), 3.91 (4H, tr, ^3J = 6.4Hz, H_4), 4.74 (10H, s, Cp), 6.83 (4H, s, H_6).

δ_C (50MHz) 2.8 (C_1), 34.2 (C_2), 34.3 (C_3), 68.3 (C_4), 85.3 (Cp), 115.5 (C_6), 153.2 (C_5), 217.6 (carbonyls).

Found: C, 58.3; H, 5.33 %; $C_{28}H_{30}O_6Fe_2$ requires C, 58.6; H 5.27%.

4.1.5. Synthesis of the bis(triphenylphoshine)diacyldiiron product **5**.

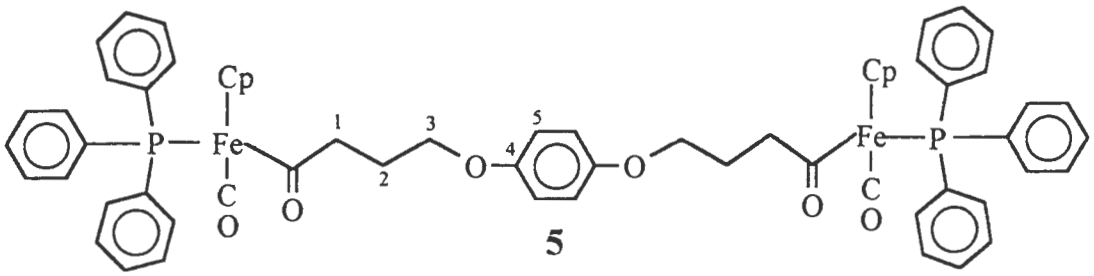

5

The product **5** was prepared by refluxing **3** (0.240 g, 0.44 mmol.) with triphenylphosphine (0.231g, 0.88 mmol.) in benzene ($10cm^3$) for 6 hours under nitrogen. The solvent was removed under reduced pressure and the resultant gum extracted with diethyl ether (4 X 10 cm^3), the combined extracts filtered and the solvent removed under reduced pressure. The brownish product mixture was investigated using thin layer chromatography with 20 % CH_2Cl_2 / 80 % hexane, 50 % CH_2Cl_2 / 50 % hexane and CH_2Cl_2. The reaction mixture was found to contain residual starting materials (**3** and triphenylphosphine), the desired more polar bis(triphenylphoshine)diacyldiiron product and a slightly less polar product which was probably the mono(triphenylphosphine)monoacyldiiron product formed by mono-substitution with carbonyl insertion (see ref. 6). This mixture, as a brown oil, was applied to an alumina column using 30 g of alumina, packed as a hexane slurry. Gradient elution using increments of 10% CH_2Cl_2 resulted in elution of unreacted starting materials (initially triphenylphosphine followed by **3**) with 20% CH_2Cl_2 / 80% hexane; 50% CH_2Cl_2 / 50% hexane eluted the less polar product which we thought to be the mono-substituted product. The bis(triphenylphoshine)diacyldiiron product, **5**, started to elute slowly with neat CH_2Cl_2. The solvent was changed to 50% CH_2Cl_2 / 50% diethylether which sped up elution of product **5**. Product **5** was isolated in 46% yield (0.205 g) as an orange powder. (m. p. 192-194^{0}C)

IR ν_{max} (CCl_4) 3059, 2927, 1919, 1610, 1507, 1434, 1231, 763 cm^{-1}.

δ_H (200MHz) 1.55 (4H, m, H_2), 2.71 (2H, dt, H_1), 3.05 (2H, dt, H_1), 3.55 (4H, m, H_3), 4.49 (10H, s, Cp), 6.72 (4H, s, H_5), 7.35 (30H, m, $P(C_6\underline{H}_5)_3$).

Bis(triphenylphoshine)diacyldiiron product, **5**, continued.

δ_C (50MHz) 24.9 (C_2), 61.7 & 61.8 (C_1), 68.0 (C_3), 85.2 (Cp), 115.3 (C_5), 127.9 - 136.9 ($P(C_6H_5)_3$), 153.0 (C_5), 220.2 (carbonyl

Found: C, 69.0; H, 5.46 %; C_{62} H_{56} Fe_2 O_6P_2 requires C, 69.5; H 5.27

4.2. Experimental details for Chapter 3.

4.2.1. Synthesis of the dibromide, **7**.

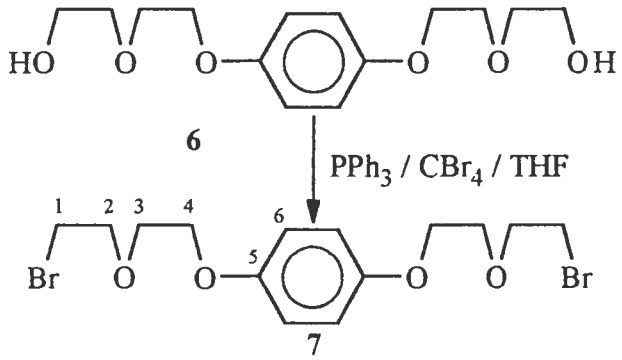

Diol, **6**, previously prepared by Stoddart and coworkers[18] was brominated by dissolving the diol, **6**, (0.43g, 1.5mmol) in THF (10cm^3) in a 2-necked 50 cm^3 round bottom flask equipped with nitrogen inlet tap and septum. To this solution was added, all at once, triphenylphosphine (0.943g, 3.6 mmol.) and CBr_4 (1.2g, 3.6 mmol.) and the reaction mixture was stirred at room temperature for one hour, after which time the reaction was quenched by the addition of water (10 cm^3), extracted with dichloromethane (3X10cm^3) and the product purified by column chromatography (the dibromide eluted with 15% ethyl acetate in hexane). The dibromide was isolated as a glassy matrix (0.72g, 86%).

IR ν_{max} (CCl_4): 2926, 1507, 1231, 801, 770 cm^{-1}.

MS, m/z: 412 (M^+, 19%), 260 (5%), 151 (11%), 109 (100%), 107(96%).

Dibromide, **7** continued.

δ_H (200MHz) 3.49 (4H, t, ^3J= 6.0 Hz, H_1), 3.87 (8H, m, H_2 & H_3), 4.09 (4H, m, H_4), 6.85 (4H, s, H_6).

δ_C (50MHz) 30.2 (C_1), 68.2 (C_2), 69.8 (C_3), 71.4 (C_4), 115.9 (C_6), 153.1 (C_5).

High resolution mass spectrometry: Found: 409.9721; $C_{14}H_{20}O_4Br_2$ requires 409.9728.

4.2.2. Synthesis of the bis-allyl product, **8**.

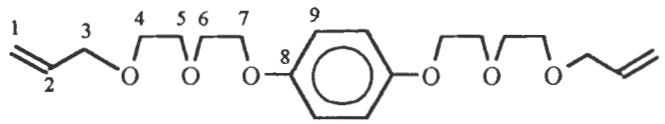

8

Diol, **6**, (1.14g, 4.0 mmol.) was dissolved in THF (40 cm^3) in a 2-necked round bottom flask equipped with a nitrogen inlet tap, magnetic stirrer and septum. To this solution was added allyl bromide (0.7cm^3, 8.0 mmol.) and sodium hydride (0.29g, 9.0 mmol. (80% in oil)). This solution was stirred for two hours and the course of the reaction was followed by thin layer chromatography by checking for the disappearance of the diol precursor. The reaction was quenched by very slow (!) addition of water and the crude product was extracted into dichloromethane. The crude yield was well in excess of 100% due to the presence of the oil from the sodium hydride. The crude product was purified by gradient elution on a silica column. The desired bis-allyl product eluted with 30% ethyl acetate / 70% hexane and isolated as an oil in 100% yield. The bis-allyl product was readily detected using thin layer chromatography with 50% ethyl acetate / 50% hexane to give a strongly UV active spot with R_f = 0.75.

IR ν_{max} (CCl_4) 3080, 2922, 1507, 1232, 995, 926, 803, 764 cm^{-1}.

MS, m/z: 366, (26%), 322 (2%), 129 (11%), 110 (6%), 85 (24%), 41 (100%).

δ_H (200MHz) 3.58 - 4.09 (20H, m, H_3, H_4, H_5, H_6, H_7.), 5.19 (4H, m, H_1), 5.89 (2H, m, H_2), 6.83 (4H, s, H_9).

δ_C (50MHz) 68.0, 69.4, 69.8, 70.7, 72.2, (C_3, C_4, C_5, C_6, C_7.)
115.5 (C_9), 117.0 (C_1), 134.6 (C_2), 153.2 (C_8).
High resolution mass spectrometry: Found: 366.2047; $C_{20}H_{30}O_6$ requires 366.2042.

4.2.3. Synthesis of the diol product, **9**.

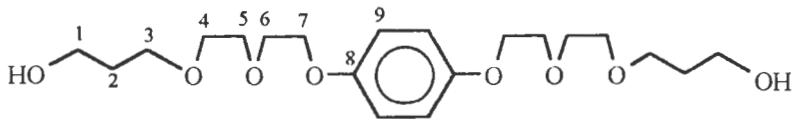

9

This diol was synthesised by a sterically controlled hydroboration-oxidation reaction. Bis-allyl product, **8**, (1.15g, 3.1mmol.) was dissolved in THF (15cm^3) in a 100 cm^3 2-necked flask equipped with nitrogen inlet tap, magnetic stirrer and septum. The THF solution of bis-allyl product was cooled to 0°C in an ice bath and 9-BBN (6.25 mmol., 12.5 cm^3 of a 0.5 M solution) was slowly syringed into the THF solution. The temperature of the hydroboration was kept at 0°C for one hour after which time the ice bath was removed and the reaction allowed to equilibrate to room temperature. The hydroboration reaction was allowed to stir for a further 8 hours after which time the reaction mixture was cooled to 0°C and the aqueous oxidant solution was slowly added by syringe. The aqueous oxidant solution was prepared by dissolving NaOH (0.15g) in methanol (5cm^3), to which was added 30% H_2O_2 (0.86 cm^3). Methanol was added by Pasteur pipette until the solution became homogenous. The oxidation step was stirred at 0°C for one hour after which time the ice bath was removed and the oxidation allowed to stirr for a further 18 hours at room temperature. The resulting solution was then extracted with ethyl acetate (4 X 20 cm^3), dried over magnesium sulphate and the solvent removed under reduced pressure. The crude product was an off-white coloured gum. Thin layer chromatographic investigation of this gum suggested that the desired diol product was a very polar compound having an R_f= 0.21 in neat ethyl acetate. In addition a polar spot was identified having an R_f = 0.50 in neat ethyl acetate and this spot was thought to be due to 9-BBN borinic acid residues. This off-white coloured gum was dissolved in the minimum ammount of solvent (80% ethyl acetate / 20% hexane) and applied to a column made up with a slurry of silica (80g) in 30% ethyl acetate / 70% hexane. Gradient elution in increments of 10% ethyl acetate / 50cm^3 was used and the borinic acid residues were

eluted by 80% ethyl acetate, 20% hexane. Gradient elution was then continued through 90% ethyl acetate / 10% hexane till 100% ethyl acetate was reached after which time the solvent system was changed to 2% methanol / 98% ethyl acetate and the polarity of this solvent was increased in increments of 2% methanol / 50cm^3. The desired polar diol product began to elute slowly with 10% methanol / 90% ethyl acetate and no further diol could be detected by thin layer chromatography in the eluent by the time 20% methanol / 80% ethyl acetate eluent was in use. The diol, **9**, was isolated as a golden yellow syrup in 56% yield.

IR ν_{max} (CCl_4) 3520, 3049, 2923, 1507, 1232, 803, 760 cm^{-1}.

MS, m/z:402 (70%), 344 (5%), 256 (4%), 147 (22%), 110 (16%).

δ_H (200MHz) 1.79 (4H, q, ^3J = 5.7Hz, H_2), 2.85 (2H, br s, -OH),
3.60 - 4.07, (24H, m, H_1, H_3, H_4, H_5, H_6, H_7), 6.81 (4H, s, H_9).

δ_C (50MHz) 31.9 (C_2), 61.3 (C_1), 68.0, 69.8, 70.0, 70.2, 70.6, (C_3, C_4, C_5, C_6, C_7.)
115.5 (C_9), 153.0 (C_8).

Found: C, 59.5; H, 8.55 %; C_{20} H_{34} O_8 requires C, 59.7; H 8.51.

Note that both the allylation and hydroboration-oxidation reactions were scaled up and repeated in order to accumulate enough product to proceed with subsequent reactions.

4.2.4. Synthesis of the bis-tosylpolyether, **10**.

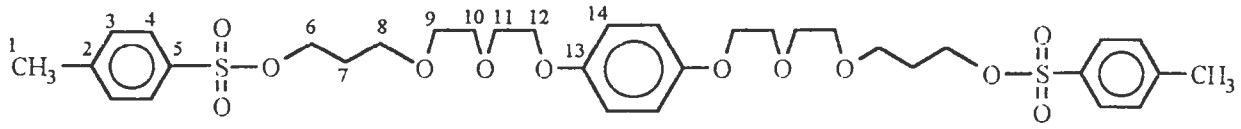

10

Diol, **9**, (2.0g, 5 mmol.) was dissolved in a solvent made up using a mixture of pyridine (1.58g, 20mmol.) and ethyl acetate (20 cm^3) in a 100 cm^3 2-necked flask equipped with nitrogen inlet tap, septum and magnetic stirrer. This solution was cooled to 0°C in an ice bath, tosyl chloride (2.3g, 12 mmol.) was added all at once and the reaction mixture allowed to stir for 12 hours. The ethyl acetate was then removed under reduced pressure using a rotary evaporator and the pyridine was removed under high vacuum. The crude product was chromatographed on silica gel (60g), eluted with 75% ethyl acetate / 25% hexane and the final product isolated in 40% yield as a viscous oil. This procedure was used in preference to the normal tosylation work-up (crystallisation on ice) since an initial attempt showed that the tosylate was highly labile and would not crystallise with the ice work-up and therefore required a solvent extraction.

IR ν_{max} (CCl_4) 2905, 1508, 1084, 820, 756 cm^{-1}.

MS, m/z: 710 (M^+, 100%), 539 (56%), 410 (100%), 368 (25%), 180 (85%) 171 (52%), 155 (100%) 110 (100%).

δ_H (200MHz) 1.90 (4H, q, ^3J = 6.08 Hz, H_7), 2.42 (6H, s, H_1), 3.6 - 4.2, (24H, m, H_6, H_8, H_9, H_{10}, H_{11}, H_{12}), 6.82 (4H, s, H_{14}), 7.32 (4H, d, ^3J = 8.1 Hz, H_3), 7.77 (4H, d, ^3J = 8.1 Hz, H_4)

δ_C (50MHz) 21.6 (C_1), 29.3(C_7), 66.6, 67.7, 68.0, 69.8, 70.3, 70.6 (C_6, C_8, C_9, C_{10}, C_{11}, C_{12}), 115.6 (C_{14}), 127.9 (C_2), 129.8 (C_3), 133.1 (C_4), 144.7 (C_5), 153.1 (C_{13}).

High resolution mass spectrometry: Found: 710.2438; $C_{34}H_{46}O_{12}S_2$ requires 710.2431.

4.2.5. Synthesis of the dibromopolyether, **11**.

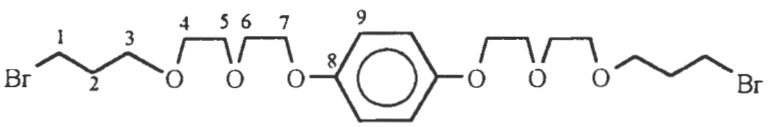

11

Diol, **9**, (0.603g, 1.5mmol.), triphenylphosphine (1.10g, 3.3mmol.) and CBr_4 (2.30g, 12 mmol.) were dissolved in 10 cm^3 of THF in a 50 cm^3 2-necked flask equiped with nitrogen inlet tap, septum and magnetic stirrer. The reaction was allowed to stirr for 2 hours at room temperature after which time the product was investigated using thin layer chromatography with 50% dichloromethane / 50% hexane; the R_f values were as follows: dibromide, R_f = 0.26; triphenylphosphine, R_f = 0.76; CBr_4 R_f = 1.00. The reaction was quenched by adding 20cm^3 of water and extracted with dichloromethane(3X15cm^3). The extracts were combined and the crude product chromatographed on silica gel using 50% dichloromethane / 50% hexane followed by 50% ethyl acetate / 50% hexane as elution solvents. The dibromopolyether was isolated as a clear oil in 64% yield. This oil formed a gold coloured wax at -30°C which promptly reverted back to the oil at room temperature.

IR ν_{max} (CCl_4) 2874, 1507, 1232, 760, 523 cm^{-1}.

MS, m/z: 528 (M^+, 72%), 318 (4%), 209 (23%), 165 (25%), 121 (74%), 110 (24%), 41 (100%), 28 (27%).

δ_H (200MHz) 2.09 (4H, q, ^3J = 6.3 Hz, H_2), 3.50 (4H, t, ^3J = 6.6Hz, H_1)
3.56 - 3.84 (20H, m, H_3, H_4, H_5, H_6), 4.07 (4H, t, ^3J = 5.2Hz, H_7)
6.84 (4H, s, H_9).

δ_C (50MHz) 30.6 (C_2), 32.7 (C_1), 68.0, 68.6, 69.8, 70.3, 70.7, (C_3, C_4, C_5, C_6, C_7.),
115.5 (C_9), 153.0 (C_8).

Found: C, 45.9; H, 6.28 %; C_{20} H_{32} O_6Br_2 requires C, 45.5; H 6.11.

4.2.6. Synthesis of the diironpolyether, **12**.

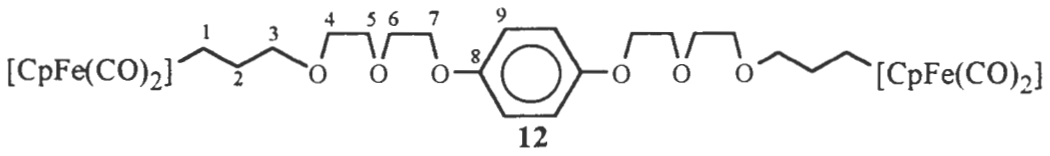

12

Note that **12** was prepared from both **10** and **11**. Both procedures are given here and both involve the use of excess $Na[CpFe(CO)_2]$ as a THF solution.

1). Synthesis of **12** using the bis-tosylpolyether, **10.**

$[CpFe(CO)_2]_2$, (0,28g, 0.79 mmol.) was dissolved in THF ($1.5cm^3$) over sodium amalgam (0.1g Na / $1cm^3$ Hg) in a small Schlenk tube. This solution was stirred vigorously for three hours during which time the colour of the solution changed from red to pale brown yielding a solution of $Na[CpFe(CO)_2]$. Bis-tosylpolyether, **10**, (0.23g, 0.32 mmol.) was dissolved in $2cm^3$ of freshly distilled THF in a $50cm^3$ 2-necked flask and this solution was cooled down to -78°C in a dry ice / acetone bath. The $Na[CpFe(CO)_2]$ solution was syringed dropwise into the cooled bis-tosylpolyether solution over a period of 5 minutes. The temperature of the reaction mixture was kept at -78°C for one hour after which time the dry ice bath was removed and stirring continued for a further hour after which the solvent was removed under reduced pressure and the residue extracted with dichloromethane ($3X50cm^3$). The product was investigated using thin layer chromatography (tlc.) prior to chromatography and this data is tabulated in Table 4.2.6.

Table 4.2.6. tlc. observations for the diironpolyether, **12**.

tlc. Solvent.	Remarks and R_f values.
Et_2O	A single spot observed running on the solvent front.
CH_2Cl_2	$[CpFe(CO)_2]_2$ spot ran with the solvent front and a large yellow spot observed extending from R_f= 0.71 to R_f= 0.93.
70% CH_2Cl_2 / 30% Hexane.	$[CpFe(CO)_2]_2$ spot ran with the solvent front and a large yellow spot observed extending from R_f= 0.67 to R_f= 0.86.
40% CH_2Cl_2 / 60% Hexane.	$[CpFe(CO)_2]_2$ spot ran to R_f=0.82 and a large yellow spot observed extending from R_f= 0 to R_f= 0.27.

The resulting viscous brown oil was chromatographed on alumina (35g) using 40% dichloromethane / 60% hexane initally, followed by 70% dichloromethane / 30% hexane, and finally dichloromethane which began to elute the product slowly. The eluent was changed to 50% dichloromethane / 50% diethyl ether which eluted the product. The eluent was removed under reduced pressure and the product isolated as a viscous yellow oil (0.123g, 44%).

2). Synthesis of **12** using the dibromopolyether, **11**.

$[CpFe(CO)_2]_2$, (0.57g, 1.6 mmol.) was dissolved in THF ($3cm^3$) over sodium amalgam (0.2g Na / $2cm^3$ Hg) in a small Schlenk tube. This solution was stirred vigorously for three hours during which time the colour of the solution changed from red to pale brown which yielded a solution of $Na[CpFe(CO)_2]$. Dibromopolyether, **11**, (0.43g, 0.81 mmol.) was dissolved in THF ($5cm^3$) in a $50cm^3$ 2-necked flask and cooled to -78°C in a dry ice / acetone bath. The $Na[CpFe(CO)_2]$ solution was slowly syringed into the cooled dibromopolyether solution over 5 minutes.

The temperature of the reaction mixture was kept at -78°C for one hour after which the dry ice / acetone bath was removed and stirring continued for a further hour. The solvent was removed under reduced pressure, the residue extracted with dichloromethane ($3X50cm^3$) and the crude product isolated as a viscous brown oil which was chromatographed on 35g of alumina as desribed in procedure no. 1. The diironpolyether, **12**, was isolated as a viscous yellow oil (0.54g, 92%). This product was characterised by ^1H NMR spectroscopy, ^{13}C NMR spectroscopy, infrared spectroscopy and mass spectrometry.

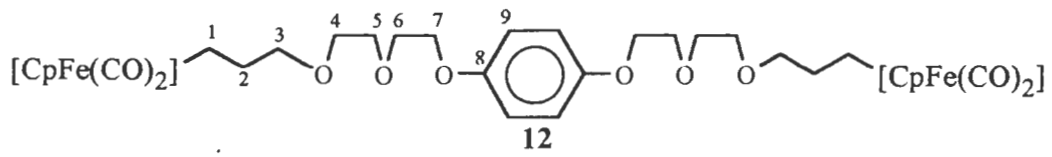

12

IR ν_{max} (CH_2Cl_2) 3023, 2925, 2001, 1942, 1506, 1208, 760 cm^{-1}.

MS, m/z: 722 (M^+), 666 (M- 2(CO))

δ_H (200MHz) 1.34 (4H, m, C_1), 1.74 (4H, m, C_2), 3.40 (4H, t, ^3J= 6.9 Hz, C_3),
3.6 - 4.1 (16H, m, H_4, H_5, H_6, H_7), 4.73 (10H, s, Cp), 6.84 (4H, s, H_9).

δ_C (50MHz) -2.1 (C_1), 37.4 (C_2), 67.8, 69.5, 69.7, 70.5, 74.2 (C_3, C_4, C_5, C_6, C_7), 85.1 (Cp), 115.3 (C_9), 152.8 (C_9), 217.2 (Carbonyls).
(Corrected according to $CDCl_3$ standard 77.00.)

MS, m/z: 722 (M^+, 6%), 666 (M- 2CO), 515 (72%), 368 (100%), 338 (42%), 238 (63%) 198 (56%), 153 (32%), 110 (100%).

4.2.7. Synthesis of the bis(triphenylphosphine)diacyldiiron polyether, **13**.

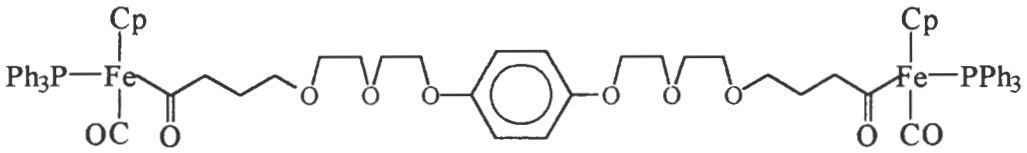

13

The product **13** was prepared by refluxing **12** (0.50 g, 0.70 mmol.) with triphenylphosphine (0.46g, 1.75 mmol.) in benzene (20cm^3) for 8 hours under nitrogen. The solvent was removed under reduced pressure and the resultant orange-yellow gum extracted with dichloromethane (4 X 10 cm^3), the combined extracts filtered and the solvent removed under reduced pressure. This yielded an orange-yellow gum which was investigated using thin layer chromatography with a three component solvent system of hexane, dichloromethane and acetonitrile, which gave clear spot resolution compared to CH_2Cl_2 / hexane mixtures. These R_f values are tabulated in table 4.2.7 overleaf.
The crude product was found to contain residual triphenylphoshine as well as the bis(triphenylphosphine)diacyldiiron polyether, **13**. This orange-yellow gum was dissolved in the minimum amount of dichloromethane and chromatographed on 35g of alumina, packed using a 40% CH_2Cl_2 / 60% hexane slurry. An orange-yellow band was observed at the top of the column and the eluant polarity was increased to 60% CH_2Cl_2 / 40% hexane, then to 80% CH_2Cl_2 / 20% hexane and then to neat CH_2Cl_2 which began to move the orange-yellow band slowly. The eluant was changed to 50% CH_2Cl_2 / 50% diethylether which sped up elution of product **13**. The product, **13**, was isolated in 44% yield (0.380g, 0.305mmol) as an orange-yellow gum.

Table 4.2.7. TLC Rf data of **13** for varied eluant polarity using the three eluant components as indicated.

(%) Hexane	(%) CH_2Cl_2	(%) CH_3CN	R_f
85	10	5	0.03
80	10	10	0.05
75	10	15	0.38
69	23	8	0.50
72	18	10	0.74
50	37	13	0.89

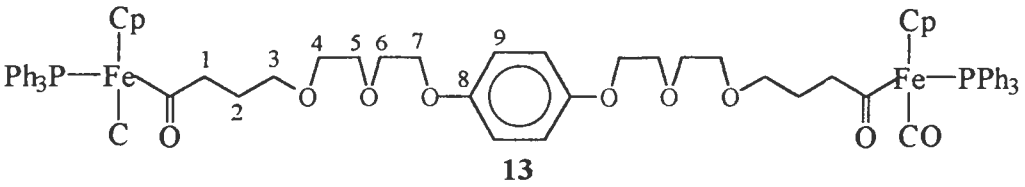

13

IR ν_{max} (CCl_4) 3058, 2870, 1917, 1611, 1507, 1435, 1232, 796 cm^{-1}.

δ_H (200MHz) 1.32 (2H, m, C_1), 1.50 (2H, m, C_1), 2.60 (2H, m, C_2), 2.94 (2H, m, C_2), 3.14 (4H, m, C_3), 3.4 - 4.2 (16H, m, C_4, C_5, C_6, C_7), 4.40 & 4.41 (10H, s, Cp, Cp'), 6.83 (4H, s, C_8), 7.3 (30H, m, PPh_3).

δ_C (50MHz) 25.0 (C_2), 62.0 (C_1), 62.1 (C_1'), 68.1 (C_3), 69.8, 70.0, 70.7, 70.9, (C_4, C_5, C_6, C_7), 85.2 (Cp), 115.6 (C_8), 153.1 (C_9), 127.9 - 136.9 (PPh_3), 220.9 (CO).

4.3. Experimental details for the clipping experiment.

Bis(triphenylphosphine)diacyldiiron polyether, **13,** (0.690g, 0.55mmol), "horseshoe" (0.131g, 0.184mmol) and dibromoxylene (0.049g, 0.184mmol) were dissolved in CH_3CN ($15cm^3$) and the solution allowed to stir at room temperature under N_2 for 2 days. The reaction was monitored by thin layer chromatography to ascertain whether or not the thread had decomposed. After two days, $AgBF_4$ (0.072g, 0.368mmol) was added and the solution allowed to stir for another three days. At this stage a further addition of $AgBF_4$ (0.072g, 0.368mmol) and dibromoxylene (0.049g, 0.184mmol) was made and the solution was allowed to stir for a further two days. It was then evident from thin layer chromatography that **13** had not decomposed. Thin layer chromatography showed the presence of dibromoxylene, **13**, a polar product corresponding in polarity to bluebox and a product slightly less polar than bluebox, thought to be the rotaxane product sought. Thin layer chromatography used (MeOH / aqueous ammonium chloride / nitromethane) 7:3:1 as eluant, when checking for charged species (i.e. "horseshoe", "bluebox" or a rotaxane); when checking for presence of dibromoxylene or **3**, (hexane / CH_2Cl_2 / CH_3CN) 7:2:1 was used as eluant.

A silica gel column was prepared by packing silica gel (20g) as a methanol slurry. The reaction mixture was dissolved in the minimum amount of (MeOH / aqueous ammonium chloride / nitromethane) 7:3:1 solvent and applied to the column. Initially $400cm^3$ of methanol eluted excess **13** as a viscous orange-red band (0.431g). This band was identified as **13** initially by thin layer chromatography and later confirmed by 200 MHz ^1H NMR spectroscopy. Note that elution from the column was extremely slow due to the polarity of the solvent. The eluant was then changed from methanol to (methanol / aqueous ammonium chloride / nitromethane) 7:3:1 which brought the rate of elution down to $1cm^3$ / 10 minutes. Once a number of fractions had been collected, thin layer chromatography showed that two UV active bands had been eluted, one corresponded in polarity to "bluebox" and the other slightly less polar than "bluebox", thought to be a possible rotaxane. Both bands were treated with NH_4PF_6 to exchange the counter ions to PF_6 thus making the respective products soluble in nitromethane. Each aqueous fraction was extracted with nitromethane ($3X15cm^3$).

Two products were isolated, the first as a reddish gum (63mg, 15%) and was investigated as being a rotaxane; the second product was a yellow solid identified as "bluebox" by thin layer chromatography (52mg, 0.055mmol, 30% relative to the amount of horseshoe used initially).

The investigation of the first product eluted was carried out by ^{1}H NMR spectroscopy; ^{13}C NMR spectroscopy was unsucessful due to the poor solubiltiy of this product in the NMR solvent (DMSO-d_6). The NMR of the possible rotaxane is included in the discussion section 3.4. of Chapter 3. This ^{1}H NMR spectrum shows signals expected for "bluebox", as well as signals expected for **13**. The polyether methylene signal is larger than expected. The shifts of the signals observed for "bluebox" suggest that **13** is encircled by bluebox. This NMR spectrum is discussed in detail on page 61.

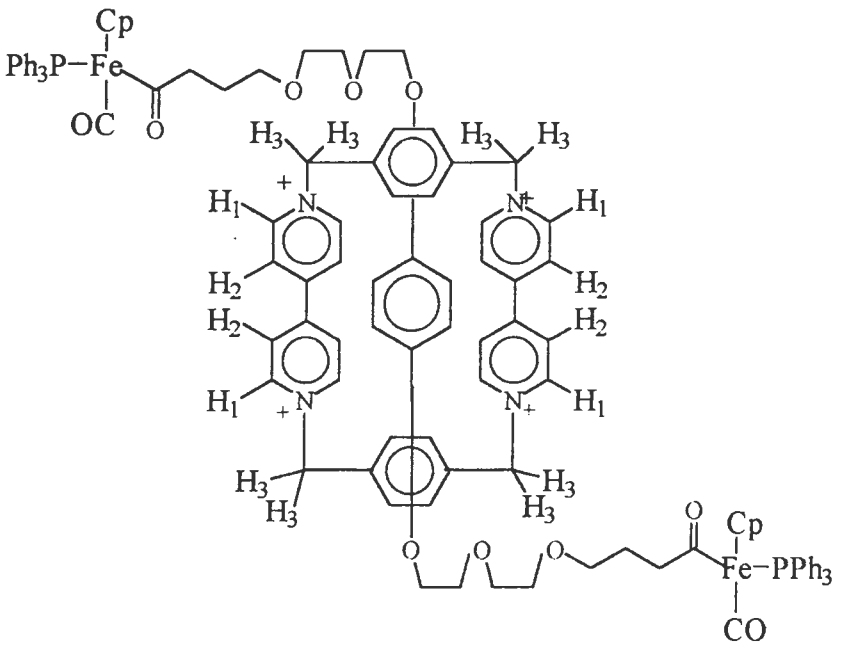

IR ν_{max} (CH_3NO_2) 3043(Aryl C-H), 2953, 1917 (Fe-CO), 1652 (C=O, acyl), 1495, 1210 cm^{-1}(ether).

δ_H (400MHz) 9.48 (4H, d, ^{3}J = 7.2 Hz, H_1), 9.45 (4H, d, ^{3}J = 7.2 Hz, H_1), 8.71 (4H, d, ^{3}J = 5.5 Hz, H_2), 8.70 (4H, d, ^{3}J = 5.4 Hz, H_2), 7.4 - 7.8 (28H, m, PPh_3), 5.93 (4H, s, H_3) and 5.92 (4H, s, H_3), 4.42 (10H, s, Cp), 3.4 - 4.0 (polyether methylenes).

References.

1. I. T. Harrison, *J. Chem. Soc. Chem. Commun.,* 1972, 231.

2. I. T. Harrison, *J. Chem. Soc. Chem. Commun.,* 1974, 301.

3. J. P. Sauvage, *Acc. Chem. Res.*, **1990**, *23*, 319.

4. C. O. Dietrich-Buchecker and J. P. Sauvage, *Chem. Rev.,* 1987, **87**, 795.

5. C. O. Dietrich-Buchecker, A. Khemiss and J. P. Sauvage, *J. Chem. Soc. Chem. Commun.* 1986, 1376.

6. F. Diederich, C. O. Dietrich-Buchecker J. F. Nierengarten and J. P. Sauvage, *J. Chem. Soc. Chem. Commun.* 1995, 781.

7. J. C. Chambron, C. O. Dietrich-Buchecker J. F. Nierengarten and J. P. Sauvage, *Pure & Appl. Chem.,*1994, **66**, 1543 and references therein.

8. H. Sleiman, P. Baxter, J. M. Lehn and K. Rissanen, *J. Chem. Soc. Chem. Commun.*, 1995, 715.

9. J. F. Stoddart, *Chemistry in Britian*, August 1991, 714.

10. (a) B. Odell, M. V. Reddington, A. M. Z. Slawin, N. Spencer, J. F. Stoddart and D. J. Williams, *Angew. Chem. Int. Ed. Engl.* 1988, **27**, 1547.

    (b) T. T. Goodnow, M. V. Reddington, J. F. Stoddart and A. E. Kaifer, *J. Am. Chem. Soc.* 1991, **113**, 4335.

11. P. R. Ashton, B. Odell, M. V. Reddington, A. M. Z. Slawin, N. Spencer, J. F. Stoddart and D. J. Williams, *Angew. Chem. Int. Ed. Engl.,* 1988, **27**, 1551.

12. M. V. Reddington, A. M. Z. Slawin, N. Spencer, J. F. Stoddart, C. Vincent and D. J. Williams, *J. Chem. Soc. Chem. Commun.,* 1991, 630.

13. P. L. Anelli, P. R. Ashton, N. Spencer, A. M. Z. Slawin, J. F. Stoddart and D. J. Williams, *Angew. Chem. Int. Ed. Engl.,* 1988, **30**, 1036.

14. P. L. Anelli, N. Spencer and J. F. Stoddart, *J. Am. Chem. Soc.,* 1991, **113**, 5131.

15. P. R. Ashton, D. Philp, N. Spencer and J. F. Stoddart, *J. Chem. Soc. Chem. Commun.,* 1991, 1677.

16. P. R. Ashton, T. T. Goodnow, A. E. Kaifer, M. V. Reddington, A. M. Z. Slawin, N. Spencer, J. F. Stoddart C. Vincent and D. J. Williams, *Angew. Chem. Int. Ed. Engl.,* 1989, **28**, 1396.

17. W. Geuder, S. Hunig, and A. Suchy, *Tetrahedron,* 1986, **42**, 1665.

18. P. L. Anelli, P. R. Ashton, R. Ballardini, V. Balzani, M. Delgado, M. T. Gandolfi, T. T. Goodnow, A. E. Kaifer, D. Philp, M. Pietraskiewicz, L. Prodi, M. V. Reddington, A. M. Z. Slawin, N. Spencer, J. F. Stoddart, C. Vincent and D. J. Williams, *J. Am. Chem. Soc.,* 1992, **114**, 193.

19. P. R. Ashton, D. Philp, N. Spencer, J. F. Stoddart and D. J. Williams., *J. Chem. Soc. Chem. Commun.*, 1994, 181.

20. D. B. Amabilino, P. R. Ashton, M. Belohradsky, F. M. Raymo amd J. F. Stoddart, *J. Chem. Soc. Chem. Commun.*, 1995, 747.

21. D. B. Amabilino, P. R. Ashton, A. S. Reder, N. Spencer and J. F. Stoddart, *Angew. Chem. Int. Ed. Engl.*, 1994, **33**, 1286.

22. R. B. King, *Inorg. Chem.*, 1963, **2**, 531.

23. L. Pope, P. Sommerville, M. Laing, K. Hindson and J. R. Moss., *J. Organometal. Chem.*, 1976, **112**, 309.

24. J. R. Moss, L. G. Scott, M. E. Brown and K. J. Hindson, *J. Organometal. Chem.*, 1985, **282**, 255.

25. J. R. Moss and L. G. Scott, *J. Organometal. Chem.*, 1989, **363**, 351.

26. Y-H Liao, Ph. D. thesis, University of Cape Town, 1994.

27. J. R. Moss, *Trends in Organometallic Chemistry*, 1994, **1**, 211.

28. Y-H Liao and J. R. Moss, Organometallics, 1995, **14**, 2130.

29. R. Dagani, *Chemical and Engineering News*, 1994, **72** , 31.

30. P. R. Markies, T. Namoto, O. S. Akkerman, F. Bickelhaupt, W. J. Smeets and A. L. Spek, *J. Am. Chem. Soc.,* 1988, **110**, 4845.

31. G. M. Gruter, F. J. de Kanter, P. R. Markies and F. Bickelhaupt, *J. Am. Chem. Soc.,* 1993, **115**, 12179.

32. A. C. Benniston and A. Harriman, *Angew. Chem. Int. Ed. Engl.*, 1993, **32** 1459.

33. A. C. Benniston and A. Harriman, *J. Am. Chem. Soc.,* 1995, **117**, 5275.

34. W. Beck, N. Burkhard and M. Weiner, *Angew. Chem. Int. Ed. Engl.*, 1993, **32**, 923 and references therein.

35. C. J. Pouchert, The Aldrich Library of NMR Spectra, 1, Aldrich Chemical Company, Inc.

36. J. R. Moss, *J. Organomet. Chem.*, 1982, **231**, 229.

37. H. B. Friedrich, P. A. Makhesha, J. R. Moss and B. R. Williamson, *J. Organomet. Chem.*, 1990, **384**, 325 and references therein.

38. L. G. Scott, M. Sc. thesis, University of Cape Town, 1984.

39. N. Aktogu, H. Felkin and S. G. Davies, *J. Chem Soc. Chem Commun.*, **1982**, 1302 and references therein.

40. A. Davidson and N. Martinez, *J. Organomet. Chem.*, 1974, **74**, C17.

41. V. Balzani and L. De Cola (eds), *Supramolecular Chemistry*, Kluwer Academic Publishers, The Netherlands, 1992, 1.

42. S. F. Mapolie and J. R. Moss, S. Afr. J. Chem., 1987, **40**, 12.

43. D Barton and W. Ollis, "The synthesis and reactions of organic compounds," in *Comprehensive Organic Chemistry*, Pergamon Press, Oxford, 1979, **3**, 713.

44. D. H. Williams and I. Fleming, *Spectroscopic methods in organic chemistry,* (3rd edn.), McGraw-Hill, Berkshire, England, 1980, 139.